IMPACT OF LAND USE CHANGES ON HYDROLOGICAL RESPONSE OF HUMID AND SUB-HUMID CATCHMENTS IN KARNATAKA STATE, INDIA

Thesis

Submitted in partial fulfilment of the requirements for the degree of

DOCTOR OF PHILOSOPHY
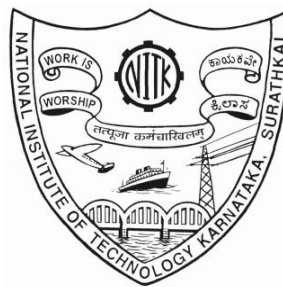
by

GANASRI B P

AM12F03

Under the guidance of

Dr. G S Dwarakish

Professor and Head

Department of Applied Mechanics and Hydraulics

NITK, Surathkal

DEPARTMENT OF APPLIED MECHANICS AND HYDRAULICS

NATIONAL INSTITUTE OF TECHNOLOGY KARNATAKA,

SURATHKAL, MANGALORE -575025

November, 2016

D E C L A R A T I O N

By the Ph.D. Research Scholar

I hereby *declare* that the Research Thesis entitled **Impact of land use changes on hydrological response of humid and sub-humid catchments in Karnataka State, India** which is being submitted to the **National Institute of Technology Karnataka, Surathkal** in partial fulfilment of the requirements for the award of the Degree of **Doctor of Philosophy** in **Applied Mechanics and Hydraulics Department** is a *bonafide report of the research work* carried out by me. The material contained in this Research Synopsis has not been submitted to any University or Institution for the award of any degree.

121153AM12F03, GANASRI B. P

(Register Number, Name & Signature of the Research Scholar)

Department of Applied Mechanics and Hydraulics

Place: NITK-Surathkal

Date:

C E R T I F I C A T E

This is to *certify* that the Research Thesis entitled **Impact of land use changes on hydrological response of humid and sub-humid catchments in Karnataka State, India** submitted by GANASRI B. P. (Register Number: 121153AM12F03) as the record of the research work carried out by her, is *accepted as the Research Thesis submission* in partial fulfilment of the requirements for the award of degree of **Doctor of Philosophy**.
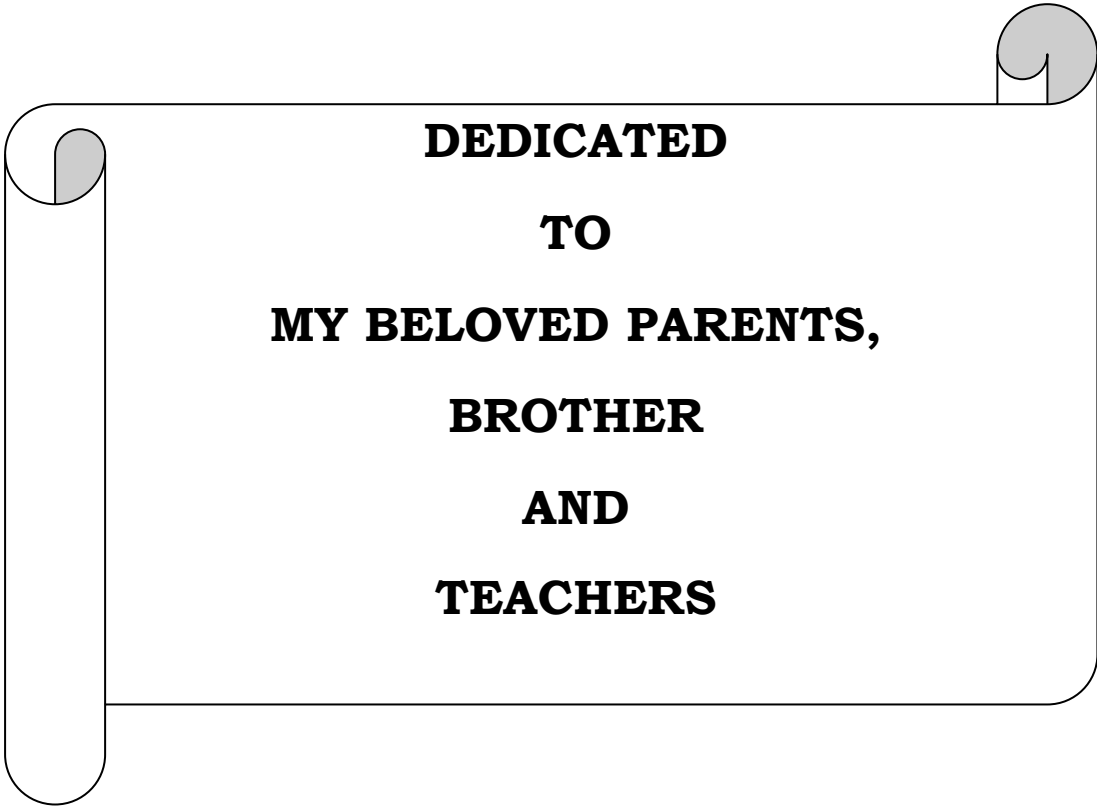
Dr. G. S. Dwarakish

Professor

Research Guide

(Name and Signature with Date and Seal)

Chairman - DRPC

(Signature with Date and Seal)

DEDICATED

TO

MY BELOVED PARENTS,

BROTHER

AND

TEACHERS

ABSTRACT

Due to activities aimed at improving the socio-economic status and wellbeing of people, natural resources are exploited, and, as a result, environment has changed in terms of climate and land use. These changes have great influence on the local hydrologic cycle and hydrologic response of the catchment. In addition to climatic factors, the flow characteristics of a stream depend upon catchment characteristics such as topography, soil, geology and land use and land cover. The land use experiences rapid spatio-temporal changes that become one of the critical factors influencing the pattern of streamflow.

The major objective of the present thesis work was to analyze and investigate the interaction between hydrologic response and the land use/land cover (LU/LC) pattern in two contrasting catchments namely Netravati river basin, a humid catchment and Harangi catchment, a sub-humid catchment of Karnataka State, India. This research work was explicitly carried out to: a) perform LU/LC classification and identifying the driving factors using multi-date satellite images, b) prediction of future trends in LU/LC pattern using Land Change Modeler (LCM) and CA-Markov model, c) estimate Actual Evapotranspiration (AET) and Land Surface Temperature (LST) using satellite images, d) explore the applicability of the semi distributed model to estimate streamflow, e) explore the applicability of monthly rainfall-runoff polygon in explaining hydrological processes in humid and sub-humid catchments, and f) analyse the relationship between changes in hydrological response and LU/LC change pattern. Study areas selected for the present work: Netravati river basin and Harangi catchment. The Netravathi basin geographically lies between 75º 01′ E and 75º 46′ E longitude and 12º 29′ N and 13º 11′ N latitude with an area of 3312.74 sq. km. Harangi catchment geographically lies between 75^0 38' E and 75^0 55' E longitude and 12^0 24' N and 12^0 40' N latitude with an area of 417.54 sq. km.

The study utilized LCM and CA-Markov models for the prediction of LU/LC for the years 2010 and 2016 in Netravati river basin and 2013 and 2016 in Harangi catchment by considering LU/LC maps of 2005, 2007 and 2007, 2010 as base maps respectively. LCM and CA-Markov model predicted the LU/LC change by 2010 with an accuracy of 80.1% and 82.13%, respectively in Netravati river basin. An accuracy of 86.6% and 80% is obtained in Harangi catchment by using LCM and CA-Markov model respectively. The result of land change prediction for the

year 2016 by CA-Markov model in Netravati river basin shows a decrease in forest, fallow land and land with or without scrub land between 2010 and 2016, contributing to an increase in built-up land and plantation. Predicted map of Harangi catchment for the year 2016 shows that the plantation is increasing from 175.77 to 220 sq.km area, but forest, fallow and wasteland are showing a decreasing trend. Then, the present study estimated AET by using Priestley Taylor method based on satellite data in Netravati and Harangi catchments. The Split Window (SW) algorithm was utilized for spatial mapping of LST. Result shows that AET has increased during the study period of 1997-2015. Since the AET estimation method is based on brightness temperature and fractional vegetation cover, the increase in LST and decrease in fractional vegetation cover has lead to increase in AET.

The present research work discussed about calibration of continuous hydrological model to predict runoff volume in Netravati river basin. The result of simulation run for the calibration period shows that the model is underestimating peak flows during monsoon and overestimating low flows during summer. The Nash Sutcliffe Efficiency determined for calibration period is about 0.251. This indicates that this model which required 19 parameters seem to be data intensive and necessitated the development of simple methodology to estimate streamflow. Therefore, the study developed a simple methodology to study the hydrological response to changes in two contrasting catchments namely Netravati river basin and Harangi catchment by using rainfall-runoff polygon method. The methodology involved qualitative and quantitative interpretation of runoff coefficient and geometric properties of polygon in relationship with the catchment behavior. Netravati river basin is represented by the less steep and wider polygon indicates the fact that the catchment response to rainfall is variable in each month especially from June to September during all periods. Harangi catchment is characterized by more steep and narrow polygon implies the consistent variation of catchment response to rainfall pattern in each month especially from the end of June to the end of August during all the periods. The analysis concluded that the influence of LU/LC change on rainfall-runoff conversion mechanism is predominant in Netravati river basin when compared to Harangi catchment. This is clearly represented by wider polygon and smaller over all slope of polygon w.r.t x-axis.

Keywords: hydrologic modeling, land use and land cover change, LCM, CA-Markov, AET, rainfall-runoff polygon

ACKNOWLEDGEMENTS

(Ganasri B P)

TABLE OF CONTENTS

LIST OF FIGURES

LIST OF TABLES

ABBREVIATION

SYMBOLS	DESCRIPTION
ABM	Agent Based Modelling
ACRU	Agricultural Catchments Research Unit
AET	Actual Evapotranspiration
ANN	Artificial Neural Network
C0 to C6	Split-Window Coefficient values
CA	Cellular Automata
CLUE-S	Conversion of Land Use and its Effects at a Small regional extent
CWC	Central Water Commission
DA	Dual-Angle
DEM	Digital Elevation Model
DHSVM	Distributed Hydrology-Soil Vegetation Model
DN	Digital Number
dr	Inverse relative earth sun distance
EBMs	Equation Based Models
EF	Evaporative Fraction
E_{rel}	Relative Efficiency
ET	Evapotranspiration
FAO	Food and Agricultural Organization
FCC	False Colour Composite
FVC	Fractional Vegetation Cover
G	Soil heat flux
GCMs	Global Circulation Models
GCPs	Ground Control Points
GIS	Geographic Information System
GLUE	Generalized Likelihood Uncertainty Equation

HSPF	Hydrological Simulation Program—Fortran
HUP	Hydrologic Uncertainty Processor
IDW	Inverse Distance Weighting
IMD	Indian Meteorological Department
IPCC	International Panel on Climate Change
J	Sequential day of year
K1 and K2	Thermal conversion constant
k_s	Saturated hydraulic conductivity
LAI	Leaf Area Index
LCM	Land Change Modeller
LSE	Land Surface Emissivity
LST	Land Surface Temperature
LU/LC	Land Use and Land Cover
LUCC	Land Use and Land Cover Change
LUP	Land Use Planning
MAM	Multi Actor Modelling
MLP	Multi-Layer Perceptron
MSL	Mean Sea Level
NAM	Nedbor-Afstromnings Model
NBSS	National Bureau of Soil Survey
NDVI	Normalised Difference Vegetative Index
NDVIs	NDVI for soil
NDVIv	NDVI for vegetation
NRSC	National Remote Sensing Centre
OK	Ordinary Kriging
OM	Organic Matter
P	Mean monthly precipitation
p	Power factor
Q	Runoff

R	Net daily radiation
R1down	Long wave downward radiation
R1up	Long wave upward radiation
RBF	Radial Basis Function
RCa	Annual runoff coefficient
RCm	Mean monthly runoff coefficient
RCMs	Regional Climate Models
RMSE	Root Mean Square Error
RR	Rainfall-Runoff
Rrc	Runoff to rainfall ratio of current month
Rrp	Runoff to rainfall ratio of preceding month
Rs	Incoming solar radiation
RS	Remote Sensing
S	Watershed storage
SC	Single-Channel
SD	System Dynamics
SEBAL	Surface Energy Balance Algorithm for Land
SEBI	Surface Energy Balance Index
SEBS	Surface Energy Balance System
SMA	Soil Moisture Accounting
SOI	Survey of India
SR	Atmospheric Spectral Radiance
SRES	Special Report on Emissions Scenarios
SVAT	Soil-Vegetation-Atmosphere Transfer
SW	Split-Window
SWAT	Soil Water Assessment Tool
TB	Brightness Temperature
TIR	Thermal Infra-Red
TSM	Two Source Models

VIC	Variable Infiltration Capacity
W	Atmospheric water vapour content
WBNM	Watershed Bounded Network Model
Z	Elevation in meter
α	Surface albedo
$\Delta\varepsilon$	Difference in LSE
ε	Mean LSE of Thermal Infra-Red bands
ε_a	Atmospheric emissivity
$\boldsymbol{\varepsilon}s$	Soil emissivity values
ε_s	Surface emissivity
εv	Vegetative emissivity
θ	Solar angle
λ	Latent heat of water
σ	Stefan-Boltzmann constant
τ_{sw}	Two way atmospheric transmissivity
p	Density of water

1.1 PREFACE

Water is the most essential natural resource for life next to air and is likely to become a scarce resource in many regions of the world. On the other hand, water can also constitute as a threat, for example, in the case of floods (Mauser and Bach 2009; Wijesekara et al. 2012; Ozturk et al. 2013). The strong connection between human and water makes it necessary in several practical applications to have the best knowledge as possible on specific hydrological processes at spatial and temporal scale of interest. This is essential to effectively plan, develop and manage the water resources, as well as to prevent its adverse effects (Lin et al. 2009; Tong et al. 2012). Global advances in the economy and standards of living have resulted in a growing dependency on water resources (Nandakumar and Mein, 1997; Legesse et al. 2003). In addition to climate change, land use change is one of the important human interventions altering the quality and quantity of both surface and ground water. The study of hydrological cycle and hydrological response of a catchment have become very complex due to complicated inter-relationship between various hydrological components such as precipitation, evaporation, transpiration, infiltration and runoff. Both climate and land use change have adverse implications on the natural hydrologic system in terms of variation in the runoff regime, evapotranspiration (ET), sub surface flow, infiltration etc., (Xu and Singh, 1998; Lorup et al. 1998; McColl and Aggett, 2007). Combined with rainfall and runoff, ET controls the availability and distribution of water at the Earth's surface, and for this reason, is of significance to a number of water-related research and application areas. The spatial variations in ET from a heterogeneous catchment can be significantly large on account of differences in climate, vegetation and soil properties. Therefore to assess the natural hydrologic system, researchers have investigated the relationship between climate, land use and hydrological processes (Nandakumar and Mein, 1997; Bormann et al. 2009; Tang et al. 2011).

1.2 THE HYDROLOGIC CYCLE

The hydrologic cycle describes the continuous movement and changes in the state of water between the earth and atmosphere. This cycle includes the processes illustrated in Figure 1.1: evapotranspiration (water going into the atmosphere), condensation (forming of clouds); precipitation (in various forms, such as rain, snow, sleet and hail), runoff (flow of rainwater on the earth's surface and in surface water bodies) and percolation (water infiltrating into the earth to form and/or recharge groundwater bodies). The water movement from the earth's surface to the atmosphere is supported by the solar radiation, while the water movement at and below the surface of the earth is mainly driven by gravity. The main effect of the hydrologic cycle is that of maintaining the heat balance of the earth, through moving and redistributing water masses (Chow et al. 1988).
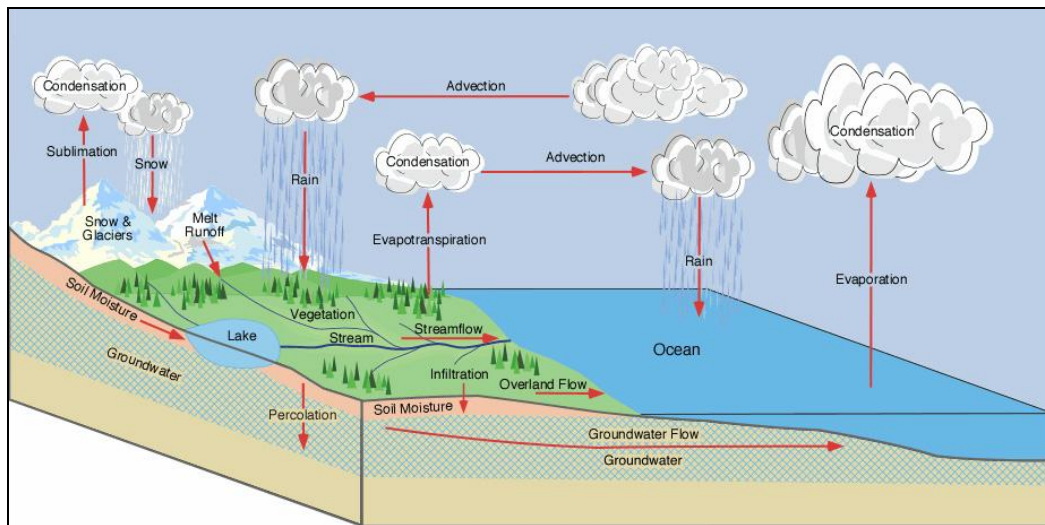
Figure 1.1 The hydrological cycle (Department of Natural Resource Ecology and Management" (NREM) at Iowa State University)

Hydrology means the science that deals with the occurrence, circulation and distribution of water of the earth and earth's atmosphere. It provides a knowledge of various phases of water as it passes from the atmosphere to the Earth and returns to the atmosphere (Subramanya 2008). In addition, it forms the basis for water resources assessment and management and the solution of practical problems relating to floods and droughts, erosion and sediment transport and water pollution (Daofeng et al. 2004). Increasing stress on the available water resources in the search for improved

economy and well-being of people, leading to the pollution of surface water and groundwater, has highlighted the central role of hydrology in all water and environmental initiatives (Xu and Singh 1998).

Hydrologic response of a watershed is highly complex due to heterogeneous distribution of various hydrologic components within the watershed. In addition to climatic factors, the flow characteristics of a stream depend upon catchment characteristics such as topography, soil, geology, land use/land cover (LU/LC) (Siriwardena et al. 2006, Isik et al. 2013). Over a period of time, topography, soil and geology remains more or less constant in a catchment. However, land use experiences rapid spatio-temporal changes, which becomes a critical factor influencing the pattern of streamflow (Lorup et al. 1998; Niehoff et al. 2002; Delgado et al. 2010). Response of these factors to runoff can be determined by modeling.

1.3 HYDROLOGIC MODELS

Due to increased need for water for various day to day activities and agricultural purpose, water resource management becomes a challenge for planners and policy makers (Costa et al. 2003; McColl and Aggett 2007; He and Hogue 2012). Hydrologic models have become increasingly important tools for the management of the water resources (Sarkar and Kumar 2012; Shirke et al. 2012). They are used for flow forecasting to support reservoir operation, for flood protection, in spillway design studies and for many other purposes. Runoff models are probably what most hydrologists spontaneously refer to when discussing hydrological models. The basic principle in hydrologic modeling is that the model is used to calculate stream flow based on meteorological data and catchment characteristics, which are available in a basin or in its vicinity (Lorup et al. 1998; Ye et al. 2013; Zhou et al. 2013).

Hydrologic models have become an indispensable tool for the study of hydrological processes and the impact of modern anthropogenic factors on the hydrologic system. The broad classification of hydrologic models is as shown in Figure 1.2.
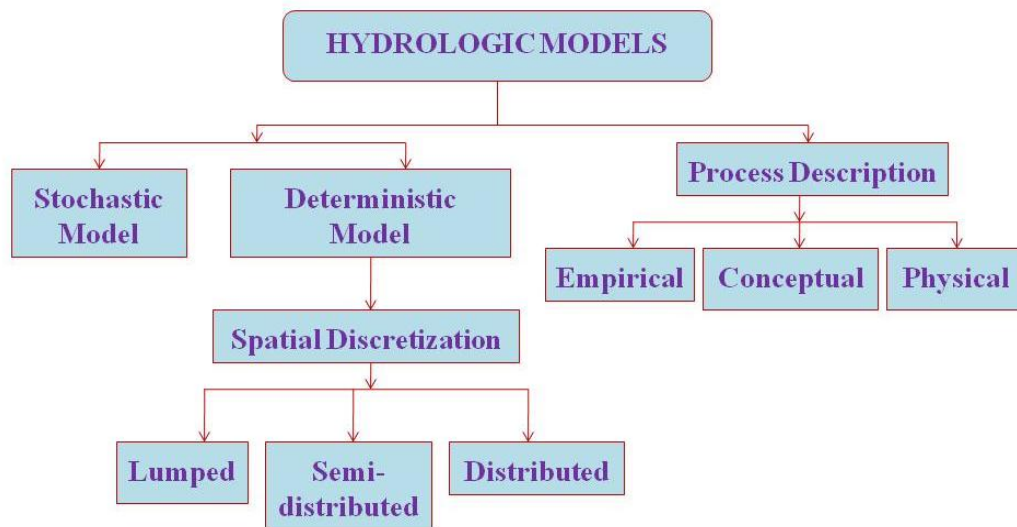
Figure 1.2 Classification of hydrologic models

Hydrologic models can be classified into the following categories based on the presence of random variables, their distribution in space, and temporal variation (Chow et al. 1988):

1. Deterministic models: Randomness is not considered; a given input always produces the same output. Therefore, these models can be used for forecasting.

   a) Deterministic lumped model: A lumped model is generally applied to a single point or a region without dimension for the simulation of various hydrological processes (Niel et al. 2003). The parameters used in the lumped model represent spatially averaged characteristics in a system. The conceptual parameterization in the models is simple and computationally efficient.

   b) Deterministic semi-distributed model: It divides the whole catchment into Hydrologic Response Units (HRUs) based on other variables in addition to land use and land cover, soil type and slope and simulates the various hydrological processes in each HRU.

   c) Deterministic distributed model: It considers the hydrological processes taking place at each grid and defines the model variables as functions of the space dimensions (Beven et al. 1980; Feyen et al. 2000).

Watershed-scale models can further be categorized on a spatial basis as lumped, semi-distributed or distributed models. The lumped modeling approach considers a watershed as a single unit for computations where the watershed parameters and variables are averaged over this unit (Niel et al. 2003; Magar and Jothiprakash, 2011; Cheng, 2011). The semi-distributed models partition the whole catchment into sub-basins or hydrologic response units (HRUs) (Daofeng et al. 2004). In contrast, the spatial heterogeneity is represented by grids in the case of distributed models. Compared to lumped models, semi-distributed and distributed models better account for the spatial variability of hydrologic processes, input, boundary conditions and watershed characteristics (Legesse et al. 2003; Thanapakpawin et al. 2006; Lin et al. 2008; McColl et al. 2007; Elfert and Bormann 2010).

2. Stochastic models: The output of these models is at least partially random. Therefore, these models make statistical predictions. Stochastic models are classified as space independent or space correlated depending on whether random variables in space influence each other.

The hydrological models can also be classified according to whether the hydrological processes are described as conceptual, empirical, or fully physically based (Figure 1.2). Empirical models such as Artificial Neural Networks (ANNs), Fuzzy Logic, Genetic Algorithm (GA) etc., are used to establish a relationship between rainfall and runoff to predict runoff in different catchments (Halff et al. 1993; Shirke et al. 2012; Chen et al. 2013). Empirical models contain no physical transformation function to relate input to output; such models usually build a relationship between input and output based on hydro-meteorological data (Sudheer et al. 2002; Sarkar and Kumar, 2012). ANN models are capable of modeling non-linear relationships between inputs and outputs. Thus, daily runoff forecasting using ANN models has become quite important for effective planning and management of water resources (Shirke et al. 2012). Ondieki (1997) has investigated four catchments ranging from semi-humid to semi-arid catchments to evaluate the water resource potential of non-perennial streams. This study has concluded that rainfall would have some relationship with runoff as well as suspended sediment load. However, the rainfall alone could not explain the runoff variance efficiently, which can be attributed

to antecedent moisture content, rainfall intensity and physical catchment characteristics such as geology, soil, slope and land use and land cover conditions (Costa et al. 2003). The major limitation of empirical models is the absence of explicit consideration of physical processes such as sub surface flow, surface runoff and infiltration in the catchment. In addition, these numerical models are not capable of modeling the influence of change in vegetation on various hydrological components.

Conceptual rainfall-runoff models are simplifications of the complex processes of runoff generation in a catchment. The particular components of these models often have to be described by empirical functions based on the observation of certain processes. Viviroli et al. (2009) introduces a semi-distributed hydrological modeling system PREecipitation-Runoff-EVApotranspiration HRU Model (PREVAH) that implements a conceptual process-oriented approach and has been developed especially to suit conditions in mountainous environments with their highly variable environmental and climatic conditions. Also, a built-in automatic calibration model significantly reduces the amount of user intervention that is usually required for tuning the model parameters. Monte Carlo model is the one, which can be used to obtain estimates of parameter uncertainties. Valent et al. (2012) have used lumped conceptual model, Hron rainfall runoff model which is a modified version of Hydrologiska Bryåns Vattenbalansavdelning (HBV) model to predict runoff and also to test the calibration procedure. Results suggested that the model has uncertainties with respect to conceptualization of complex runoff generation process and the quality of input data (Tian et al. 2013). Parajka et al. (2006) have utilized scatterometer data in a conceptual semi-distributed model to study the soil moisture dynamics which alter the hydrological processes.

In contrast, the physically based distributed models are able to explicitly represent the spatial variability of the important land surface characteristics such as topographic elevation, slope, aspect, vegetation, soil as well as climatic parameters including precipitation, temperature and ET distribution (Grayson, 1992; Wijesekara et al. 2012; Niehoff et al. 2002; Akbari and Singh, 2012). Shen and Phanikumar (2010) utilized the Process-based Adaptive Watershed Simulator (PAWS) to evaluate the integrated hydrological response of the surface–subsurface system using a novel

non-iterative method that couples runoff and groundwater flow to vadose zone processes approximating the 3D Richards equation. The model solves the governing equations for the major hydrological processes efficiently so that large-scale applications become relevant. The model performance may deteriorate in catchments dominated by perched water table dynamics because the model assumes that soil moisture does not flow laterally in the unsaturated part of the soil column.

1.4 HYDROLOGIC RESPONSE TO LU/LC CHANGE DYNAMICS

Recent studies have demonstrated the potential of an integrated modeling approach to evaluate the impact of land use changes on water resources (McColl and Aggette, 2007; Wijesekara et al., 2012). Choi and Deal (2008) combined a semi-distributed hydrologic model and a dynamic urban growth model (LEAMluc) for examining the implications of urbanization on the hydrological processes in the basin. They found that the land use scenarios generated by the model show noticeable changes in surface flow in some areas as a result of very high population growth. He and Hogue (2012) have used a semi-distributed model to evaluate the impact of future urbanization on flow regimes and found that increasing development increases the total annual runoff and wet season flows. Integrating land use models with a precipitation-runoff model provides quantitative information about the effects of land use intensities and strategies on hydrological output. Different land uses in different sub-watersheds yield significantly different hydrologic output (Lin et al., 2009).

1.5 ANALYSIS OF HYDROLOGIC RESPONSE CHARACTERISTICS THROUGH RUNOFF COEFFICIENT

Any water resources engineering structure design necessitates accurate estimation of surface water yield and peak flow that is usually calculated based on runoff coefficient and precipitation characteristics. The runoff coefficient in any watershed is influenced by many concerned factors including precipitation intensity and duration, Land use/Land cover (LU/LC), geology, infiltration rate, soil type and topography. In recent past, runoff values are highly modified in urbanized catchments due to anthropogenic effects (Kadioglu and Sen 2001). Rodriguez-Blanco et al. (2012) considered a series of rainfall-runoff events to analyse the principle hydrological patterns and identified the factors, which impel the hydrological response. Their study

indicates that water yield mainly depends on antecedent moisture condition in addition to the rainfall amount. In addition, the hydrographs with quick increase and slow recession indicates that subsurface flow is probably the prevailing process effecting the runoff response of the catchment to rainfall events. However, hydrologic response of a catchment is most commonly expressed through runoff coefficient. Since it represent the amount of rainfall becomes runoff in relationship with catchment physical properties (Nazir et al. 2015). In any water resources design, the runoff coefficient value is chosen instinctively from the pre-defined table based on the personal judgement rather than hard data. Nevertheless, the runoff coefficient estimated in any river basin varies widely from storm to storm depending on the antecedent moisture condition (Kadioglu and Sen 2001; Rodriguez-Blanco et al. 2012). Furthermore, the runoff coefficient value varies temporally with changes in rainfall of that particular area. The increase in percentage of imperviousness may increase the value of runoff coefficient. This is because of the decrease in the amount of infiltration and storage due to imperviousness. On the other hand, the vegetation rich area may produce high surface runoff due to saturated watershed storage conditions (Nazir et al. 2015). Goldshleger et al. (2009) made an effort to generalize the relationship between percentage of impervious area and storm runoff coefficient that reflects the global trends of expansion and densification of urban zones; wherein the surface imperviousness have been derived from RS data including aerial photographs.

1.6 ROLE OF REMOTE SENSING IN HYDROLOGIC MODELING

Physically based hydrologic models are an important evolutionary step in representing hydrological processes using spatially distributed data. Better representation of physical processes in space and time needs the availability of digital products (e.g., distributions of elevation, soil, vegetation) and remotely sensed data (e.g., soil moisture, vegetation), along with new technologies for measuring temporal and spatial variability in precipitation (Daofeng et al 2004; Ruelland et al. 2008). The distributed hydrological models need spatially variable rainfall and temperature data, which now can be obtained from Tropical Rainfall Measuring Mission (TRMM) precipitation products, Advanced Very High Resolution Radiometer (AVHRR),

Moderate Resolution Imaging Spectroradiometer (MODIS), and Landsat images with high spatial and temporal resolution (Haigen et al. 2015). For topography-based hydrologic models, digital elevation models (DEMs), Shuttle Radar Topography Mission (SRTM), and ASTER are routinely used to device the land-surface topography, which contains crucial information about the surface water flow and the interaction of surface water and ground water (Khan et al. 2013). With the development of remote sensing and satellite technology, the satellite data can be used to derive a variety of surface parameters such as radiant surface temperature and vegetation fraction, and their spatial and temporal comparison. Also, these variables can be used for regional hydrologic modeling of important hydrological processes. One of the important hydrologic model inputs such as land use and land cover can be obtained from Landsat TM images, LISS-III and LISS-IV images (Bhagyanagar et al. 2012). The recent missions of European Space Agency included Sentinel series operational satellites with an aim to meet requirements of earth observation. These satellites are capable of providing data for various applications including sea-surface topography, sea-surface height and significant wave height, ocean and land-surface temperature, ocean and land-surface colour, sea and land ice topography, sea-water quality and pollution monitoring, inland water monitoring, climate monitoring and modelling, land-use change monitoring, fire detection, weather forecasting, and measuring earth's thermal radiation for atmospheric applications (https://earth.esa.int/web/guest/missions/esa-operational-eo-missions).

1.7 SCOPE OF THE RESEARCH WORK

The human activities are the major drivers leading to dynamic changes in land use and climate, which in turn made it complex to ascertain the hydrologic response, since the hydrologic components are distributed heterogeneously. In order to model the complex system many models have been developed which began with lumped conceptual and extended up to physically based distributed models. Among them, the physically based models are capable of representing the physical characteristics of watershed in an explicit way. In contrast, the semi-distributed and fully-distributed models are efficient in representing the spatial heterogeneity of the watershed. However, physically based models are data demanding and therefore necessitates the

development of simple methodology with limited availability of data to study the hydrologic response characteristics of a catchment.

As the earth's environment is undergoing rapid change, there is a necessity to analyse and predict the impact of plausible future changes in vegetation pattern and climate on hydrological response. Most of the previous studies have evaluated the impact of land use change on hydrologic response by considering catchments in a single climatic condition. However, it is equally important to analyse the variation in the hydrologic response in catchments with different land use characteristics and climatic conditions. Therefore, the catchment comparison studies mainly focus on seasonality and variability in hydrologic responses of different geo-climatic catchments.

1.8 STUDY OBJECTIVES

With the aim of analysing and evaluating the interaction between hydrologic response and the land use pattern in contrasting geo-climatic settings, the following objectives are formulated for this study:

1. To perform LU/LC classification and identifying the driving factors for LU/LC changes in two study catchments using multi date satellite images

2. To predict the future trends in LU/LC pattern using Land Change Modeler (LCM) and CA-Markov model and to validate them

3. To estimate Actual Evapotranspiration (AET) and Land Surface Temperature (LST) using satellite images

4. To explore the applicability of the semi distributed model to estimate stream flow in Netravati river basin

5. To explore the applicability of monthly rainfall-runoff polygon in explaining hydrological processes in contrasting catchments in humid and sub-humid catchments

6. To analyse the relationship between changes in hydrological response and LU/LC change pattern

1.9 STUDY AREAS

The study to accomplish the above-mentioned objectives is conducted in the following two catchments located in different hydro climatic regions of Karnataka State, India:

1. Netravati river basin (Humid climate)

2. Harangi catchment (Sub-humid climate)

1.9.1 Netravati river basin

The Netravati River originates at Bellaraya Durga in the Dakshina Kannada district and flows westward up to its confluence with the Arabian Sea. The study area geographically lies between 75^0 01' E and 75^0 46' E longitude and 12^0 29' N and 13^0 11' N latitude, and covers an area of 3288.3 km^2 (Figure 1.3 a). This river basin consists of many sub basins namely, Kumaradhara, Kallaji hole, Gowri hole, Belthangadi hole, Netravati hole, Neriya hole, and Shisla hole. The heavy rainfall in the area supports luxurious growth of vegetation. The upper portion of the basin covered with dense timber forest of evergreen trees with or without scrub, at varying growth stages from small trees to fully grown forest, lies in the Western Ghats. The southwest monsoon period is the coolest part of the year with the mean daily temperature below 20^0C. The mean daily temperature during the months March to May is 35^0C. The weather is highly humid all through the year and particularly, during the southwest monsoon when mean humidity exceeds 85%. The highest and lowest reliefs are formed at 1463 m and 3 m, respectively, above the mean sea level. The annual rainfall over the area varies between 1300 mm and 5700 mm. The mean annual rainfall is 3621.44 mm.
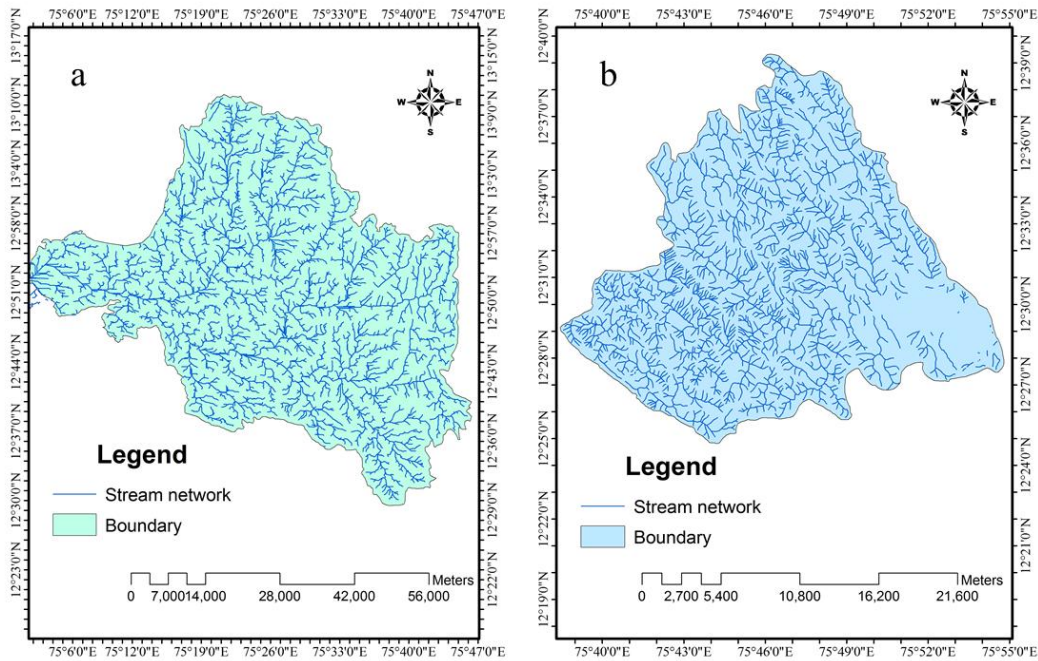
Figure 1.3 a) Netravati river basin and b) Harangi catchment

1.9.2 Harangi catchment

Harangi river is a major tributary of river Cauvery and has its origin in Pushpagiri Hills, Coorg District situated on its western part and separated from Bhagamandala (the source of Cauvery) by a high ridge. The study area geographically lies between 75^0 38' E and 75^0 55' E longitude and 12^0 24' N and 12^0 40' N latitude, with an area of 417.54 km^2 (Figure 1.3 b). Harangi catchment is blessed with bountiful rainfall in the upper reaches and has important tributaries like Madapura and Hotti hole. Heavy rainfall, steep valleys and absence of any storage reservoirs has led to the practice of irrigation in patches in some valleys mostly depending on rains during Southwest monsoon. The climate is characterized by high humidity and mild temperature. The temperature generally varies from 10^0 C to 12.8^0 C in December to about 32^0 C to 35^0 C in the summer months of April and May. The highest and lowest reliefs are formed at 1525 m and 884 m respectively above the mean sea level. The mean annual rainfall is 2332.59 mm.

1.10 ORGANIZATION OF THESIS

The thesis comprises of five chapters and list of references. A brief description of the each chapter is presented here.

Chapter 1 introduces the problem being considered for the study, describes the present state-of-the-art knowledge, scope of the research work, the objectives of the study and details of study areas.

Chapter 2 deals with the review of literature regarding: i) models to analyse LU/LC change, ii) the effect of LU/LC change on stream flow pattern and other hydrologic components such as infiltration, sub surface flow, and evapotranspiration, iii) model comparison and performance evaluation, iv) the importance of satellite based evapotranspiration estimation v) application of monthly rainfall-runoff polygons in explaining hydrological processes, ending with vi) closure.

Chapter 3 describes the detailed methodology adopted to accomplish the research objectives in two catchments namely, Netravati river basin (humid climate) and Harangi catchment (sub-humid climate) located in different hydroclimatic regions of Karnataka State, India.

Chapter 4 presents the results obtained from the study and the elaborative discussion on the results obtained.

Chapter 5 lists out conclusions from the study and discusses scope for future research on the topic.

2.1 GENERAL

Hydrological processes are complex in nature. Studying their complexity is the fundamental step in various hydrological applications such as flood prediction, hydro power estimation, sewer design, water supply network design and irrigation projects (Mishra et al. 2005; Warburton et al. 2012). The spatial and temporal variability of hydrological processes has its significant dependency on rainfall pattern, and physical and hydraulic properties of the watershed. Hydrological models provide a better understanding of outcome of processes by evaluating the response of watershed to various inputs such as rainfall, evapotranspiration and watershed properties etc., (Tong et al. 2012). Few studies have studied the applicability of numerical, lumped and semi distributed models in the prediction of stream flow, which is necessary to optimize water availability for various applications such as reservoirs and dams design and drinking water supply. Li et al. (2009); Choi and Deal (2008); Mao and Cherkauer (2009) assessed the effect of change in land use and landscape on hydrologic response of catchment and inferred that the spatial and temporal variability of land use pattern has significant influence on hydrological processes in the catchment. However, analyzing the LU/LC change and identifying the driving factors is very complex. Using multi-temporal land use information, numerous models have been proposed to explore the process of land use and land cover change (LUCC) (Niehoff et al. 2002; Jain and Chaudhry 2003; Zak et al. 2008; Yu et al. 2011).

Based on the previous studies, this chapter presents: i) a brief description of models used to analyse LU/LC change, ii) a review of available literature pertaining to the effect of LU/LC change on stream flow pattern and other hydrologic components such as infiltration, sub surface flow, and evapotranspiration, iii) a brief discussion on model comparison and performance evaluation, iv) importance of satellite based evapotranspiration estimation v) application of monthly rainfall-runoff polygons in explaining hydrological processes, ending with vi) closure.

2.2 DIFFERENT APPROACHES FOR DETECTION OF LAND USE AND LAND COVER CHANGES

LU/LC change is one among the prominent human interventions altering the earth's environment. The study of causes, processes and effects of LUCC is one of the important research topics of landscape ecology (Lee et al. 2008; Liu et al. 2009). Models that study land use change facilitate the analyse the causes and consequences of land use changes in order to better ascertain the functioning of the land use system and to help in land use planning and policy. Furthermore, models can be used for the exploration of future land use changes under different scenarios (Verburg et al. 2004). Modeling land-use change as a function of biophysical and socio-economic driving factors is one technique for unraveling the complex relationships in land-use change systems and provides insights into the extent and location of land-use change (Aspinall 2004).

Driving factors are the forces that cause changes in the land use over a period of time at a specific location. The driving factors form a complex system of dependencies, interactions, and feedback loops and they effect at several temporal and spatial levels. It is therefore difficult to analyze and represent them comprehensively. Due to the human–environment relationship, for ascertaining the process behind the change in landscape and its causes, it is necessary to study the interrelationship between human and nature (YueChen and ChunYang 2008). Evaluating the driving forces and forecasting future trend requires a thorough understanding of methods and critical interpretation of socio-economic and environmental data. The studies by Campbell et al. 2005; Liu et al. 2009; Yu et al. 2011; Wang et al. 2011 classified four types of driving factors such as economic, biophysical, institutional/policy and social/cultural which alter the land use pattern. The economic driving forces include market forces, trade policy and agreements, economic policy, land use policy, and land tenure policy. Biophysical factor includes rainfall, run-off, and topography. Institutional/policy driving forces include national and international policies to conserve biodiversity and natural climate. Social/cultural driving forces include urbanization, immigration, population dynamics, and cultural change. Usually the change in each land use type depends on neighboring land use type as well as

population growth and economic growth trend (Yu et al. 2011). According to Lin et al. (2009), the factors that drive land-use change in any watershed include the altitude, slope, distance from river, soil erosion, soil drainage, distance from major roads, distance from a built-up area and population density. Wang et al. (2011) considered natural and socio-economic driving factors to simulate the land use change dynamics. Natural factors are relatively stable and have cumulative effect on regional environment, whereas socio-economic factors are highly variable which have a direct relationship with the human activities. However, it is necessary to consider the different policies and scenarios to forecast future trend in land use change (Liu et al. 2009; Wang et al. 2011; Yu et al. 2011).

2.2.1 Sources of Data and Pre-processing

The study of the change in pattern of land use over a period of time and identification of driving factors requires spatial and non-spatial data. Hence, inputs to the land use change models are derived from variety of sources including remote sensing, field survey and other mappings. Many ecosystem processes are difficult to monitor directly. The remote sensing data is one of the efficient sources which can provide spatial and temporal data (Liu et al. 2009). Land use change takes place in any spatio-temporal manner. Identification of causes for change involves the collection of precise and valid data comprising spatial and non-spatial information (Jing-an et al. 2006). Satellite data is available at various resolutions ranging from coarser resolution (MSS-79m, TM-30m, LISS III-23.5m) to finer resolution (LISS IV-5.8m, Cartosat I-2.5m and Cartosat II-less than 1m). Different resolution satellite images are used in some applications in order to compensate the inconsistency in data (Yu et al. 2011). Generally raw satellite images do not have spatial reference and sometimes radiometric errors will be induced. Hence, the images will have to be geometrically corrected and geocoded to the respective coordinate system (eg. Transverse Mercator coordinate system, Geographic Coordinate System etc.,) using topographic maps. More than 50 Ground Control Points (GCPs) are necessary to accomplish geo-referencing process (Liu et al. 2009; Yu et al. 2011).

Non-spatial data has been collected through historic data statistics and field survey. As these data are collected manually, errors and gaps will be induced which

reduces the data consistency and reliability (Jing-an et al. 2006). Due to the developmental activities in the area, there may be a change in administrative boundary. Hence, the social and economical data collected for a period is inconsistent. The interpolation techniques have been used to create spatially and temporally consistent data (Yu et al. 2011). The integration of remote sensing data with non spatial data is necessary to model the land use change and also to study the impacts of socio-economic, natural, and cultural factors.

2.2.2 Modeling the Land Use Change Dynamics

The land use change models can be broadly categorized as spatially explicit and aspatial models. In contrast to spatial optimization models, empirical–statistical models have been developed to identify the factors that influence land-use changes, and predict future land-use change patterns upon changes in driving factors as specified in scenarios. CLUE-S (Conversion of Land Use and its Effects at a Small regional extent) model is one of the well known examples of empirical–statistical models (Lin et al. 2009; Verburg et al. 2006). Many geographers and economists have analysed and predicted the location of LUCCs using empirical-statistical models (Verburg et al. 1999; Veldkamp et al. 2001; Yu et al. 2011; Lin et al. 2008), and rule based models especially cellular automata (YueChen and ChunYang 2008). The selection of models also depends on type of influencing factors: spatial and non-spatial factors. Many existing models are incapable of handling both spatial and non-spatial factors in the process of modeling the land use change (Lin et al. 2008; Verburg et al. 2006). Among spatial and aspatial models, Yu et al. (2011) have emphasized only on aspatial model for two reasons: first is that for ascertaining the process of land conversion, it is sufficient to determine the quantity and rate of LUCC but not their spatial location. Second, the LUCC process is very complex as it depends upon several driving factors and choice of a particular land depends on the interest of users. And so, it is difficult to develop a rule based spatially explicit model to predict the future location of LUCC.

It is true that all existing simulation models are not capable of taking the complexity of both macro-driving factors and micro spatial pattern in LUCC (Verburg el al. 2006; Lin et al. 2008; Yu et al. 2011; Changhong et al. 2011). There are mainly

two types of Dynamics model: top-down dynamics model and bottom-up dynamics model. The top-down model handles the macro drivers, whereas bottom-up model reflects the micro spatial pattern. System Dynamics model (SD) and Artificial Neural Network (ANN) come under top-down model, Cellular Automata (CA) model is a representative type of bottom-up approach (YueChen and ChunYang 2008; Yu et al. 2011). SD describes the interrelationship between the rate of change of input variables and different land use types (YueChen and ChunYang 2008; Zheng et al. 2012). ANN is based on the principle of neural system and uses nonlinear functions. Therefore it is capable of modeling nonlinear complex systems such as land use and land cover change. Usually ANN was extensively used in classification applications. Also, with the advancement in research, ANN is gradually applied to simulation studies, as it can model nonlinear complexities (YueChen and ChunYang 2008). CA model is designed to simulate the complicate relationship among the micro spatial pattern of land use change. Hence, bottom-up approach is an efficient method to study the complexity in the spatial automatic changes (YueChen and ChunYang 2008; Wang et al. 2011). Wang et al. (2011) utilized the advantages of both top-down and bottom-up approaches by integrating three models such as SD model, ANN and CA. The integrated models are thus capable of analyzing both macro driving factors and micro spatial pattern change.

Verburg et al. (1999) had taken up a study to assess the short term LUCC and its ecological consequences using CLUE-S model. In the CLUE-S model, specific land use conversion elasticity has been assigned to each land use type based on expert knowledge and observed behavior in the recent past (Verburg et al. 2001; Lin et al. 2008; Liu et al. 2009; Zheng et al. 2012). CLUE-S is suitable for spatially explicit and multi-scale simulation of land use change under certain assumptions of possible future developments, defined as scenarios. However, the CLUE-S model is not meant for predictions, but rather gives possible spatial outcomes of feasible land use developments (Verburg et al. 1999). SD model is suitable for studying the dynamic behavior of complex system over a period of time. However, it could not express the dynamics on a spatial scale. SD model can express 'when' and 'how much' change has taken place, whereas CLUE-S model can answer 'where' the change has been occurred. To bridge the gap between temporal land demand and spatial supply, Zheng

et al. (2012) have coupled SD and CLUE-S models to simulate future landscape pattern.

In a number of models, temporal dynamics are taken into account using initial land use as a criterion for the resultant changes. The MameLuke settlement model aims at modeling the dynamics between demography and ethnic identity in a spatially and temporally explicit way. This model allows for stakeholder integration in formulating rules based on real actions (Huigen 2004). In addition, Cellular automata do this explicitly by using decision rules that determine the conversion probability (Hong et al. 2011). Zak et al. (2008) suggested that no single factor is capable of bringing change in land use and highlighted the importance of considering the nonlinear effects of combining climatic, socio economic and technology based factors. In contrast to spatial optimization models, empirical-statistical models such as equation based models (EBMs) have been designed to predict the future trend in the pattern of land use based on specified scenarios (Lin et al. 2008). One deficiency in EBMs is that they cannot deal with non-mechanistic, nonlinear variation of the variables and their relationships. A multi actor modeling (MAM) based on agent based modeling (ABM) framework has been used to overcome the difficulties in EBM. ABM is a conceptual model that has rules (agents) (Ralha et al. 2013).

2.3 HYDROLOGICAL MODELS

Hydrological processes at the catchment scale are not stationary as the changes taking place in the catchment are highly variable in nature (Mauser and Bach, 2009; Cornelissen et al. 2013). Various models are available to solve the hydrological problems. Rainfall-Runoff (RR) prediction is one of the most complicated processes in environmental modeling. This is due to the spatial and temporal variability of topographical characteristics, rainfall patterns, and the number of parameters to be derived during the calibration (Nandakumar and Mein 1997).

2.3.1 Functionality and Complexity of Models

While choosing a model for specific application, it is important to consider its applicability to simulate the impact of land use and climate change and also prediction performance (Schreider et al. 2002; Ty et al. 2012; Abushandi and Merkel 2013). The

functionality and complexity of the models are the major criteria in model selection. The functionality of a model depends on the hydrologic process representation, the equations adopted to simulate these processes and model discretization (Xu and Singh, 1998; Hogue et al. 2006). Whereas, complexity of a model comprises of estimated data, resources, time and cost that are required to parameterize and calibrate a model, as well as the professional judgment and experience required to operate these models (Verma et al. 2010; Shen and Phanikumar 2010).

The descriptions of several widely-used hydrological models are provided in Table 2.1. These models can simulate hydrologic processes such as, i) Soil-Vegetation-Atmosphere Transfer (SVAT) processes: canopy rain interception and evaporation, stem flow, canopy snow interception, snowmelt, vegetation transpiration and soil evaporation; ii) Soil moisture storage and runoff generation processes: infiltration, depression storage, subsurface runoff, Horton (infiltration excess) overland flow; iii) channel routing; and iv) other processes: groundwater flow, glacier melt, lakes, wetlands (Post and Jones 2001; Thanapakpawin et al. 2006; Jiang et al. 2007). The equations adopted to simulate these processes vary between models. Empirical approaches are based on experimentally derived simple relationships such as linear regressions. Empirical methods for calculating evaporation include radiation-based equations (e.g., Priestley-Taylor) (Wu and Johnston 2007) and snow melt phenomena using degree-day method, whereby the rate of melting increases as the air temperature increases (Wijesekara et al. 2012). Whereas, the analytical model use simplified assumptions to derive solutions for the governing equations for conservation of mass, momentum, and/or energy. Examples include the Green-Ampt equation, which describes the infiltration of rainfall or snowmelt into the subsurface (Li et al. 2009). In physically-based models, mass transfer, momentum and energy are simulated using partial differential equations which are solved by various numerical methods such as the Saint-Venant equations for surface flow (Kim et al. 2012), the Richards equation for unsaturated zone flow (Elfert and Bormann 2010), and the Penman-Monteith equation for evapotranspiration which is recommended for calculating reference evapotranspiration by the Food and Agricultural Organization (FAO) (Mackay 2001; Wu and Johnston 2007; Mao and Cherkauer 2009; Cornelissen et al. 2013). In contrast to empirical and analytical models, the physically based

models are characterized by higher intrinsic accuracy for predicting the effect of land use disturbances or climate change. However, these models are quite data intensive (Shen and Phanikumar 2010).

The functionality of a model also depends on the model's ability to spatially discretize the watershed based on soil and vegetation (Wooldridge et al. 2001; He and Hogue 2012). The purpose of discretizing a watershed into different units is to account for the spatial variability and pathways of water movement and to describe geologic and land cover variability and the effects of slope and aspect on hydrologic response (Wu and Johnston 2007; Chien et al. 2013). Apart from spatial discretization, the time step at which model simulations are performed (i.e., temporal discretization) is also important. Some models can only run at a specific time interval (e.g., sub-daily, daily or monthly). Time discretization may affect the ability of a model to predict the output. In addition, temporal discretization has important implications such as data availability and preparation (model complexity) (Chien et al. 2013).

The complexity of a model is equally important while evaluating the ability of the models to simulate the desired land use and climate change scenarios. In many applications, modelers face data scarcity problems which lead to the selection of low complexity lumped and/or conceptual models. However, when more detailed results are needed, a fully distributed and/or physically based approach would be required and it may be necessary to collect the various data to run the model (Elfert and Bormann 2010). The low-complexity models are typically characterized by modest requirements regarding meteorological data (e.g., monthly temperature and precipitation data) and low input data requirements, whilst the medium-complexity models involve higher requirement of meteorological data (e.g., daily temperature and precipitation data) and medium model input requirements. The highly-complex models, on the other hand require more frequent meteorological data (e.g., hourly to daily temperature and precipitation data) and very high model input requirements (Chien et al. 2013; Niu and Sivakumar 2013). The set of models presented in Table 1 are of high complexity, since these models require minimum 5 to 10 years of input datasets for the calibration and validation. These models require more simulation time

period, because of semi-distributed or distributed based watershed discretization. For example, HEC-HMS model performs continuous simulation based on soil moisture and linear reservoir volume accounting model, which requires 10-12 model parameters to represent surface and sub-surface hydrological processes. This requires more number of input data to estimate these parameters, which makes the model complex (Verma et al. 2010).

Table 2.1 Popular Hydrologic models and methods of computing their inputs

Model	Main components	Evapo-transpiration	Overland flow	Subsurface flow	Spatial scale
HEC-HMS [Verma et al. 2010]	Precipitation, Losses, Baseflow, Runoff transformation and Routing	Priestley-Taylor	CN, kinematic wave Equations, Soil Moisture Accounting Model	Linear reservoir volume accounting model, Exponential recession model	Semi-distributed
MIKE SHE [Wijesekara et al. 2012]	Interception, Overland/ Channel flow, Unsaturated/ Saturated zone, Snowmelt; Aquifer/ rivers exchange, Advection/dispersion of solutes, Plant growth, soil erosion and irrigation	Based on canopy storage and soil evaporation	2-D diffusive wave equations (St. Venant equations)	3-D groundwater flow (Green Ampt infiltration Method)	Distributed
SWAT [Wu and Johnston, 2007]	Hydrology, Weather, Sedimentation, Soil temperature and	Penman–Monteith, Hargreaves, Priestley-Taylor	CN method	Lateral subsurface flow/	Semi-distributed

				ground flow (Green and Ampt Equation)	
	properties, Crop growth, Nutrients, Pesticides, Agricultural management and Channel and Reservoir routing				
WaSiM [Elfert and Bormann, 2010]	Evapotranspiration, Soil module, Infiltration, Overland flow, Interflow, Base flow Routing	Penman–Monteith	Horton overland flow	Green and Ampt Equation	Distributed
DHSVM [Thanapakpawin et al. 2006]	Surface and subsurface flow, Soil moisture, Snow cover, Runoff and Evapotranspiration	Penman–Monteith equation	Saturation excess and infiltration excess mechanisms	Saturated subsurface flow	Distributed
Variable Infiltration Capacity (VIC) model [Mao and Cherkauer, 2009]	Infiltration, Runoff, Baseflow processes, Evapotranspiration.	Penman–Monteith equation	Soil property based surface flow simulation	Variable infiltration capacity curve	Distributed

PAWS [Shen and Phanikumar, 2010]	Overland flow, Snowpack, Soil moisture, Groundwater flow and Stream flow	Penman Monteith + Root extraction	Manning's formula + Kinematic wave formulation + Coupled to Richards equation	Green and Ampt equation	Distributed

2.3.2 Application of Hydrologic Models to Study the Impact of LUCC

The water and energy balances are significantly influenced by land cover pattern via its effect on transpiration, interception, evaporation and infiltration (Ozturk et al. 2013; Nandakumar and Mein 1997; Mao and Cherkauer 2009; Delgado et al. 2010). The transformation of earth's land surface has many consequences for biophysical and ecological system in terms of urban heat islands, alteration in stream flow pattern, global atmospheric circulation and extinction of living species (Schreider et al. 2002; Yu et al. 2011). The rapid increase in population has led to change in land use in terms of deforestation aimed at improving agricultural production (Lorup et al. 1998). In a number of semi-arid regions, this has resulted in land degradation due to soil erosion, reduced productivity and drought (Ondieki 1997; Lorup et al. 1998; Legesse 2003; He and Hogue 2012). In the upper Midwestern United States, the hydrology is effected by human activities through conversion of forest and prairie grasslands to agricultural lands (Mao and Cherkauer 2009). Jing and Ross (2015) assessed the possible relationship between LUCC and streamflow due to mining activities by using Hydrological Simulation Program—Fortran (HSPF) model. The study showed that the mining affected basins experienced tremendous increase in streamflow; necessitating reclamation schemes to improve the hydrological condition of the basin.

The heterogeneous distribution of various hydrologic components made it difficult to study the hydrologic response to changes (Siriwardena et al. 2006; Delgado et al. 2010; Niu and Sivakumar 2013). In recent years, many researchers have investigated the relationship between land use change and hydrologic response in catchments (Ozturk et al. 2013; Nandakumar and Mein 1997; Mao and Cherkauer 2009; Ondieki 1996; Lorup et al. 1998; Legesse et al. 2003; He and Hogue 2012; Niel et al. 2003; Isik et al. 2013). The methods used are lumped, distributed, conceptual or physical models. Lorup et al. (1998) have combined a statistical method with hydrological modeling i.e., Nedbor-Afstromnings Model (NAM), a lumped conceptual model in order to distinguish between the effects of climate variability and LULC change on runoff through studying six semi-arid catchments. As model gave reasonably good performance, the difference between simulated and observed flow

was considered to be a key test variable to assess the impact of land use change on catchment runoff.

While analyzing the effect of vegetation pattern, one should consider not only the percentage of different land use categories, but also the variation in the characteristics of specific land use class, e.g., type of crop and other management aspects (Lorup et al. 1998; Warburton et al. 2012). Thanapakpawin et al. (2006) utilized the Distributed Hydrology-Soil Vegetation Model (DHSVM), a spatially explicit landscape/hydrology model that considers spatial heterogeneity of the watershed to simulate forest-crop expansion and crop to forest reverse expansion scenario based on land use transition during the period 1989-2000. They found that the expansion of crop fields in high land zone led to slightly higher annual and wet season water yields compared to similar expansion in lowland- midland zone.

A better knowledge of basin hydrology and the relationship between land use change and relative variation in ET, baseflow and surface runoff generation and associated water distribution will be helpful to watershed planners and decision makers (Thanapakpawin et al. 2006; Tang et al. 2011; Wang et al. 2012). Assessment of the rainfall-runoff relationship is vital in modeling and designing urban drainage (Laouacheria and Mansouri 2015). Numerical models such as regression, ANN, fuzzy and GA are data driven models which are not capable of modeling spatially explicit relationship of hydrologic response with respect to physical characteristics of the basin. In contrast, process based distributed models have the potential to quantify and forecast the dynamics of water availability with land use and climate change (Haigen et al. 2015). However, these models are data intensive and not applicable to catchments with sparse datasets (Thanapakpawin et al. 2006; Elfert and Bormann 2010; Lin et al. 2008). Lorup et al. (1998) first used a hydrological model for predicting the effect of land use change on runoff but faced lack of data to validate the results. Thanapakpawin et al. (2006) adopted the Diurnal interpolation scheme using Variable Infiltration Capacity (VIC) model and to obtain the required data, sub-divided the daily records into three-hourly temperature, radiation and relative humidity.

28

Clearance of tropical forest land is known to lead to increase in the annual runoff. Costa et al. (2003) studied the relationship between precipitation, discharge, ET and LULC change in a large catchment (175360 sq. km) considering 50 years data using statistical analysis. Their study revealed that the conversion of forest land to grass land leads to reduction in ET value and an associated increase in runoff. The change of hydrologic response of a catchment due to land use change will be influenced by the intensity of conversion of natural vegetation and location of the change. The interaction of land use and hydrologic processes exhibits spatial and temporal variation, as fluxes of water within a catchment vary vertically and laterally.

Niehoff et al. (2002) investigated the impact of changes of land surface condition on storm-runoff generation from three catchments with different land use patterns. Later, Warburton et al. (2012) studied the difference in hydrological response in three South African catchments with different vegetation covers using the conceptual and physical, Agricultural Catchments Research Unit (ACRU) model. To analyse the influence of heterogeneity associated with the vegetation cover on stream flow patterns, three different catchments were selected. Results showed that the stream flow generated was not proportional to the relative area of that land use. The location of a specific land use within a catchment has a role in the response of the stream-flow from the catchment.

2.3.3 Scenario based Simulation of Hydrological Response in a Catchment

It is of interest to simulate the effect of possible changes in climate variables and land use that may occur in the near-future by considering scenario conditions. Climate change has its direct influence on runoff which is one of the major components of hydrological cycle (Huang et al. 2015). Westmacott and Burn (1997) used the Mann-Kendall trend test and a regionalization procedure to quantify the severity of climatic effects within the river basin, which is helpful to increase awareness of future consequences for water resource systems planning and management strategies. Results indicate that the timing of a hydrologic event was influenced to a greater extent due to changes in temperature. Legesse et al. (2003) assessed the sensitivity of water resources to land use change as well as climatic variability in a semi-arid to sub-humid basin. Results show that the physically based semi-distributed model is

capable of representing the dynamics of the hydrograph at monthly scale better than at the daily scale. The climate scenario study revealed that the hydrologic system seems to be more reactive to an increase in rainfall than to a decrease in rainfall. Also, the system response depends not only on the quantity but also on the quality of rainfall and the number of rainy days. This requires the model to run at less than a day interval, which is very much data intensive.

Li et al. (2009); Ozturk et al. (2013) observed that the influence of climatic variability is more significant on surface hydrology than land use change. The impact of change in temperature is difficult to assess clearly because the temperature fluctuation will have its own effect on other hydro-meteorological variables also (Legesse et al. 2003). Huang et al. (2015) simulated the runoff of the upstream of Minjiang River for nine climate change scenarios by varying precipitation, temperature and potential evapotranspiration. The study inferred that precipitation variation has more influence on simulated runoff than the temperature variation. The upstream of Minjiang River is located in alpine-cold region, which is a plateau climate and subtropical climate region. In the study area, the rainfall drops from Songpan, Heishui to Mao, Wenchuan county, and increases from Wenchuan to downstream of Dujiangyan. The daily maximum precipitation is more than 200 mm, and annual average evaporation is 600–800 mm.

Simulating the hydrologic response of a catchment to different scenario conditions involves calibrating and validating the model using present conditions and running the model with parameters for newly framed scenarios and comparing the results (Legesse et al. 2003; Siriwardena et al. 2006; Elfert and Bormann 2010; Li et al. 2009; Isik et al. 2013; Niu and Sivakumar 2013). Model calibration is a process of manual/automatic adjustment of model parameters to match between predicted and observed values based on objective functions. Normally, physically based models such as PRMS, SWAT etc., involves large number of model parameters making the models complex. However, sensitivity analysis can suggest as to which parameter is more sensitive than others in predicting simulation results. Model validation is a process of evaluating the ability of model to simulate the hydrological components of a catchment by calibrated model parameters for different conditions than calibration

period. Therefore, model simulation period is divided into two different sets; calibration and validation data set (Legesse et al. 2003). Siriwardena et al. (2006) formulated calibration strategies based on time step (monthly and annually) and exponent 'c' of objective function (0.5 and 1.0). It is observed that slightly better results were obtained by calibrating the model using these strategies. Elfert and Bormann (2010) have done manual calibration of WaSiM-ETH by comparing predicted result with observed values for a period of 10 years data set. Initial two years of data was used as warm-up period to reduce the effect of model's initial conditions on the output. WaSiM-ETH model was calibrated and validated by considering three quality measures namely mean absolute water balance error, coefficient of determination and model efficiency. In the physically based spatially distributed model, the temporal aggregation of fluxes as well as increased spatial scale resulted in improvement of model efficiency (Elfert and Bormann 2010).

In order to study the effect of future LU/LC patterns on hydrological systems, researchers formulated various scenarios, which are as shown in Table 2.2. The agricultural scenarios based on Special Report on Emissions Scenarios (SRES) of International Panel on Climate Change (IPCC) and also national policy measures were implemented to observe the variations in hydrologic components. Mainly, conversion of agricultural land to urban, forest land and grassland was considered for the analysis (Wu and Johnston 2007; Niu and Sivakumar 2013). Scenario-based studies imply that even a validated catchment model might not be able to simulate significant changes in the water flows when large parts of the catchment of interest are affected by an extreme land use change (Legesse et al. 2003). According to Mao and Cherkauer (2009), forests have the lowest total spring runoff, which is mainly due to higher annual ET that keeps soil moisture levels low, leading to increased infiltration. However, grassland, woodland and cropland have higher total spring runoffs because of their lower ET losses and more rapid loss of winter snow cover. In addition, the scenarios based on land use policy and urban development provide opportunity to take valid decisions in selecting land use policies that can reduce natural hazard (McColl and Aggett 2007; He and Hogue 2012). Generally scenario based studies do not try to reconstruct the vegetation history but only attempt to

propose the possible and plausible scenarios for studying the potential impact on hydrology.

With advances in research, many hydrological models are integrated with land use change models. The spatial pattern optimization model (OLPSIM) and Conversion of Land Use and its Effects at a Small regional extent (CLUE-s) model were integrated with a hydrologic model, Hydrologic Engineering Center's Hydrologic Modeling System (HEC-HMS) based on Soil Conservation Service Curve Number (SCS-CN) (Nagaraj and Yaragal 2008) approach to investigate the impact of more realistic developmental scenarios on watershed by considering driving factors (Lin et al. 2009). More recently, Sahua et al. (2012) compared the performance of four modified SCS-CN methods in computing surface runoff in two catchments in Maharashtra State, India. Their study mentioned that in spite of the much larger catchment area of the Kalu watershed compared with those of the U.S. watersheds, used for developing the SCS-CN model, all the four modified SCS-CN-based models performed reasonably well. Wijesekara et al. (2012) tried to assess the impact of potential land use changes over next 20 years on the hydrologic processes by combining the Cellular Automata (CA) model and MIKE-SHE/MIKE11 hydrologic model. The results showed that there was a reduction of net capacity of water retention on surface due to the expansion of built-up and agricultural area which has led to an increase in surface runoff caused by reduction in infiltration.

Table 2.2 Land use and land cover change scenarios

Serial No.	Author(s) Name	Scenario Details
1	Thanapakpawin et al. (2006)	1. Reversal of all croplands back to evergreen needleleaf forests (above 1000 MSL) and to deciduous broadleaf forests (below 1000 MSL) 2. Doubling the cropland area by adding new crop cells 3. Doubling of cropland that is limited to either highland zones or lowland 4. Doubling of cropland that is limited to midland basin zones
2	Choi and Deal (2008)	1. Base economic growth (current population) 2. High economic growth (125% weight to population projection)

		3. Uber economic growth (150% weight to population projection)
3	Elfert and Bormann (2010)	1. Change from agricultural land into forest 2. Change from agricultural land into urban area 3. Change from agricultural land into forest and urban area in equal parts
4	Wijesekara et al. (2012)	1. Evergreen to Agriculture/Built-up 2. Deciduous to Agriculture/Built-up 3. Agriculture to Built-up/Rangeland/parkland 4. Rangeland/parkland to Built-up/Agriculture
5	He and Hogue (2012)	1. Scenario 1: Current development 2. Scenario 2: Doubles scenario 1 3. Scenario 3: Doubles scenario 2 4. Scenario 4: Triples scenario 2
6	Cornelissen et al. (2013)	LU1 scenario: 1. Economic growth 2. Improved political and socio-economic situation 3. Innovations in agricultural sector 4. Expansion of cultivated areas by 15% LU2 scenario: 1. Economic stagnation 2. Protected forests are not controlled 3. No new technology that enhance production 4. Expansion of cultivated areas by 30% LU3 scenario 1. Business as usual 2. Productivity does not increase 3. Expansion of cultivated areas by 20%

In recent times, Global Circulation Models (GCMs) and Regional Climate Models (RCMs) models are being used to generate estimates for future changes in climate. GCMs are efficient in studying the future changes in climate. GCMs have high temporal resolution with low spatial resolution. It is essential to downscale GCM results to regional climate variable. Downscaling is a process of developing the relationship between large scale variables and small scale variables to represent the local climatic conditions (Wibig et al. 2015; Ribalaygua et al. 2013). Despite the ongoing development in GCMs and RCMs, uncertainty exists on the magnitude of the changes in temperature, precipitation, Green house gases, aerosols etc., (Merritt et al. 2006; Ghosh and Misra 2010). These global and regional models are less reliable in simulating detailed spatial and temporal features. Given the difficulties in deducing future climatic trends by using GCMs and RCMs, Tong et al. (2012) preferred to use

a range of hypothetical climate scenarios. Wang et al. (2015) considered hypothetical scenarios and inferred that, streamflows are highly correlated to precipitation, while weakly correlated to temperature under humid climatic conditions. Soil moisture and actual evaporation are likely to vary with temperature. The integration of models provided a comprehensive picture of the watershed by incorporating the dominant land use transitions and their impact on the land phase of the hydrologic processes. This is an improvement over the use of a single scenario such as an increase in deforestation or afforestation (Niehoff et al. 2002; Tong et al. 2012; Wijesekara et al. 2012; Ozturk et al. 2013).

2.3.4 Model Comparison and Performance Evaluation

Comparison of models enables the identification of possible sources of uncertainty in hydrologic modeling and forms a basis for investigation of the effects of different model structures on model prediction (Jiang et al. 2007; Viney et al. 2009; Cornelissen et al. 2013). If hydrological models are applied within a single study, model calibration often results in reliable simulation of the past. However, the influence of model choice and model calibration on the simulation of climate and land use change impacts remains unclear, even if uncertainties and climate are considered (Kumar et al. 2013). The different model structures capture different aspects of the catchment response and, therefore, more aspects of the catchment response are captured in the combined model (Butts et al. 2004). Breuer et al. (2009) have applied 10 lumped, semi-lumped and fully distributed hydrological models to analyse their performance in scenario based runoff prediction. Depending on the spatial support and the associated data aggregation and interpolation, models deal differently with model input, which leads to differences in model output. They achieved a better comparison of model results by homogenizing important model input data such as precipitation, temperature and Leaf Area Index (LAI). However, forcing model to use comparable model inputs can help to avoid drawing wrong conclusions with respect to the effects of model structure (Huisman et al. 2009). This implies that during the selection of models to study the effect of model structure and functionality on the output, it is necessary to consider the consistency among selected model inputs and time steps. Also, when the aim is to tackle different aspects in single modeling

framework, it is more appropriate to integrate two or more models with different functionalities.

Butts et al. (2004) developed a modeling framework that permits changes in the model structure, including both conceptual and physically based process descriptions, to be considered within the same modeling tool. Their results showed that the model performance was quite sensitive to model structure. Also, the distributed routing and distributed rainfall information increase the simulation accuracy and predictive capability of the model. The sensitivity of stream flow simulations to variations in acceptable model structure was as large as uncertainties arising from parametric and measurement uncertainty, but the model simulations appeared to be less sensitive to rainfall uncertainty. Biondi et al. (2010) utilized a precipitation-dependent Hydrologic Uncertainty Processor (HUP) for assessing the hydrologic uncertainty in predicting actual stream flow based on precipitation quantity. Their study found that hydrologic uncertainty grows with the value of discharge predicted by the model and that it is higher when associated with higher precipitation values.

Singh et al. (2013) used SWAT CUP software to describe and demonstrate the use of different approaches such as the Sequential Uncertainty domain parameter Fitting (SUFI-2), Generalized Likelihood Uncertainty Equation (GLUE) for stream-flow measurement and best parameter estimation for stabilizing the correlation between the simulated parameters and observed parameters. Laouacheria and Mansouri (2015) used Watershed Bounded Network Model (WBNM) and Hydrologic Engineering Center-Hydrologic Modeling System (HEC-HMS) hydrological models to predict the runoff hydrographs of urban catchments and also evaluated the effect of parameters on the shape of the runoff hydrograph. It was inferred that, catchment size did not affect the routing calculations but it had a direct influence on the unit hydrograph.

Cornelissen et al. (2013) studied four models (WaSiM, SWAT, UHP-HRU and GR4J) that vary in complexity, spatial resolution, and process representation to compare the effects caused by different models to improve the assessment of hydrological processes and to study the influence of land use and climate change on

discharge. The variation between simulation qualities of the models can be attributed to uncertainty in input data, calibration strategy, parameterization and difference in model structure (Huisman et al. 2009; Breuer et al. 2009; Cornelissen et al. 2013).

Laouacheria and Mansouri (2015) inferred that CN and lag time were more sensitive in estimating peak discharge by HEC-HMS model, where as in the case of WBNM model, initial loss and lag parameter were more sensitive. An analysis of ensemble model predictions shows that the best ensembles are not necessarily those containing the best individual models. Conversely, it appears that some models that predict well individually do not necessarily perform well when combined with other models (Viney et al. 2009). Bormann et al. (2009) investigated the impact of data resolution of land use information on simulated water balances for current catchment conditions and land use scenarios, and found that spatially distributed models are more suitable when compared to lumped models to analyse the effects of the patterns of land use change.

To evaluate model performance, researchers used many performance measures comprising a combination of numerical measures and graphical plots. Lorup et al. (1998) used Nash-Sutcliffe efficiency (Figure 2.1A, B, E and F), error index, and model efficiency (Figure 2.1C) (Ozturk et al. 2013; Mao and Cherkauer 2009; Elfert and Bormann 2010; Thanapakpawin et al. 2006; He and Hogue 2012; Li et al. 2009) and joint plots of the simulated and observed hydrographs, scatter plots and flow duration curves to test the model performance. If Nash-Sutcliffe coefficient is zero, which indicates that model's prediction is no better than using the mean of the observed values (Choi and Deal 2008; Ozturk et al. 2013).

Different criteria assess the performance in different ways. The coefficient of efficiency (Figure 2.1E) (Siriwardena et al. 2006; McColl and Aggett 2007; Jiang et al. 2007; Bormann et al. 2009) was used to assess the goodness of fit, whereas the bias (He and Hogue 2012) and absolute percentage bias (Thanapakpawin et al. 2006; Breuer et al. 2009; Bormann et al. 2009; Li et al. 2009) were used to compare the simulated with observed long term water balance. Root Mean Square Error (RMSE) and relative RMSE (Niu and Sivakumar 2013) compare measured and simulated data (Thanapakpawin et al. 2006; Jiang et al. 2007; Li et al. 2009; Breuer et al. 2009).

Thanapakpawin et al. (2006) used Relative Efficiency (E_{rel}), a modified form of Nash-Sutcliffe efficiency because E_{rel} is more sensitive to over or under estimation in model prediction, as it is based on relative deviation. (Figure 2.1D). Bormann et al. (2009) introduced a criterion called 'scenario effect', which is defined as the difference in long-term water flow between simulations of the current state and future scenario conditions. The performance of six well-known models in estimation of runoff is shown in Table 2.3, whilst a graphical representation is presented in Figure 2.1.

Table 2.3 The performance of different models in estimating the runoff

Serial No.	Model Name	Correlation Coefficient	Efficiency	Reference Figure
1	MIKE-SHE (Ozturk et al. 2013)	0.72	0.52 (Nash-Sutcliff)	Figure 2.1A
2	VIC (Mao and Cherkauer 2009)	0.91 (Index of agreement, d)	0.74 (Nash-Sutcliff)	Figure 2.1B
3	WaSiM-ETH (Elfert and Bormann 2010)	0.83 (Coefficient of determination)	0.81 (Model efficiency)	Figure 2.1C
4	DHSVM (Thanapakpawin et al. 2006)	--	0.74 (Relative efficiency)	Figure 2.1D
5	HSPF (He and Hogue 2012)	0.87	0.72 (Nash-Sutcliff)	Figure 2.1E
6	SWAT (Li et al. 2009)	--	0.53 (Nash-Sutcliff)	Figure 2.1F

A

B

E: Coefficient of efficiency, d: Index of Agreement

C

R^2: Coefficient of determination, ME: Model Efficiency

D

E

NSE : Nash Sutcliffe Efficiency

F
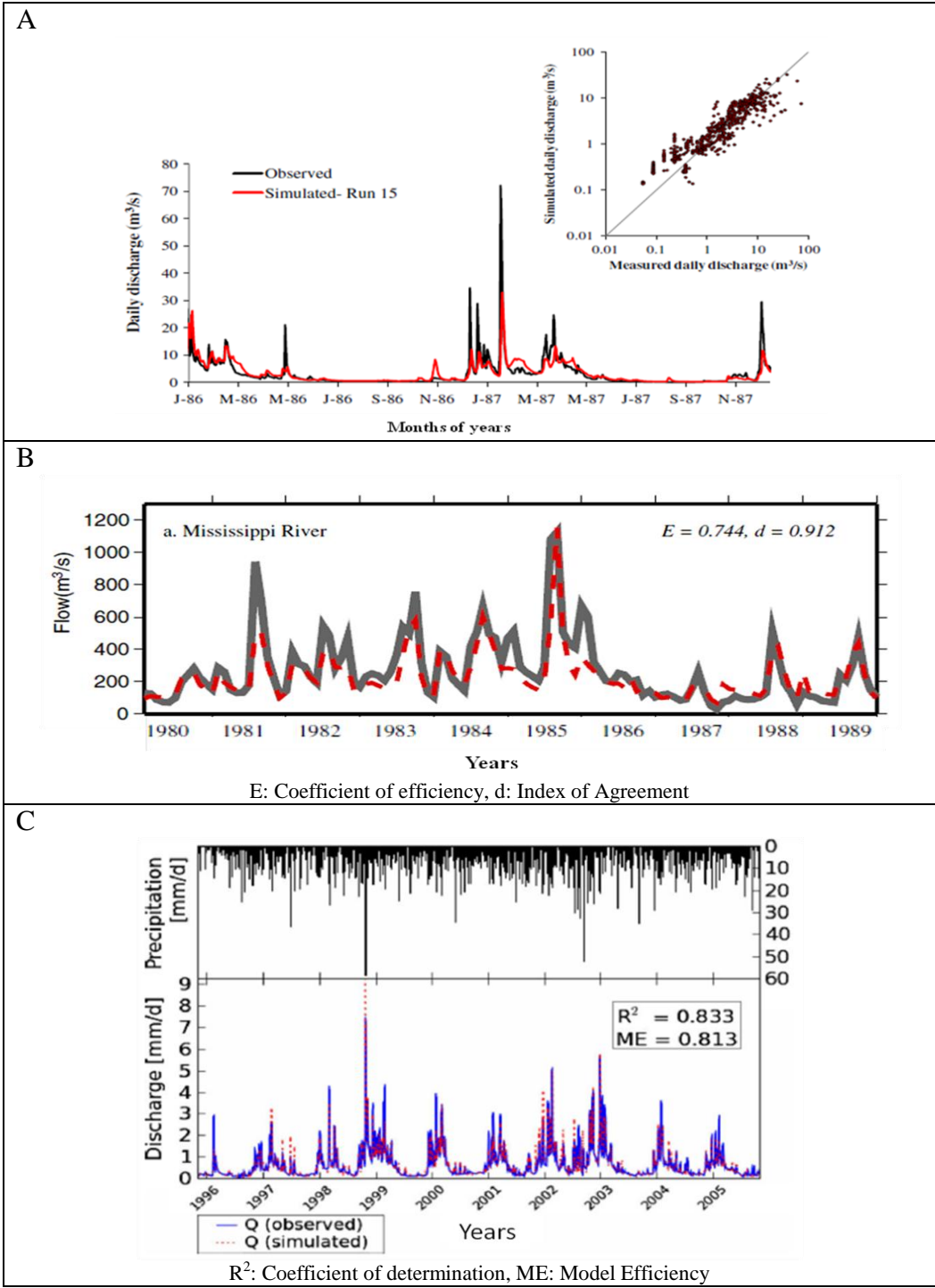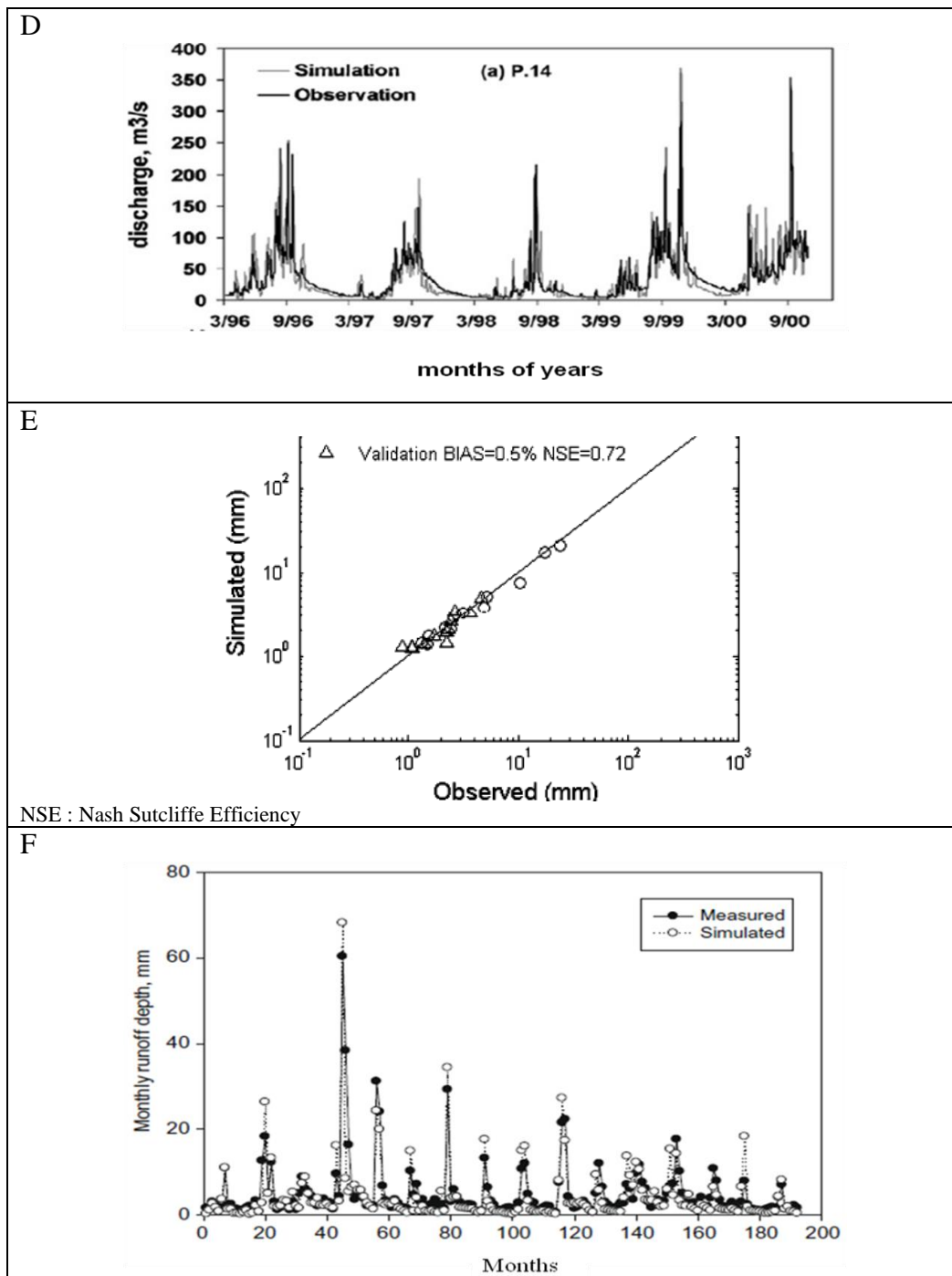
Figure 2.1 Graphical representation of performance of the six models

2.4 SATELLITE BASED EVAPOTRANSPIRATION ESTIMATION

Evapotranspiration (ET) is one of the major sources of water loss in the water balance system of any river basin. Its accurate estimation is essential to analyse hydrological, climatic and ecosystem processes (Liou and Kar 2014). The estimation of ET is essential for agricultural water management, crop yield modeling, draught monitoring

and hydrological and climatic studies (Ambsat et al. 2008). The process of ET is greatly influenced by spatio-temporal pattern of vegetation. Development of models to ascertain the relationship between LU/LC change and actual ET taking place in a watershed has become an important topic of research. Surface energy balance methods such as Surface Energy Balance Index (SEBI), Surface Energy Balance System (SEBS), Simplified Surface Energy Balance Index (S-SEBI), Surface Energy Balance Algorithm for Land (SEBAL) and Two Source Models (TSM) had been used for the estimation of ET (Liou and Kar 2014). Sobrino et al. (2005; 2007) used a Simplified Surface Energy Balance Index method (S-SEBI) on an instantaneous time basis, integrated over a day for the estimation of evapotranspiration on a daily basis. In this, a simple method for retrieving daily ET from Landsat image based on the S-SEBI model has been proposed. It is based on the estimation of the evaporative fraction from land cover classification. Remote sensing (RS) images have become an important source of data for estimation of regional as well as meso-scale level of ET from the earth surface (Rajeshwari and Mani 2014). Land Surface Temperature (LST) helps to establish the critical interaction between surface radiance and energy balance components (Liou and Kar 2014). Landsat images have been utilized for LST estimation in many studies. But atmospheric interference has to be considered in estimating surface temperature by using Landsat satellite images. This is due to the fact that, radiance will be attenuated by the atmosphere through absorption; also thermal radiance will be emitted by the atmosphere. Therefore the radiance reaching the sensor is a combination of ground thermal radiance and upwelling atmospheric emission (Qin et al. 2001). The thermal remote sensing facilitates precise estimation of surface emissivity for accurate determination of radiometric temperature. Hence, the development of any algorithm for accurate estimation of surface emissivity is certainly better than assigning default values set to one; because natural surfaces are not perfect emitters (Brunsell and Gillies 2002). Various methods such as Split-Window (SW) (Skokovic and Sobrino 2014; Jimenez-Munoz et al. 2014, 2014; Rajeshwari & Mani 2014; Latif 2014), Dual-Angle (DA) and Single-Channel (SC) method (Qin et al. 2001) have been used for LST estimation from satellite data. These methods are based on parameters such as Normalized Differential Vegetation Index (NDVI), Fractional Vegetation Cover (FVC) and emissivity (Maskova et al. 2008).

40

Rajeshwari & Mani (2014) obtained FVC values using linear relation between NDVI and FVC.

2.5 APPLICATION OF MONTHLY RAINFALL-RUNOFF POLYGONS IN EXPLAINING HYDROLOGICAL PROCESSES

Runoff coefficient based analysis of hydrological response of any river basin is useful for land use and flood management in the basin (Sriwongsitanon and Taesombat 2011). The estimation of runoff coefficient is a difficult task, since it has to account for all the factors influencing transformation of precipitation into runoff (Kadioglu and Sen 2001; Rodriguez-Blanco et al. 2012). Runoff coefficient can be estimated statistically by plotting precipitation v/s runoff to obtain the slope of regression line, assessing linear relationship between rainfall and runoff. However, the rainfall-runoff relationship is a nonlinear process due to the influence of physical characteristics of the catchment (Kadioglu and Sen 2001). Rodriguez-Blanco et al. (2012) suggested considering other factors affecting the hydrological response of a watershed. Event based runoff coefficient plays key role in catchment comparison studies since it takes into account the influence of different landscapes in transforming the rainfall into runoff. A runoff coefficient greater than 1 indicates that groundwater or snowmelt may contribute to runoff in addition to rainfall (Kadioglu and Sen 2001). Rodriguez-Blanco et al. (2012) inferred that baseflow contributes 75% of the annual water yield in any agroforestry and temperate humid catchments. Therefore, combined influence of baseflow and rainfall has to be considered in computing runoff coefficients. Nazir et al. (2015) have used the recursive digital filter method Eckhardt to separate the baseflow from the daily streamflow. Blume et al. (2007) concluded that Constant-k method for baseflow separation is more efficient than graphical methods, as it can handle events with multiple peaks.

Every catchment has different quantum of seasonality depending upon the timing, volume, intensity, frequency and duration of precipitation and runoff. Therefore, the seasonality is considered as a key signature for regionalization studies to cluster identical hydrological response. Runoff coefficient is one of the important flow response indices, which can be computed by regression against catchment properties for estimating river flows at ungauged sites (Visessri and Mclntyre 2015).

Mimikou (1984) inferred catchment size and runoff coefficient can be used for prediction of flood flows, annual runoff yield and unit graphs of various storm events for ungauged basins. Seasonality can be quantified using statistical indices to indices derived from geometrical approaches. Ali et al. (2013) highlights the applicability and usefulness of statistical approaches such as Parde coefficients, seasonality histograms, seasonality ratio, and standard flow metrics for quantifying seasonality and catchment inter-comparison studies. Burn index is one of the most commonly used geometric approach to quantify the seasonality of the maximum annual runoff or the annual maximum daily precipitation through defining the mean date and variability of occurrence of extreme events (Ali et al. 2013). Another commonly used geometrical approach namely precipitation-runoff polygon is used by Kadioglu and Sen (2001) to study the rainfall-runoff transformation in a catchment. The significant variability in the rainfall-runoff response characteristics is demonstrated effectively based on contrasting shape of polygons (Nazir et al. 2015). Most of the available statistical/geometrical indices considers the rainfall and runoff in isolation during seasonality analysis; whereas polygon based method is capable of representing the nonlinear relationship between rainfall and runoff in the same diagram. The qualitative interpretation of precipitation runoff polygon affords a descriptive way to observe the dynamics prevailing in specific months and the relationship between precipitation and runoff and their degree of seasonality (Ali et al. 2013). Ali et al. (2013) are the first to utilize precipitation-runoff polygon based interpretations along with quantitative metrics for seasonality analysis for an array of catchments across different hydro-climatic zones. The study suggested that the polygon based analysis can be used effectively for assessment of the impacts of climatic change on hydrological regime, provided the data of past, present and future precipitation and runoff is available (Kadioglu and Sen 2001). Pektss and Cigizoglu (2013) adopted a hybrid approach by combining time series decomposition with ANN and compared its performance with ARIMA, ARIMAX and ANN in predicting monthly runoff coefficients. This study concluded that the hybrid model can produce the runoff coefficient time series.

Many studies have utilized the potential benefit of physically based semi-distributed and fully distributed modelling approach to evaluate the impact of land use

changes on hydrological response (Thanapakpawin et al. 2006; McColl and Aggett 2007; Choi and Deal 2008; Lin et al. 2008; Elfert and Bormann 2010; He and Hogue 2012; Wijesekara et al. 2012; Vaizi 2014). Sriwongsitanon and Taesombat (2011) have studied the influence of changes in LU/LC over time on flood behaviour of the upper Ping river basin, Northern Thailand through evaluating the relationship between peak flow rate, runoff coefficient and LU/LC pattern. Studies under high forest cover indicate that runoff coefficient is higher for larger flood event and lower for smaller flood events. This is due to the fact that the rainfall losses due to evapotranspiration, interception and soil moisture capacity are high in forested areas during small flood events. However, the runoff coefficient is high during larger flood events because dense forest patches are associated with high antecedent moisture condition leading to less infiltration. Crooks and Kay (2015) have used Climate and Land use Scenario Simulation in Catchments (CLASSIC) model for continuous simulation of flow series in the Thames between 1890 and 2013 to answer questions such as: a) are the model parameters determined from catchment physical properties suitable for the whole period (low flows and high flows)?; b) is the data quality an issue in assessing the model output results? In such applications, it is important to use hydrological models with unchanged model parameters while estimating impacts of change with respect to data quality, and spatial variation in rainguage density. Nourani and Saeidifarzad (2016) compared the long term lag time parameter in a conceptual rainfall-runoff model to the LU/LC change using observed streamflow data coupled with computational intelligence tool such as ANN and hybrid wavelet-ANN. However, these models are data intensive and not applicable to catchments with sparse datasets. Nazir et al. (2015) used the mean rainfall-runoff polygon method to analyse the effects of LU/LC changes on the mean monthly runoff coefficient in a tropical catchment and concluded that the length of polygon peripheral is highly influenced by climate variability rather than land use characteristics, is therefore a useful method in hydrological modelling (Ali et al. 2013).

2.6 CLOSURE

The present review described the various modeling approaches to assess the impact of land use changes on hydrologic response at catchment scale and also discusses the importance of scenario based studies. In addition, a brief description about model comparison in order to identify uncertainties is provided.

Several studies indicated that the conversion of forest land to grass land or crop land leads to reduction in ET value and an associated increase in surface flow. Legesse et al. (2003); Siriwardena et al. (2006); Elfert and Bormann, (2010); Li et al. (2009); Isik et al. (2013); and Niu and Sivakumar (2013) simulated the effects of scenario based changes in land use and climate on the hydrologic system. The results of climate scenario study showed that the influence of climate variability is more significant when compared to land use change. These scenario based studies do not actually project the future changes, but can only indicate possible future changes. This shows that, it is necessary to develop models which can predict future changes in climate and land use pattern in more realistic manner.

However, integration of various models is an improvement over the use of single model. Lin et al. (2009); Wijesekara et al. (2012) have integrated the hydrologic models with land use change models to study the impact of foreseeable changes. Since, LUCC models are reasonably good at forecasting the near-future changes in LULC pattern by considering drivers such as demographic, socio-economic and national policies etc., GCM and RCM models have been developed to simulate the real future climate change pattern. However, many researchers preferred scenario based forecasting due to difficulties and uncertainties associated with downscaling techniques and representation of detailed spatial features in climate models.

Also, the present study has reviewed the importance of comparison of models in identifying possible sources of uncertainties in hydrologic modeling. Based on the literature review, it can be concluded that the variations in the simulating efficiency of various models can be attributed to uncertainty in the calibration strategy, model input and structure and parameterization. When the aim of the study is to tackle different

aspects in single modeling framework, then it is more appropriate to integrate two or more models with different functionalities.

Estimation of actual ET and reference ET is essential for studing water balance of river basin ecosystem. ET estimation at global and regional scale can be made better by use of RS data along with measured meteorological variables. As RS data can provide LST, NDVI, Leaf Area Index (LAI), surface albedo and surface emissivity, which are vital inputs for ET models (Liou and Kar 2014).

From the literature review, it is evident that many studies have been carried out to assess the impact of land use change on hydrological response of the particular catchment using various models. Among them, the physically based distributed and semi distributed models are more suitable for these studies. However, these models are data intensive and not applicable to catchments with sparse datasets. Therefore, it necessitates the development of a simpler method to analyse the impact of LU/LC change on hydrologic response characteristics of any catchment. It is found that, the comparison of different models is very much helpful to differentiate the effect of choice of model, structural uncertainty and better understanding of hydrological processes. Recently, few researchers have analysed the impact on stream flow due to land use and climate change scenarios. The models have been developed to forecast the future change in land use pattern by considering driving factors. Also, these LUCC models have been coupled with hydrological models which lead to more realistic assessment of future stream flow changes. The studies so far have analysed a single hydroclimatic condition; and very few studies have been done related to comparative evaluation in different hydroclimatic conditions.

CHAPTER 3

DATA AND METHODOLOGY

3.1 GENERAL

The rapid development in the pace of industrialization and urbanization has put pressure on the earth's natural resources leading to degradation and becoming a global problem. The intervention of humankind in the natural ecosystem is leading to changes in hydrological phenomenon in the form of floods and draughts. It is essential to model the complex relationship between various hydrological processes and their behavior in relation to human induced changes. In addition to climatic factors, hydrological response of a catchment depends upon catchment characteristics such as topography, soil, LU/LC, geology etc., Therefore, the broad objective of present research wok is to study and compare the hydrologic response characteristics such as ET and runoff coefficient to land use and land cover changes in humid and sub-humid catchments. Data used in the present study and analysis of the same are presented in next sections of this chapter.

3.2 DATA COLLECTION

Following are the data used for the study and description of the same is provided in Table 3.1.

Table 3.1 Description of the data products

Type of Data		Period	Source	Description
Conventional Data	Toposheets (1:50000)	1973	Survey of India (SOI), Bengaluru	-
	Rainfall data	1970-2013	Indian Meteorological Department (IMD), Pune	Daily rainfall data
	Meteorological data	1970-2013	Indian Meteorological Department (IMD), Pune	Daily data
	Streamflow	1970-2013	Central Water Commission (CWC), Bengaluru	Daily stream flow data
	Soil data	-	National Bureau of Soil Survey and Land Use Planning (NBSS and LUP)	Description of soil types
Remote Sensing Data	DEM	-	Bhuvan Geospatial Data Portal	Resolution: 30m
	Satellite image	1997, 2005, 2007, 2010, 2013	National Remote Sensing Centre (NRSC), Hyderabad Landsat images	LISS-III images Resolution: 23.5m Resolution: 30m
Field Data	Soil Samples from Netravati river basin	-	Field survey	38 soil samples at 0.5m and 1m depth in 19 sampling locations

3.3 METHODOLOGY

This chapter presents the detailed procedure adopted to accomplish the research objectives in two catchments namely, Netravati river basin (humid climate) and Harangi catchment (sub-humid climate) located in different hydroclimatic regions of Karnataka State, India. The overview of the methodology adopted in this research is shown in Figure 3.1 and the same is described in the following steps:
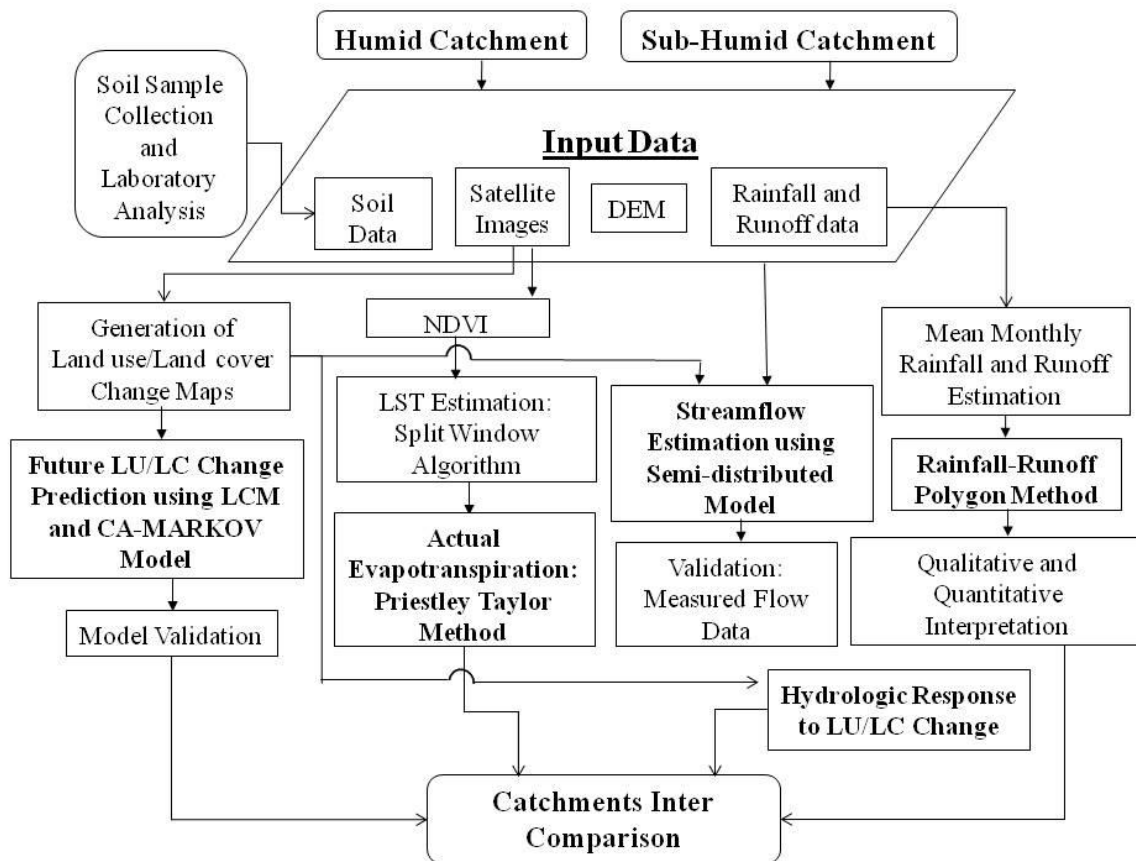
Figure 3.1 Schematic representation of overall methodology

STEP 1: Delineation of study area from the toposheet and satellite imagery.

STEP 2: Collection of data required for the study including meteorological data, toposheet, satellite images, streamflow, soil sample collection and laboratory analysis. Later, the estimated soil physical and hydraulic properties were used to calculate model parameters of SMA model.

STEP 3: Classification of satellite images and prediction of future trends in LU/LC pattern using LCM and CA-Markov model.

STEP 4: Estimation of LST and actual ET using Split Window algorithm and Priestley Tailor method respectively.

STEP 5: Estimation of streamflow using a semi-distributed model namely HEC-HMS and validation using measured streamflow data. The parameters of the model were estimated based on soil physical and hydraulic properties and the classified LU/LC maps.

STEP 6: Analysing the hydrological processes in two contrasting catchments through quantitative and qualitative interpretation of rainfall-runoff polygons

STEP 7: Analyse the hydrologic response to LU/LC change

STEP 8: Comparison of hydrologic responses such as runoff coefficient and ET between humid and sub-humid catchments

3.4 PREDICTION OF LAND USE/LAND COVER DYNAMICS

Review of literature indicates that very few studies have focused on the comparison of performance of LU/LC change models in analyzing the vegetation pattern in river basin/catchment/watershed. Therefore, the study analysed the dynamics of LU/LC change and predicted its possible future changes in Netravati river basin and Harangi catchment, Karnataka, India. This study specifically addressed: 1) Spatial and temporal changes in LU/LC classes, 3) Selection of driving factors for change, 4) Preparation of suitability maps, 5) Prediction of LU/LC changes using Land Change Modeler (LCM) and CA-Markov model and their validation 6) Comparison of two models performance in different study areas. The outline of methodology adopted is shown in Figure 3.2.
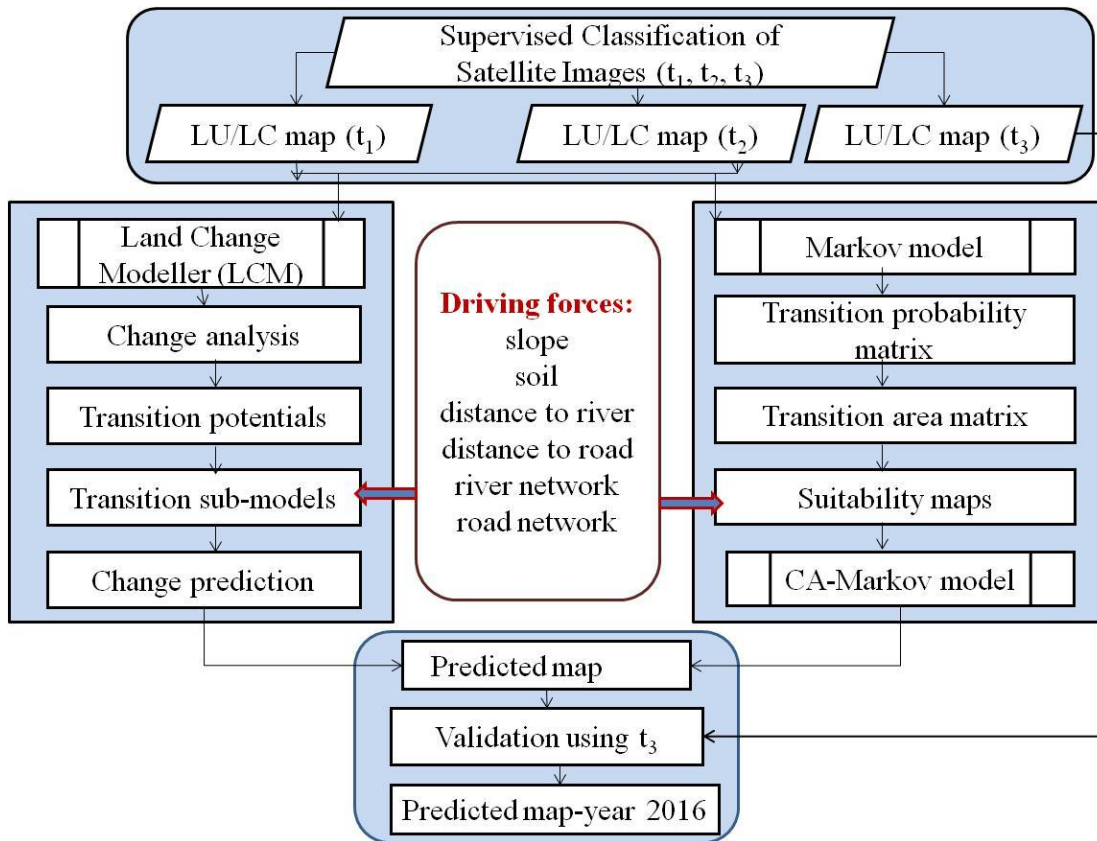
Figure 3.2 Flowchart of simulating LU/LC change using LCM and CA-Markov

3.4.1 Land Use and Land Cover Change Detection and Selection of Driving Factors

The land use/ land cover change detection was carried out through multi-date image classification based on Maximum likelihood algorithm, Minimum distance to mean algorithm and Parallelepiped algorithm using remote sensing images of the year 2005, 2007 and 2010 for Netravati river basin and 2007, 2010 and 2013 for Harangi catchment. The methodology adopted is shown in Figure 3.3. The classification algorithms are explained as follows.
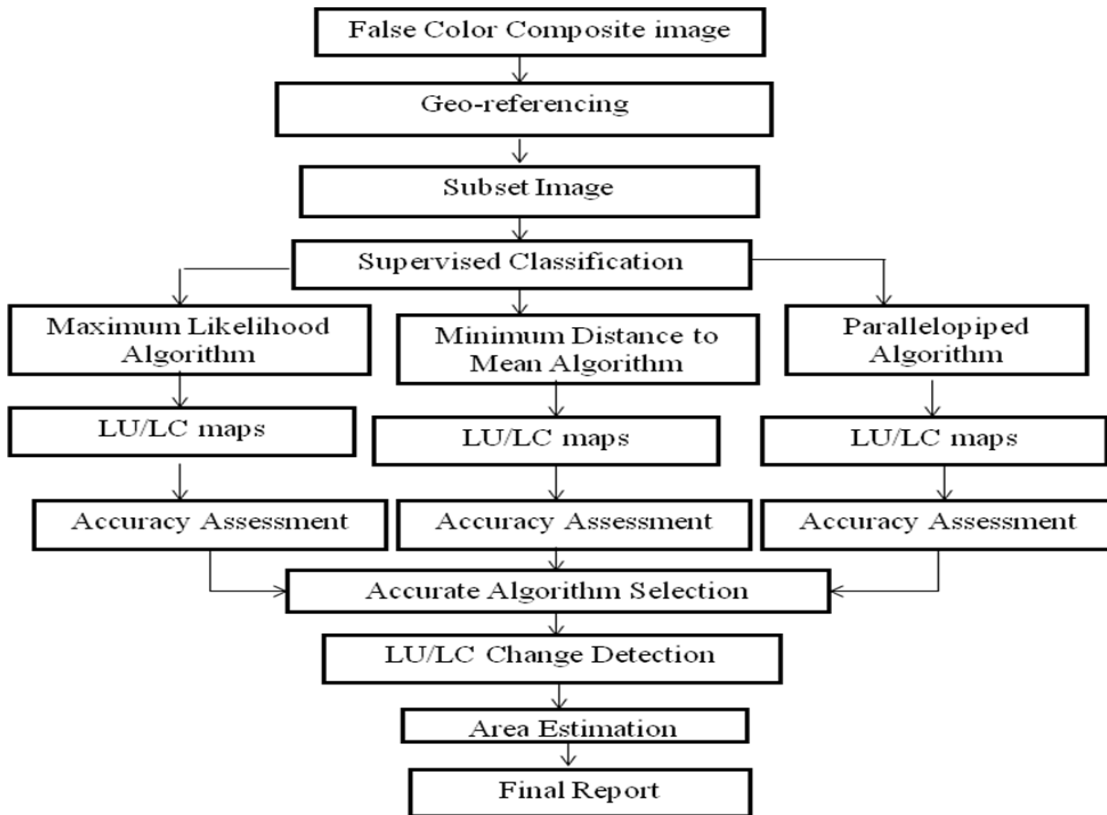
Figure 3.3 Flowchart showing the methodology for detection of LU/LC change

i. Maximum Likelihood Algorithm

The maximum likelihood method takes advantage of the probability of a pixel being a member of an information class in its decision making. This algorithm relies on the second-order statistics of the Gaussian probability density function for each class. The basic discriminate function for pixel X is

$X \epsilon C_j$ if $p(C_j/X) = max[p(C_1/X), p(C_2/X), …, p(C_m/X)]$ (3.1)

Where max $[p(C_1/X), p(C_2/X), …, p(C_m/X)]$ is a function that picks up the largest probability among those inside the bracket.

ii. Minimum Distance to Mean Algorithm

The decision rule in the minimum-distance-to-mean algorithm is based on the relativity among the spectral distances between the pixel in question and the center (mean) of all information classes that have been derived from the training samples. The decision rule behind this classifier takes the following form:

Pixel $X \in C_j$ if $d(C_j) = \min[d(C_1), d(C_2), ..., d(C_m)]$ (3.2)

Where min $[d(C_1), d(C_2), ..., d(C_m)]$ is a function for identifying the smallest distance among all.

iii. Parallelepiped Algorithm

The parallelepiped algorithm assigns a pixel to one of the predefined information classes in terms of its value in relation to the DN range of each class in the same band. This comparison is expressed mathematically as

Pixel $X \in C_j$ if min $DN_j \leq DN_x \leq$ max DN_j (3.3)

The decision rule states that pixel X under consideration is a member of information class C_j if and only if its value falls inside the DN range of that class in the same band.

      The base map of the study areas was delineated from Survey of India (SOI) toposheet of 1:50000 scale using ArcGIS 9.3 software. The satellite images were geo-referenced with respect to coordinate system of toposheet using image-to-map transformation. Seven classes were identified in Netravati river basin by the classification process of RS dataset namely built-up land, fallow, plantation, forest, land with or without scrub, sandy area, and river. Similarly in Harangi catchment also, seven LU/LC classes were delineated during classification of images namely urban area, forest area, water body, water logged area, plantation, fallow land and waste land. The study made use of ERDAS IMAGINE 9.1, a image processing software to accomplish the process of LU/LC change detection.

      After obtaining results of classification, it is necessary to check their accuracy. Accuracy assessment was carried out and the kappa coefficient was calculated for all the

three methods in order to select best the classification algorithm among them for Harangi catchment. For this process, 40 ground truth points were chosen within the study area that includes sample points in all LU/LC classes. Based on the results of accuracy assessment, best classification algorithm namely Maximum likelihood algorithm was identified and its results were utilized for change detection in Harangi catchment. The same procedure was adopted to select best classification algorithm for LU/LC classification and change detection of Netravati river basin.

Based on the trend of LU/LC change pattern and the basic knowledge of the study areas, driving factors were identified. The selected driving factors include slope, soil, road network, river network, distance to road and distance to river. Then, the maps of driving factors were generated, which have been used as input for the preparation of suitability maps by using overlay analysis in ArcGIS 10.1. The LU/LC projections were performed in LCM and CA-Markov models by creating a transition probability matrix to calculate the quantity of each land use change by a desired date. The study used LU/LC maps of Netravati river basin of the year 2005 (t_1) and year 2007 (t_2) as inputs to the model for simulating the changes in the year 2010 (t_3). Whereas for Harangi catchment, LU/LC maps of the year 2007 (t_1) and year 2010 (t_2) were used as inputs to the model for simulating the changes in the year 2013 (t_3). Result of the model was validated by comparing predicted images of the year 2010 and 2013 with original classified images of the year 2010 and 2013, respectively. The validated model was used to simulate the LU/LC change scenario during the year 2016 for both Netravati river basin and Harangi catchment.

3.4.2 Driving Factors

The driving factors are the forces that cause change in LU/LC pattern of any area. The driving factors such as socio economic, biophysical and infrastructural factors were identified based on LU/LC change analysis in the present study (Table 3.2). Different criterions were used to determine which LU/LC classes of watershed were suitable for changing from one class to another with time. Since new developments cannot usually come-up in river network, and in road–rail networks, these classes were assigned under constraints for LU/LC change.

54

The river network was considered as a constraint for all the LU/LC classes except water body. The driving forces for LU/LC change were the proximity to road–rail network, settlement, slope, river network and associated LU/LC classes. These factors were served as criterion that define some degree of suitability for an activity under consideration. Figure 3.4 and 3.5 show the driving forces used in Netravati river basin and Harangi catchment respectively. The distance to roads and river network was calculated using Euclidean distance tool. Soil map for the study area was extracted from the map obtained from NBSS and LUP.

Table 3.2 Summary of driving factors

Driver	Category	Source	References
Slope	Biophysical	ASTER DEM	
Soil	Biophysical	NBSS and LUP	
Distance to river	Biophysical	Arc map 10.1	Verburg et.al (2004)
Distance to roads	Infrastructural	Arc map 10.1	
River network	Biophysical	ASTER DEM	
Road map	Socio economic	QGIS	
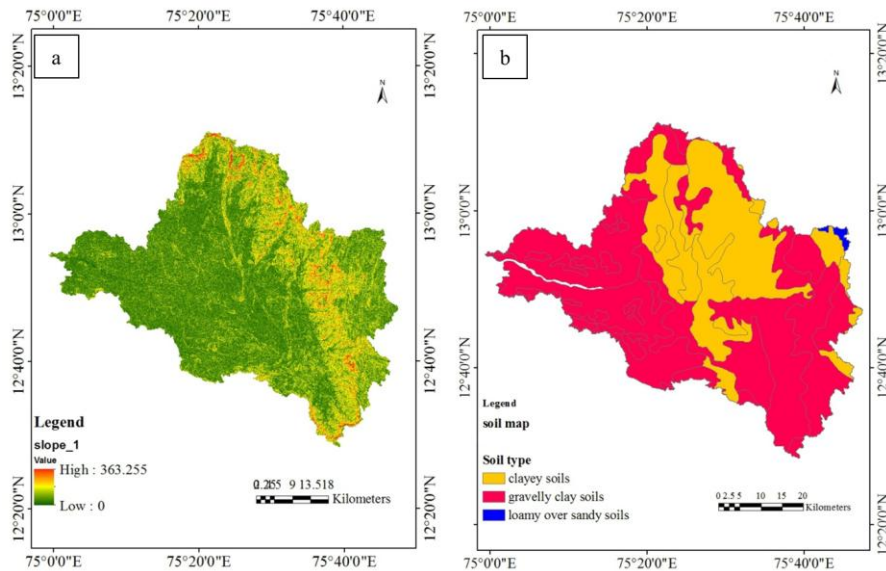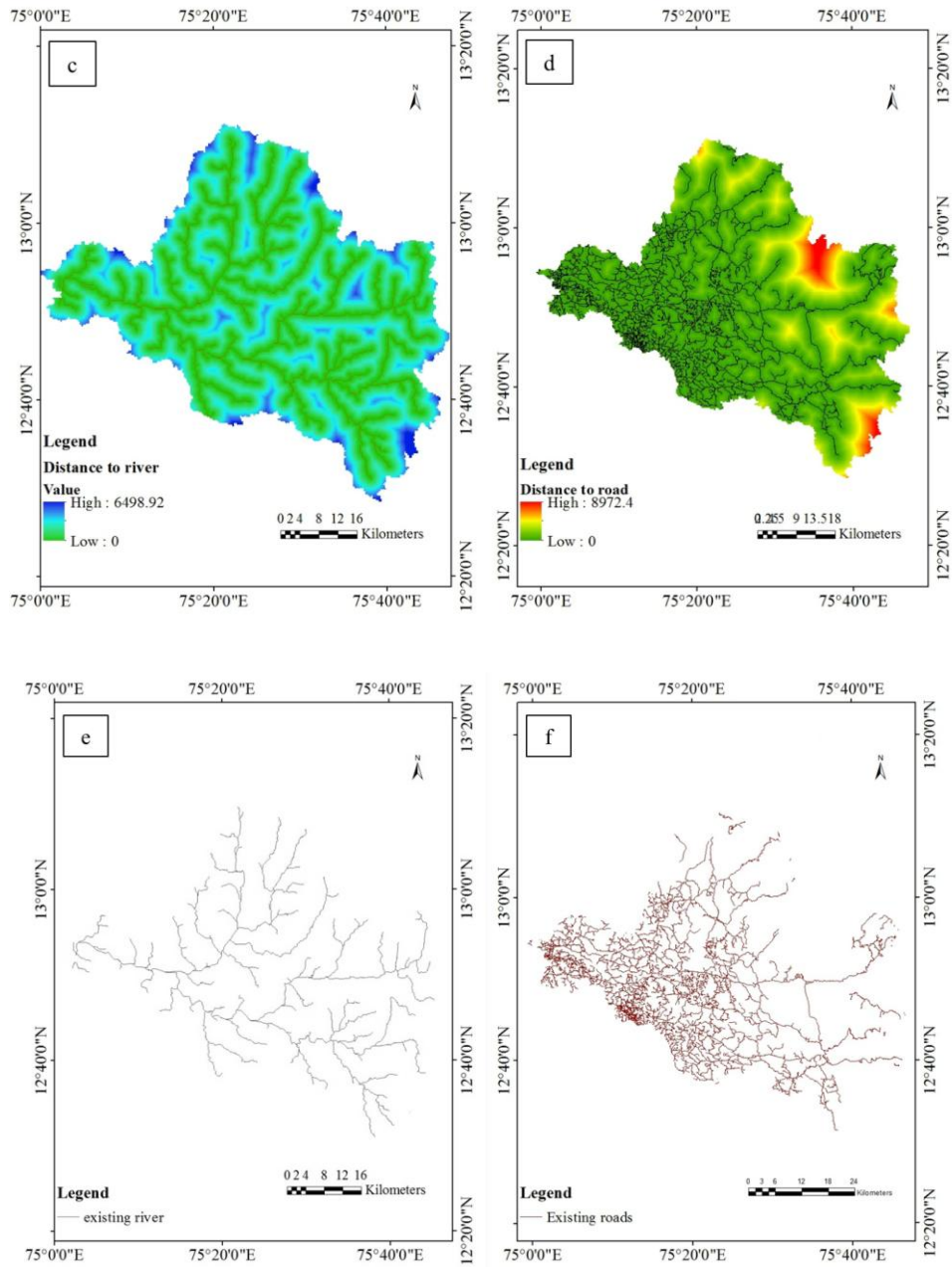
Figure 3.4 Driving factors: a) slope b) soil c) distance to river d) distance to road e) river network f) road network map of Netravati river basin
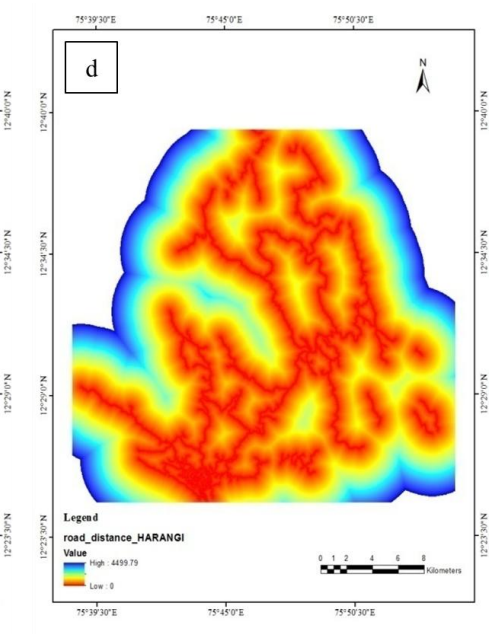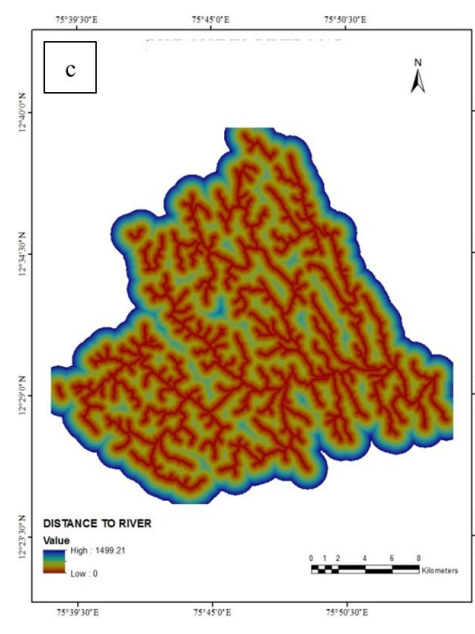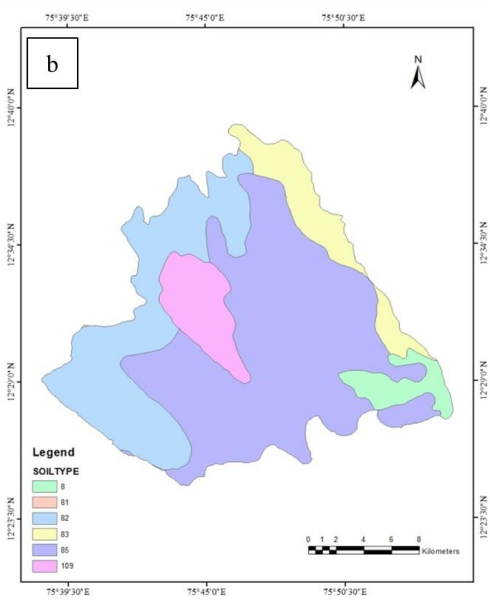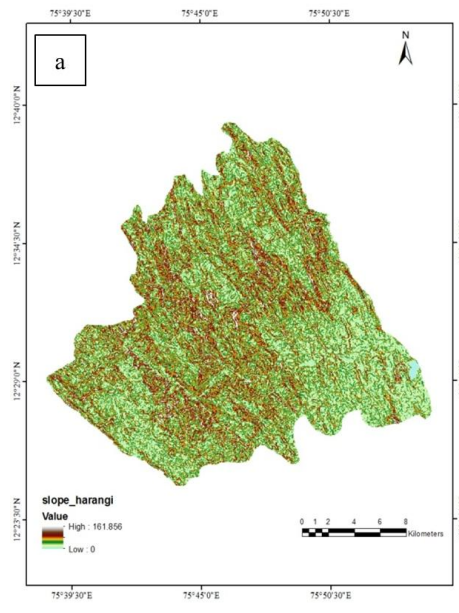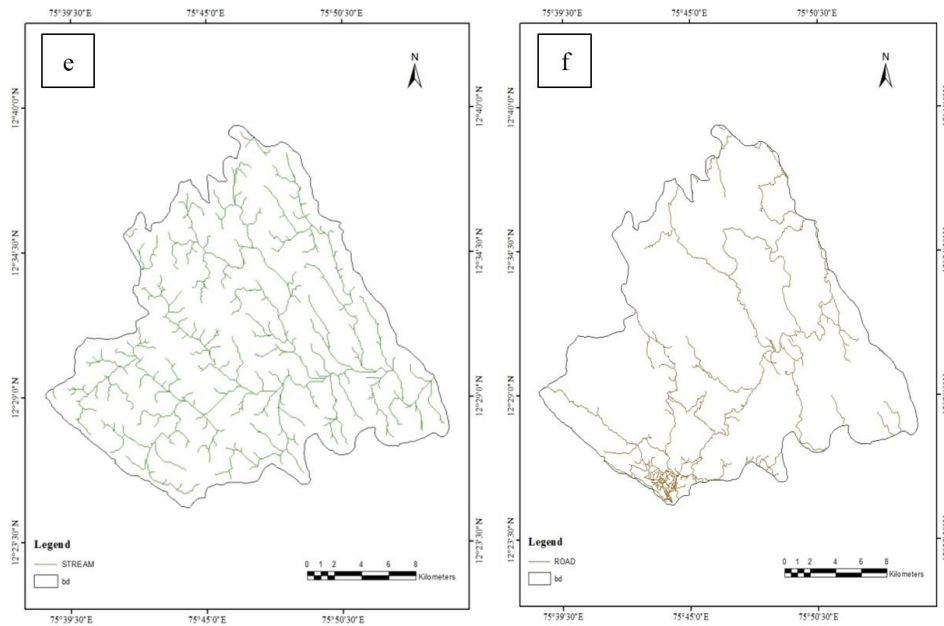
Figure 3.5 Driving factors: a) slope b) soil c) distance to river d) distance to road e) river network f) road network map of Harangi catchment

3.4.3 Suitability Maps

The term suitability is used to provide information whether areas are suitable or not for changing one class to another based on certain conditions. In this study, driving factors like slope, distance to river, distance to road, soil and different land use and land cover classes were considered to define the multiple criteria for making decisions about future status of various land use and land covers, which is essential for preparation of suitability map. The factors and the respective criteria considered for this analysis are given in Table 3.3. The generated suitability maps of Netravati river basin and Harangi catchment are as shown in Figure 3.6 and Figure 3.7 respectively. The suitability maps along with the transition probability area matrix were given as inputs to the CA-Markov model to predict future change.

Table 3.3 Criteria used for creating suitability maps.

LU/LC Classes	Slope	Road network	Soil	References
Built-up land / Urban area	0-6%-very suitable,7-13%-suitable,4-25%-residential, >15%-not suitable.	20-500m		Behera et al., 2012
Fallow	<10%	10-500m		
Plantation	<15%	>100m	Clayey soil	
Forest	2-65%	>1000m	High and medium clay content	
Land with or without scrub / waste land	<10%	10-500m		
River / water body	<1%	30-200m		
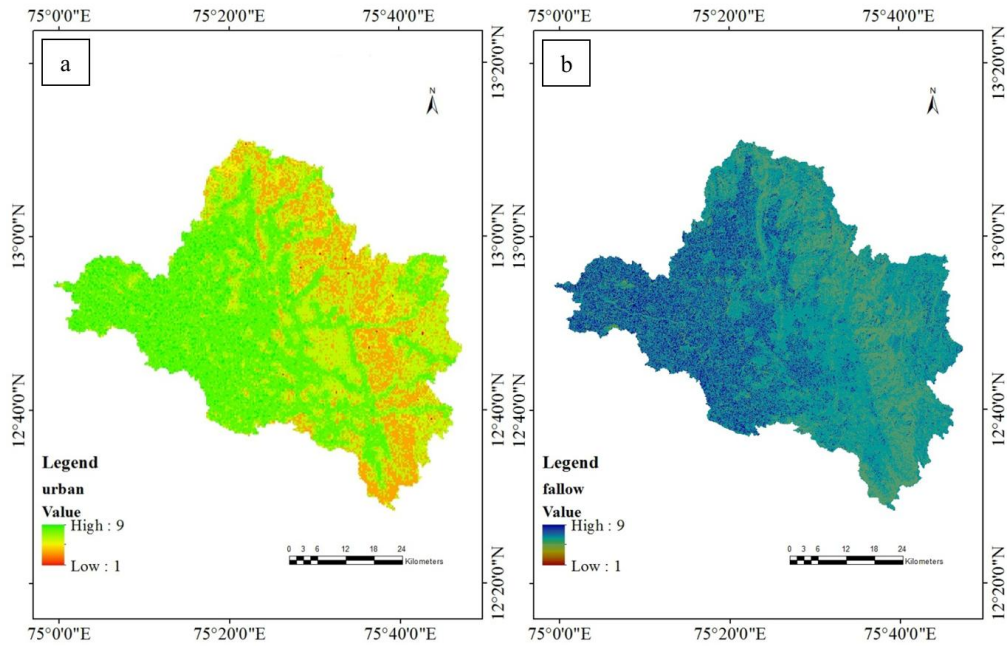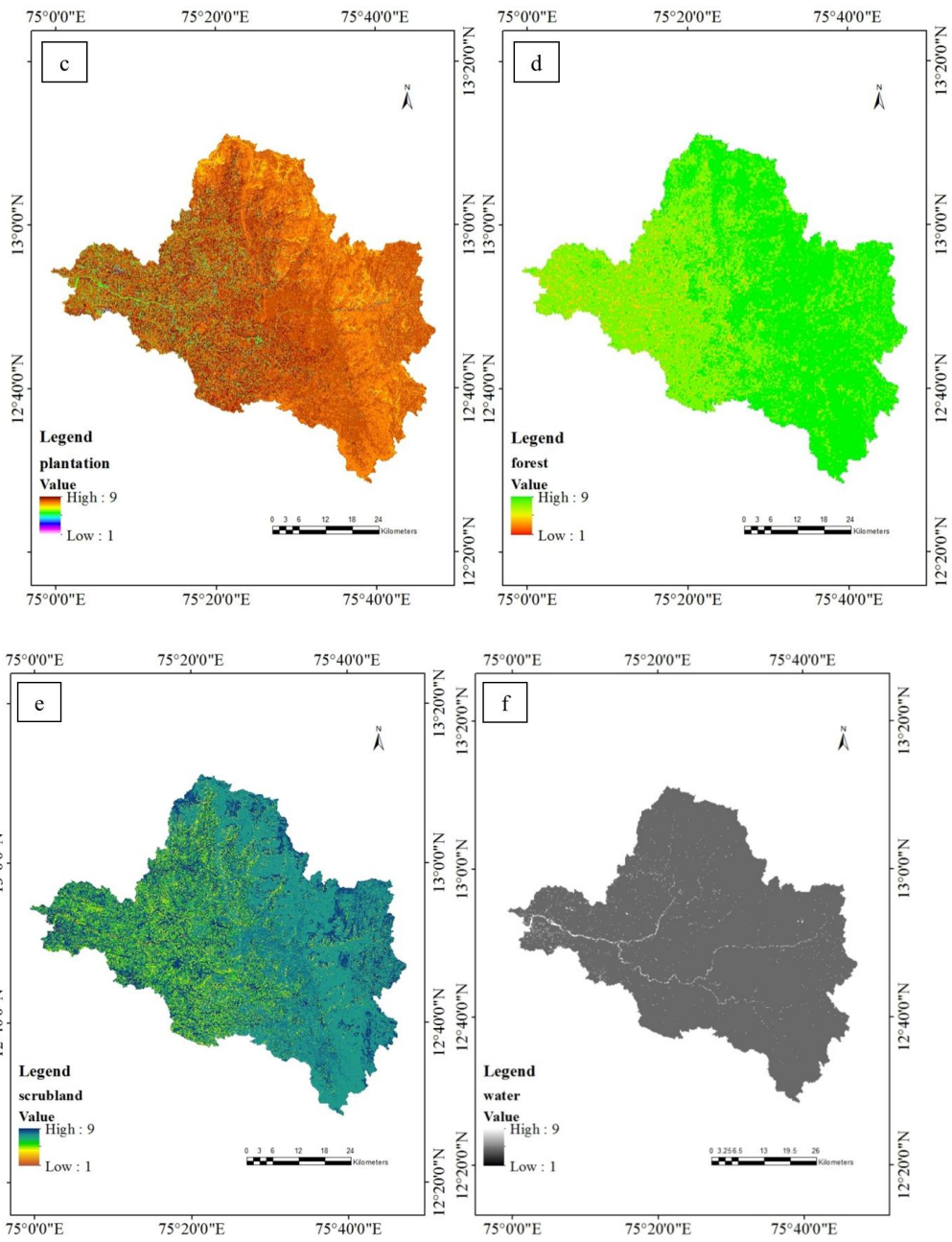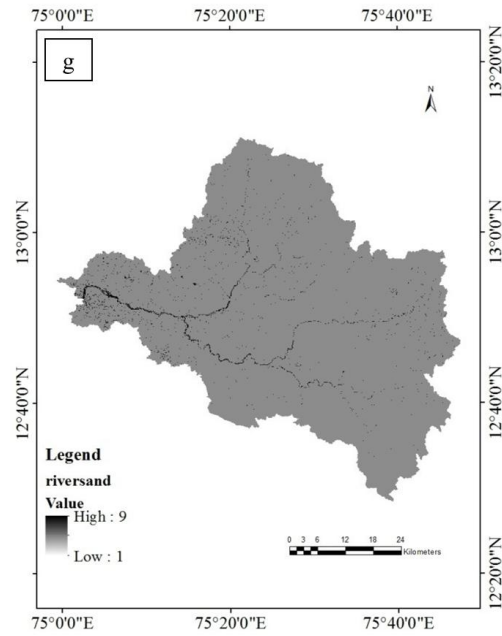
Figure 3.6 Suitability maps: a) built-up land b) fallow c) plantation d) forest e) land with or without scrub f) water body and g) river sand of Netravati river basin
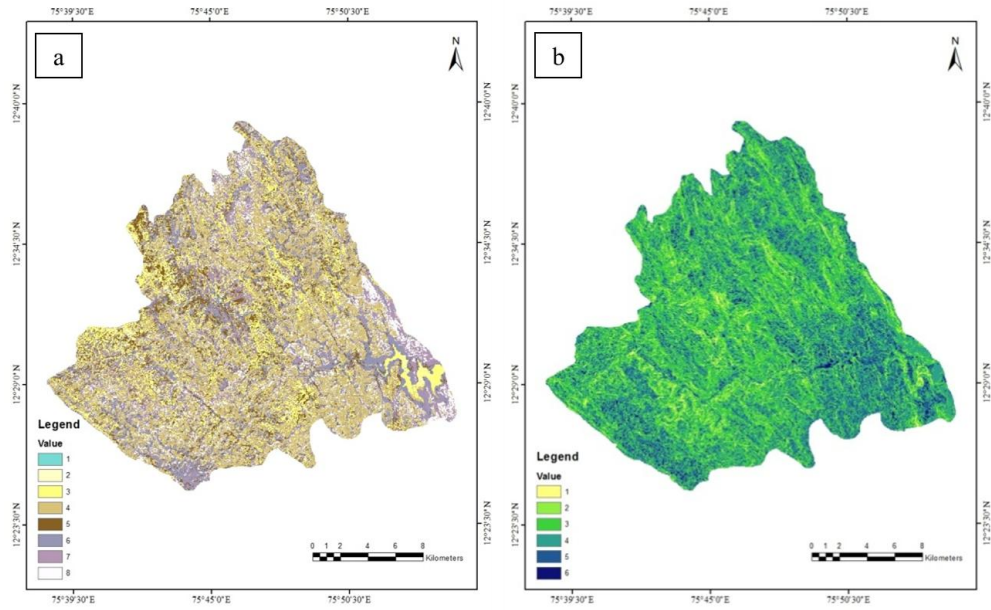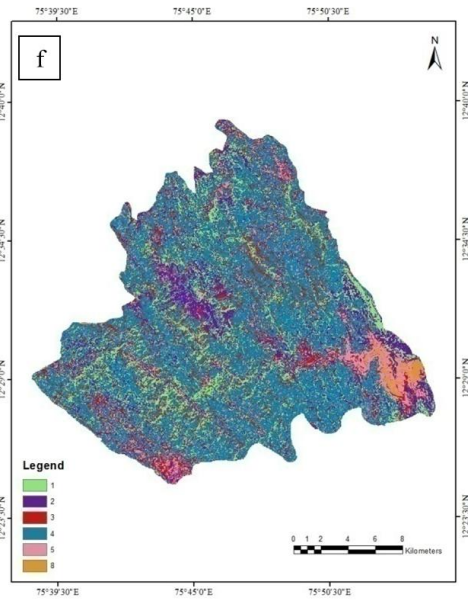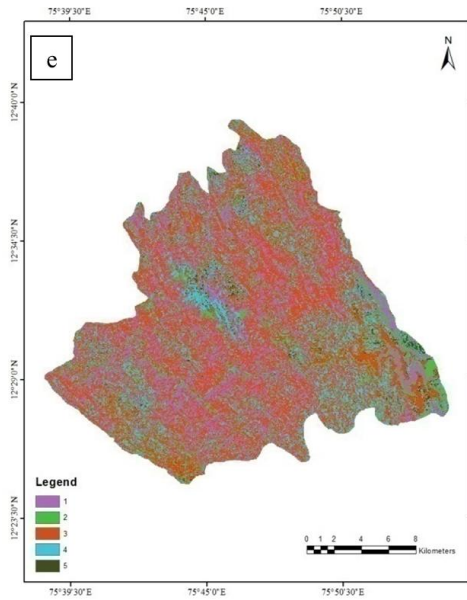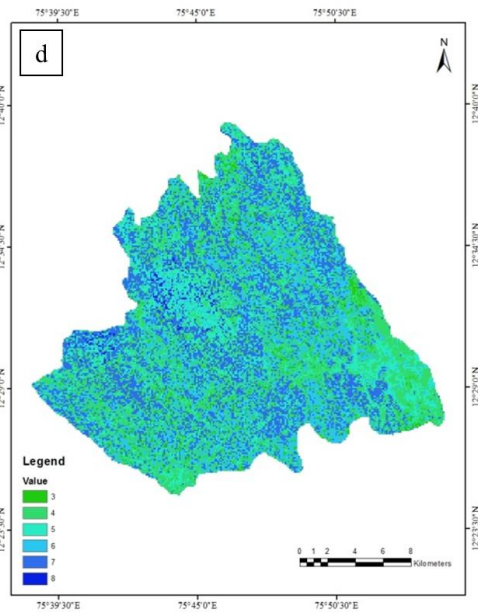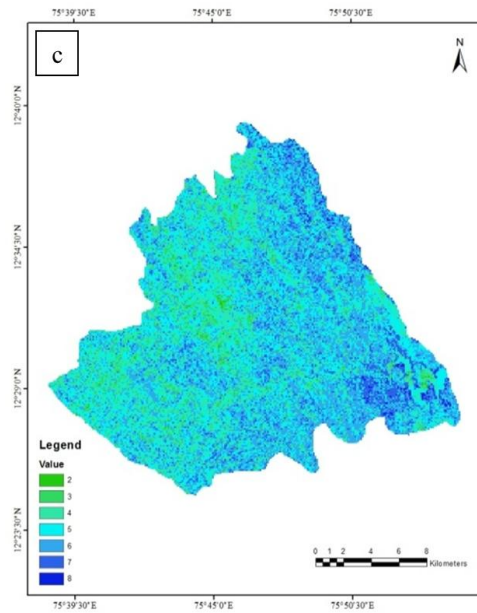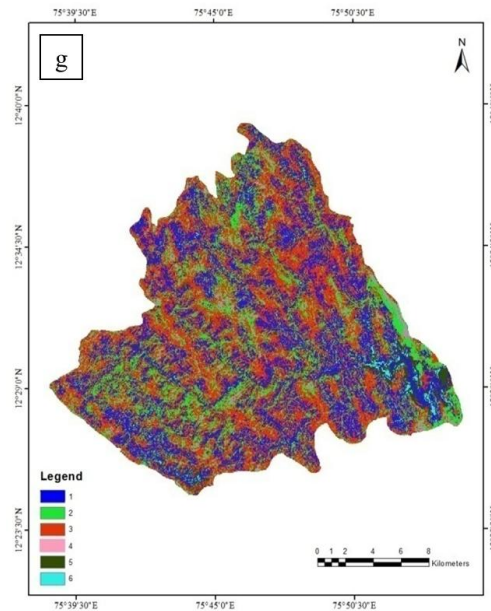
Figure 3.7 Suitability maps: a) urban area b) fallow c) plantation d) forest e) waste land f) water body and g) waterlogged area of Harangi catchment

3.4.4 Land Change Modeler (LCM)

Land Change Modeler is an integrated model within IDRISI Selva, which was used to analyze the changes in LU/LC dynamics. Land change prediction in LCM is an empirically driven process that moves in a stepwise fashion from change analysis, transition potential modeling to change prediction. It is based on the historical change from time 1 to time 2 land cover maps to project future scenarios (Schulz et al., 2010; Olmedo et al., 2013). Change analysis provides the gains and losses by category, net change by category and contributors to net change experienced by different LU/LC classes. The transition sub models were loaded with driver maps such as road, river, slope and soil map by using transition potential tool. Multi-Layer Perceptron (MLP) neural network was used to model the transitions, since multiple variables need to be modeled at the same time (Schulz et al., 2010; Kumar et al., 2015). The change prediction tool contains Markov chain, which was used to find out the transition probability matrix from which probability of changing from one class to another was obtained.

63

3.4.5 Cellular Automata-Markov (CA-Markov) Model

Markov chain is one of the most accepted methods for modelling LU/LC change using current trends because it uses evolution from 't − 1' to 't' to project probabilities of land use changes for a future date 't + 1'. These probabilities are generated from past changes and then applied to predict future changes but it does not consider spatial knowledge distribution within each category and transition probabilities are not constant among landscape states; so it may give the right magnitude of change but not the right direction (Muller and Middleton 1994). In this study, Markovian process was used to obtain a transition area matrix from transition probability matrix. The transition area matrix obtained from 't − 1' and 't' time period was used as the basis for predicting the future LU/LC scenario. CA-Markov model is a combination of Cellular Automata and Markov model (Behera et al., 2012; Wang et al., 2012). Markov model provides the states of conversion between different land use types and the rate of conversion among the land use types whereas CA-Markov provides spatial transitions in an area with time (Sang et al., 2011).

3.5 SATELLITE BASED EVAPOTRANSPIRATION ESTIMATION

3.5.1 Evapotranspiration Estimation using Priestley-Taylor (PT) method

Evapotranspiration (ET) is a key process in land surface–atmosphere studies. It mainly depends on water availability and incoming solar radiation and then reflects the interactions between surface water processes and climate. The spatial and temporal quantification of surface ET based on satellite derived products is of paramount importance in various environmental applications such as crop water monitoring, irrigation scheduling, hydrological studies, and weather forecasting. Therefore, the present research work aims to estimate actual evapotranspiration by using satellite data in Netravati river basin and Harangi catchment, Karnataka State, India. The detailed procedure adopted to estimate actual ET by using Priestley Taylor method in Netravati river basin and Harangi catchment is as shown in Figure 3.8. This study made use of cloud free (less than 10% cloud cover) Landsat image of 30m resolution for the years 1997, 1999, 2003, 2011 and 2015 during pre-monsoon period

(January to March) for the estimation of Land Surface Temperature (LST) and ET. Landsat 8 images with band 2 (green), 3 (blue), 4 (red), 5 (near infra-red), 10 (thermal infra-red 1) and 11 (thermal infra-red 2) were used for the years from 2015. Landsat 5 and Landsat 7 images were used for the year 1997, 1999 and 2003, 2011 respectively. The parameters such as saturated vapour pressure, vapour pressure deficit, net short and long wave radiation, transmissivity, psychometric constant and air pressure used in the model were obtained from Food and Agriculture Organization (FAO). ERDAS IMAGINE 9.1, a image processing software was used for modelling ET and LST.
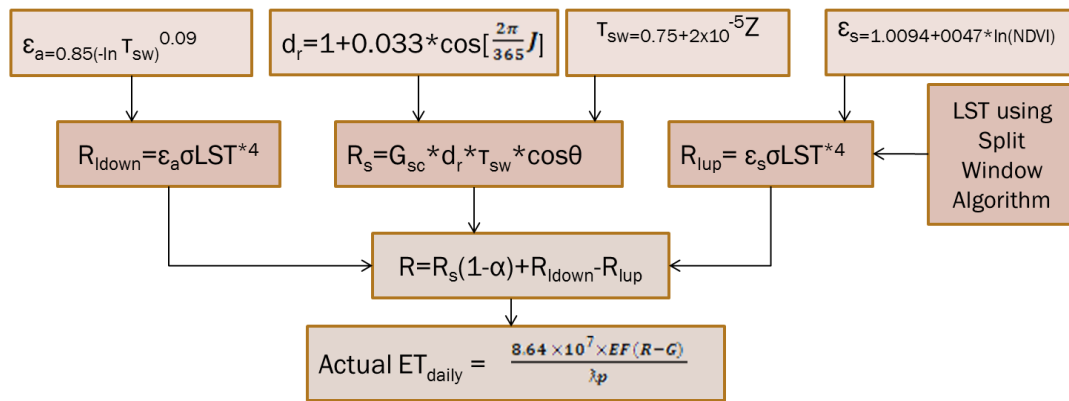
Figure 3.8 Flowchart for actual ET estimation using Priestley-Taylor method

Priestley Taylor Equation was used for the estimation of Actual ET (AET). The equation is most suitable for estimating areal ET from a wet environment where the effect of the local advection is minimal (Laxmi et al. 2015). As all the parameters were calculated from instantaneous observation, daily AET (24 hour) was estimated based on assumption that evaporative fraction remains constant. Assuming that the soil heat flux integrated over 24-hours (G_{daily}) is negligible, AET rate over 24 hours can be calculated as:

$$\mathbf{AET_{daily}} = \frac{8.64 \times 10^7 \times EF(R-G)}{\lambda p} \tag{3.4}$$

where,

λ=Latent heat of water (2.47×10^6kJkg^{-1}); EF=Evaporative Fraction

p=Density of water (1000kgm^{-3});

G=Soil heat flux (Wm^{-2}); R= Net daily radiation (Wm^{-2})

Illustration of each parameter involved in Eq. 3.4 are given in the following sub-articles

i. Estimation of Net Radiation R:

$$R=R_s (1-\alpha) + R_{1down}-R_{1up} \tag{3.5}$$

where,

R_s is incoming solar radiation (Wm^{-2})

R_{1down} is long wave downward radiation

R_{1up} is long wave upward radiation

α = Surface albedo

ii. Incoming Solar Radiation (R_s):

$$R_s=G_{sc}*d_r*\tau_{sw}*cos\theta \tag{3.6}$$

where,

G_{sc}=solar constant at the top of atmosphere $(1376 \ Wm^{-2})$

d_r=inverse relative earth sun distance; τ_{sw} =two way atmospheric transmissivity

iii. Inverse relative Earth - Sun distance:

$$d_r=1+0.033*cos[\frac{2\pi}{365}J] \tag{3.7}$$

where,

 J=sequential day of year and the angle $(Jx2\pi/365)$ is in radians

iv. Two-way atmospheric transmissivity (τ_{sw}):

τ_{sw} includes transmissivity of both direct solar beam radiation and diffuse radiation to the surface. Assuming clear sky and relatively dry condition, it can be related to elevation as below,

$$\tau_{sw}=0.75+2x10^{-5}Z \tag{3.8}$$

where,

Z = elevation in meter

v. Solar angle θ:

It is the angle between the plumb line on the surface of the earth extending vertically upwards with the direction of sun.

vi. Long wave downward radiation (R_{1down})

Downward radiation cannot be obtained or received from space born sensors. It has to be calculated from LST as per Stefan-Boltzmann law. The equation is as follows:

$$R_{1down} = \varepsilon_a \sigma LST^{*4} \tag{3.9}$$

where,

σ=Stefan-Boltzmann constant, ε_a=atmospheric emissivity

vii. Atmospheric emissivity (ε_a)

Emissivity of an object is the ratio of energy radiated by that object at a given temperature to the energy radiated by a perfect black body at same temperature. It is calculated as (Bastiaanssen 1995):

$$\varepsilon_a = 0.85(-\ln \tau_{sw})^{0.09} \tag{3.10}$$

viii. Long Wave Upward Radiation (R_{1up})

It is the radiation flux emitted from the earth surface to the temperature.

$$R_{1up} = \varepsilon_s \sigma LST^{*4} \tag{3.11}$$

where,

ε_s=surface emissivity calculated from Normalized Difference Vegetation Index (NDVI)

$$\varepsilon_s = 1.0094 + 0047*\ln(NDVI) \tag{3.12}$$

3.5.2 Split Window Algorithm

LST from Landsat 8 data was calculated by applying a structured mathematical Split-Window (SW) algorithm, which is diagrammatically represented in Figure 3.9. It uses brightness temperature of two bands of thermal infra-red (TIR), mean and difference in Land Surface Emissivity (LSE) for estimating LST of an area. The mathematical form of algorithm is as given below.

$$LST = TB_{10} + C_1 (TB_{10}\text{-}TB_{11}) + C_2 (TB_{10}\text{-}TB_{11})^2 + C_0 + (C_3+C_4W) (1\text{- } \varepsilon) + (C_5+C_6W) \Delta\varepsilon$$

$$(3.13)$$

where,

LST is Land Surface Temperature (K)

C_0 to C_6 are Split-Window Coefficient values (Table 3.4) (Skokovic and Sobrino 2014)

TB_{10} and TB_{11} are brightness temperature of band 10 and band 11 (K)

ε is Mean LSE of Thermal Infra-Red (TIR) bands;

$\Delta\varepsilon$ is Difference in LSE

W is atmospheric water vapour content

Table 3.4 Split window coefficient value

Constant	value
C_0	-0.268
C_1	1.378
C_2	0.183
C_3	54.300
C_4	-2.238
C_5	-129.200
C_6	16.400
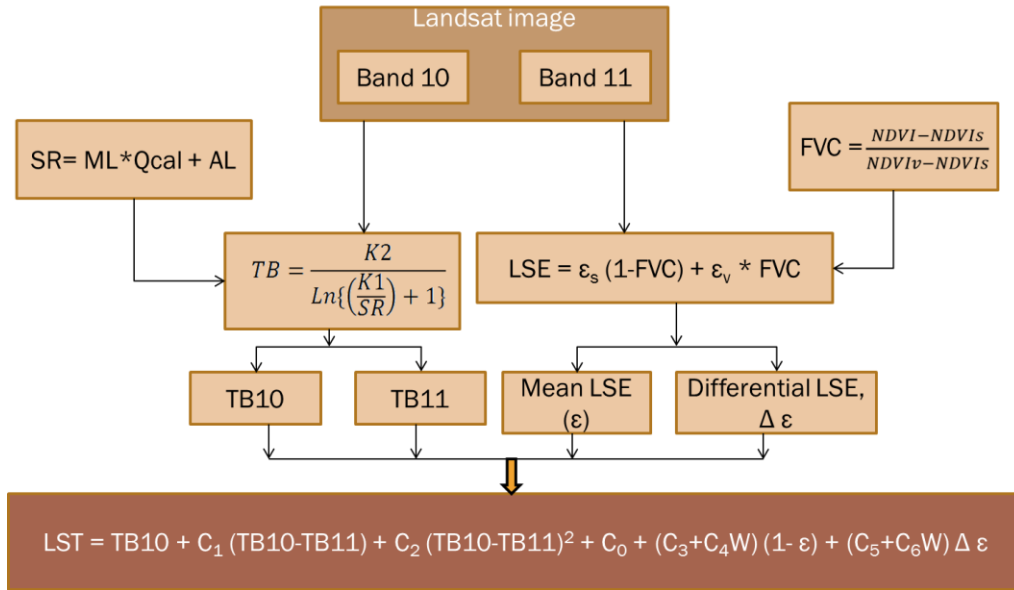
Figure 3.9 Estimation of LST using Split Window algorithm

Illustration of each parameter involved in Eq. 3.13 are given in the following sub-sections

i. Atmospheric Spectral Radiance

Atmospheric Spectral Radiance (SR) is determined by:

SR= ML*Qcal + AL $\hspace{6cm}$ (3.14)

where,

Qcal is Digital Numbers (DN) in band 10 or 11 of Landsat 8 and ML and AL are multiplicative and additive constants of corresponding band.

ii. Brightness Temperature (TB)

TB is the microwave radiation radiance traveling upward from the top of Earth's atmosphere. The calibration process was done for converting thermal DN values of thermal bands TIR to TB. The equation adopted to estimate TB for both the TIRs bands is as follows.

$$TB = \frac{K2}{Ln\{\left(\frac{K1}{SR}\right) + 1\}}$$

$\hspace{12cm}$ (3.15)

where,

K1 and K2 = thermal conversion constants which are different for the two TIR bands

iii. Land Surface Emissivity (LSE)

The LSE of the region is necessary to calculate LST of the area under study. Therefore, LSE was estimated by taking weighted average of emissivity of soil and vegetation (Table 3.5).

$$LSE = \varepsilon_s\,(1\text{-}FVC) + \varepsilon_v * FVC \tag{3.16}$$

where,

ε_s and ε_v - soil and vegetative emissivity values of the corresponding bands.

Table 3.5 Emissivity Values (Rajeshwari and Mani 2014)

Emissivity	Band 10	Band 11
ε_s	0.971	0.977
ε_v	0.987	0.989

iv. Fractional   Vegetation Cover (FVC)

Fractional vegetation cover is the estimate of fraction of area of a pixel covered with vegetation. It is estimated using NDVI normalization method (Rajeshwari and Mani 2014).

$$FVC = \frac{NDVI - NDVIs}{NDVIv - NDVIs} \tag{3.17}$$

where,

NDVIs =NDVI for soil; NDVIv = NDVI for vegetation

The above equation 3.17 is the normalization of NDVI values assuming linear relation between NDVI and FVC. A bare pixel was selected from true color composite of area and corresponding NDVI was obtained and taken as NDVIs. Then, NDVI was obtained for a fully vegetated pixel, which was taken as NDVIv. Normalization was done for the resultant image, pixel which shows values greater than or equal to 1 were assigned a value of 1 and those pixel which shows value less than or equal to zero was assigned a value of 0.

v. Mean and differential emissivity

Mean and differential LSE were calculated for Landsat 8-band 10 and 11 by using the following equations.

$$\varepsilon = (\varepsilon 10 + \varepsilon 11)/2 \tag{3.18}$$

$$\Delta\varepsilon = \varepsilon 10 - \varepsilon 11 \tag{3.19}$$

3.6 CONTINUOUS HYDROLOGIC MODELLING

3.6.1 Hydrologic Engineering Center - Hydrologic Modeling Software (HEC-HMS) model

The study adopted a methodology to estimate streamflow in Netravati river basin, Karnataka State, India, using a continuous simulation model namely Soil Moisture Accounting (SMA) model in HEC-HMS modeling framework which incorporates surface, sub-surface and ground water parameters in the process of simulation (Figure 3.10).
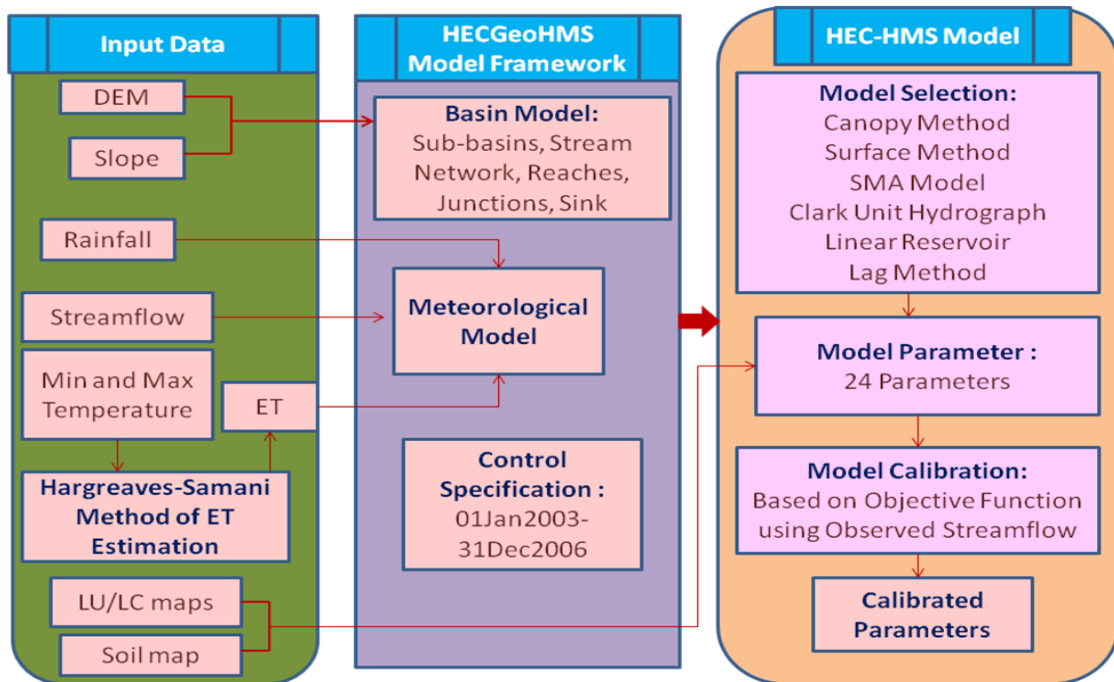
Figure 3.10 Methodology for streamflow estimation using HEC-HMS model

The HEC-HMS is developed by the US Army Corps was selected due to its simplicity and versatility for estimating streamflow in Netravati river basin, Karnataka state, India during the year 2003-2006. HEC-HMS contains three main components: basin model, meteorological model, and control specifications (Verma et al. 2010; Abushandi and Merkel 2013). The basin model stores the physical datasets describing the catchment properties; the meteorological model includes precipitation, evapotranspiration; and the control specification describes the duration and time step for continuous simulation. HECGeoHMS is an extension to ArcGIS 10.1 version was used to prepare basin model and meteorological model. The first step was to define the basin area and sub-basins, a stream network, and diversions and junctions. Second step was to prepare meteorological model based on areal distribution of rainfall which was estimated using Inverse Distance method. The HEC-HMS model requires different datasets including a DEM, weather data, soil type and land use/land cover maps. Final step was to export these models to HEC-HMS modeling framework. The HEC-HMS program offers several options to represent different components of the hydrological system, specially the rainfall-runoff transformation process. The selected options for the study are as follows:

i) Canopy method was used for representing canopy interception storage, which is removed through evaporation.

ii) Surface method accounts for water loss due to surface depression storage, which is usually removed by evaporation and infiltration.

iii) Soil Moisture Accounting (SMA) model was selected to estimate the volume of water transferred as runoff. This model is recommended to be applied for continuous simulations, since it is capable of considering soil moisture conditions, ground water storage and baseflow characteristics of river basin.

iv) Clark Unit Hydrograph model was selected to transform direct runoff into streamflow.

v) The baseflow was characterized by a linear reservoir model, to be used with SMA model

vi) The flow routing was done based on lag model. The Basin lag is estimated as 0.6*time of concentration.

i. *Soil-Moisture Accounting (SMA) Model*

The conceptual design of soil-moisture accounting model is as shown in Figure 3.11. Water is stored on the canopy, in surface depressions, in the soil profile, and in two groundwater layers. Canopy storage is considered as an initial loss that must be satisfied before any precipitation reaches the soil surface. Infiltration is deduced as the precipitation that exceeds the canopy storage capacity. Precipitation that cannot be infiltrated is allocated to depression storage. Overflow from depression storage becomes surface runoff. Canopy interception is computed for both pervious and impervious parts of the subbasin. Infiltration or depression-storage losses are not deducted from precipitation in case of impervious surfaces. Water is removed from canopy storage by evaporation. Water is removed from depression storage by evaporation and infiltration. The soil-moisture accounting model assumes that the potential infiltration rate decreases linearly with increasing water content. Soil-moisture storage is partitioned into two zones: an upper zone and a tension zone. Water is removed from the upper zone by evapotranspiration (ET) and by percolation to the upper groundwater layer. Water is removed from the tension zone by ET but not by percolation. Water is extracted from the tension zone only when the upper-zone storage is depleted. The rate of percolation between two adjacent layers depends on a user-specified maximum rate and the degrees of saturation of the two layers. The two groundwater layers are optional, the upper groundwater layer can be used to account for shallow subsurface flow processes such as drainage of saturated hill slopes. The lower groundwater layer can represent a more extensive aquifer that is hydraulically connected to the stream. Lateral outflow from the groundwater layers can be routed to the stream as baseflow (Fleming and Neary 2004).
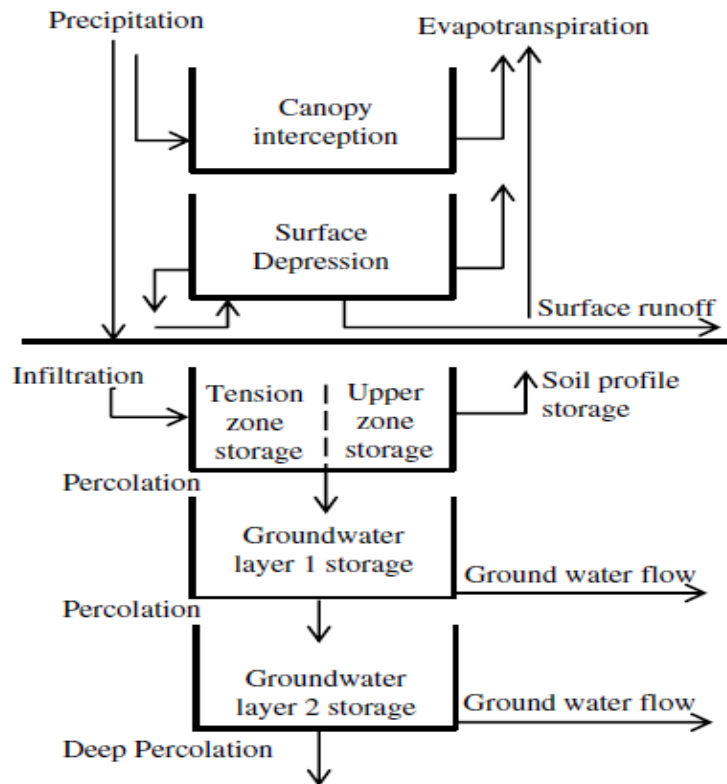
Figure 3.11 Schematic diagram of HEC-HMS soil-moisture accounting model

ii. Clark Unit-Hydrograph Method

The processes of translation and attenuation dominate the movement of flow through a watershed. Translation is the movement of flow down the gradient through watershed in response to gravity. Attenuation results from the frictional forces and channel storage effects that resist the flow. The translation of flow through the watershed could be described by a time-area curve, which expresses the curve of the fraction of watershed area contributing runoff to the watershed outlet as a function of time since the start of effective precipitation. Effective precipitation is that precipitation that is neither retained on the land surface nor infiltrated into the soil. The time-area curve is bounded in time by the watershed T_C. Thus, T_C is a hydrograph parameter of the Clark unit-hydrograph method. Attenuation of flow can be represented with a simple, linear reservoir for which storage is related to outflow as (Straub et al. 2000):

74

$$S = RO \tag{3.20}$$

where,

S is the watershed storage,

R is the watershed-storage coefficient, and

O is the outflow from the watershed.

iii. Linear Reservoir Model

The linear reservoir baseflow model is used in conjunction with the continuous SMA model. This baseflow model simulates the storage and movement of subsurface flow as storage and movement of water through reservoirs. The reservoirs are linear: the outflow at each time step of the simulation is a linear function of the average storage during the time step. The outflow from groundwater layer 1 of the SMA is inflow to one linear reservoir, and the outflow from groundwater layer 2 of the SMA is inflow to another. The outflow from the two linear reservoirs is combined to calculate the total baseflow for the basin (HEC-HMS Manual).

3.6.2 Calibration of the Model

It was necessary to establish values for 19 parameters to model hydrological processes in each sub-basin: 12 for the SMA model, 2 for Clark's model, 4 for the independent linear storage tanks model used to represent baseflow and 1 for Lag method of routing. Furthermore, 5 parameters corresponding to the initial content of canopy and surface storage included in the SMA model had to be considered. The list of parameters considered for the present study as given in Table 3.6. In the present study attempt has been made to optimize model parameters through the process of calibration by considering four years input data between years 2003-2006, in order to get goodness of fit between computed and observed streamflow, which was decided based on RMSE and Nash Sutcliffe Efficiency, through manual calibration procedure.

The model parameters related to infiltration and soil layer were considered based on the laboratory measurement, characterization and spatial interpolation of soil physical and hydraulic properties. The details of laboratory measurement are as follows:

I. *Laboratory Measurement and Characterization of Soil Physical and Hydraulic Properties*

Soil is one of the highly heterogeneous natural resources on earth surface. The soil physical and hydraulic properties have greater influence on hydrological processes including baseflow, infiltration and ground water flow. Soil layer acts as a boundary which separates rainfall into runoff and infiltration. Primary reason for the poor management of ground water resources is due to the insufficient knowledge about hydraulic properties of the soil formations. So, the knowledge of hydraulic properties of soil is significant for the improved planning and management of water resources. Soil hydraulic properties depend mainly on soil structure, soil texture, organic matter content, and bulk density. Soil properties are spatially variable; hence, to simulate realistic field conditions, a large number of samples are required. The continuous modeling of streamflow using semi-distributed models such as HEC-HMS requires soil physical and hydraulic properties. Therefore, soil samples were collected from Netravati river basin for estimating soil properties. The NBSS LUP has provided soil map of Netravati river basin that includes description of seven soil classes. By keeping NBSS LUP map as reference, 38 soil samples were collected at 0.5m and 1m depth in 19 sampling locations. The soil samples were collected at 0.5m and 1m depth because surface soil properties have the greatest effect on hydrology (infiltration, soil moisture retention and water holding capacity). The physical and hydraulic properties of soil measured in laboratory include bulk density, particle size distribution, organic matter content and hydraulic conductivity. The spatial variability of soil properties was analyzed by using three interpolation techniques such as Ordinary Kriging (OK), Inverse Distance Weighting (IDW) and Radial Basis Function (RBF).

Table 3.6 Initial model parameter values assigned under different models

Model	Parameter	Initial Value	Reference
Canopy Method	1. Initial Storage (%)	5-25	Dijk and Bruijnzeel 2001
	2. Max Storage (MM)	1-9	Grimmond and Oke 1991
	3. Crop Coefficient	1	Hamel and Guswa 2015
			Sridhar 2007
Surface Method	4. Initial Storage (%)	1-5	Garcia et al. 2008
	5. Max Storage (MM)	6.4-9.4	
Loss Method-SMA Model	6. Soil (%)	25-40	Garcia et al. 2008
	7. Groundwater 1 (%)	50-65	
	8. Groundwater 2 (%)	40-75	
	9. Maximum Infiltration (MM/HR)	3-5	
	10. Impervious (%)	0.5-4.5	
	11. Soil Storage (MM)	50-85	
	12. Tension Storage (MM)	50-68	
	13. Soil Percolation (MM/HR)	1-8	
	14. GW 1 Storage (MM)	456-767	
	15. GW 1 Percolation (MM/HR)	1.5-2.25	
	16. GW 1 Coefficient (HR)	0.04-0.1	
	17. GW 2 Storage (MM)	330-671	
	18. GW 2 Percolation (MM/HR)	0.75-1.1	
	19. GW 2 Coefficient (HR)	0.01-0.2	
Transform Method: Clark Unit Hydrograph	20. Time of Concentration (HR)-Kirpich method	5.3-9.73	Straub et al. 2000
	21. Storage Coefficient (HR)	1.38-3.95	
Baseflow Method: Linear Reservoir Model	22. GW 1 Initial Discharge (M3/S)	0.0014-0.0043	HYSEP Method
	23. GW 2 Initial Discharge (M3/S)	0.00014-0.00043	
Routing Method: Lag Model	24. Lag time (Minutes)	0-316	HEC-HMS manual

*i. **Bulk Density:*** Bulk density is an indicator of soil compaction. It is calculated as the weight of soil divided by its volume as given in Equation 3.21. This volume includes the volume of soil particles and the volume of pores among soil particles. Bulk density is typically expressed in g/cm^3 and is dependent on soil texture, densities of soil mineral (sand, silt, and clay) and organic matter particles, as well as their packing arrangement.

$$Bulk\ density = \frac{Weight\ of\ dry\ soil}{Volume\ of\ soil}$$

(3.21)

ii. Particle-size distribution: The particle size distribution (also called grain size distribution) is one of the most important characteristics of the soil. It has an effect on many properties of the soil such as the ease of tillage, the capillary conductivity of soil, the available moisture, the permeability of soil, compaction, etc. Particle size analysis is the standard laboratory procedure for the determination of the particle size distribution of soil and it is required in classifying the soil (Lambe 1967). The mechanical sieve analysis was performed to determine the particle sizes larger than 0.075 mm and the hydrometer method (Figure 3.12) was used to determine the particle sizes smaller than 0.075 mm. clay is defined as particles with diameter less than 0.005 mm. Silt has a particle diameter ranges from 0.005 mm to 0.05 mm and sand has particle diameter ranges from 0.05 mm to 1mm. Larger particles with grain sizes greater than 1 mm were considered as gravels (Punmia et al. 2005). The triangular classification of U. S. Public Roads Administration, textural classification system was used to categorize the soil based on the percentage of sand, silt and clay sizes (Figure 3.13).

Figure 3.12 Experimental setup of Hydrometer analysis
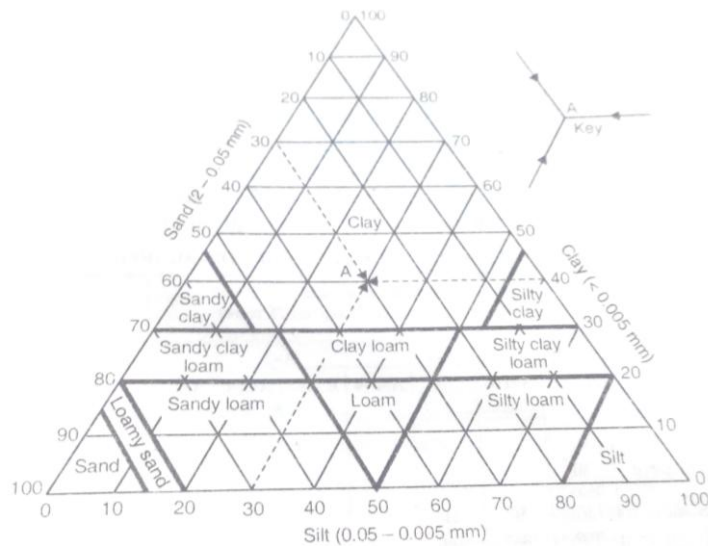
Figure 3.13 Textural classification chart: U. S. Public Road Association

iii. Organic matter content: Organic matter in soils is widely distributed over the earth's surface occurring in almost all terrestrial and aquatic environments (Schnitzer, 1978). Soils contain a large variety of organic materials ranging from simple sugars and carbohydrates to the more complex proteins, fats, waxes, and organic acids. Walkley and Black, (1934) method for determining the soil organic matter (OM) content uses a specified volume of acidic dichromate solution reacting with a determined amount of soil in order to oxidize the OM (Figure 3.14 a).

iv. Saturated hydraulic conductivity (k_s): Soil saturated hydraulic conductivity is one of the most important soil hydraulic parameters as it charecterizes the soil's ability to transmit water. It is a fundamental input for modeling runoff, drainage, and movement of solutes in soil. In laboratory, the value of k_s can be determined by several different instruments and methods such as permeameter, pressure chamber and consolidometer. In this study, falling head method using permeameter was used to determine k_s (Figure 3.14 b).

Figure 3.14 Experimental setup of a) Organic matter content test and b) Saturated hydraulic conductivity test

II. *Spatial Interpolation using Geostatistical Wizard*

The spatial distribution maps of soil properties such as sand, silt, clay, saturated hydraulic conductivity, organic matter content and bulk density were prepared by using three different interpolation techniques. First step is to select appropriate interpolation technique. In order to select the appropriate technique, the predicted results obtained from different techniques were compared with observed values. A technique is considered accurate when the root mean square error is approaching zero. The second step is to choose a suitable semivariogram model in case of kriging interpolation technique. The soil samples were divided into training and validation data sets. The training data set was utilized for preparing the semivariogram model and validation data set was to test the developed model. Validation statistics obtained for each model were compared as in the earlier step for selecting appropriate interpolation technique. Based on the validation statistics, the techniques selected for preparing spatial distribution maps of soil properties include Ordinary Kriging, Inverse Distance Weighting (IDW) and Radial Basis Function. The present study used power factor p=2 for IDW spatial interpolation; a greater value of p gives more weight to closer observations.

3.7 RELATIONSHIP BETWEEN HYDROLOGICAL RESPONSE AND LANDUSE CHANGE PATTERN

In the present research work, an effort has been made to assess the potential of mean monthly rainfall-runoff polygons in explaining the rainfall-runoff transformation processes in two contrasting catchments -Netravati river basin (Humid) and Harangi catchment (Sub-humid). This study specifically focuses on: i) the applicability of monthly rainfall-runoff polygons in explaining hydrological processes in contrasting catchments in humid and sub-humid environment, ii) the relationship between changes in hydrological response and LU/LC change pattern.

The detailed systematic approach adopted to analyse the relationship of climate variability and LU/LC change with hydrological response of two hydrologically different catchments is as shown in Figure 3.15. The study determined the mean monthly and annual runoff coefficient at Netravati river basin and Harangi catchment for period 1, period 2 and period 3. The details of three periods are given in Table 3.7. The data used for the study includes rainfall, discharge, toposheet, and satellite images. Measured daily discharge time series data at Bantwal station of Netravati river basin and Kudige station of Harangi catchment was collected from Central Water Commission (CWC), Pune, India. The corresponding recorded daily rainfall time series data was collected from Indian Meteorological Department (IMD), Pune, India. The raingauge stations considered for analysis in Netravati river basin include Bantwal, Belthangady, Dharmasthala, Mani, Subramanya, Koila/Puthur, Kokkada, and Sunkadakatte, whereas Harangi catchment includes Galibeedu, Harangi, Madapur, Merkera, Somawarapete, Kudige and Surlabi. The data consist of daily time series observation from 2003-2010 in Netravati river basin and 2005-2012 in Harangi catchment.

Table 3.7 The period of analysis: period 1, period 2 and period 3 in Netravati river basin and Harangi catchment

Period of Analysis	Netravati river basin		Harangi catchment	
	LU/LC Map	Rainfall and Runoff data	LU/LC Map	Rainfall and Runoff data
Period 1	2005	2003, 2004, 2005	2007	2005, 2006, 2007
Period 2	2007	2005, 2006, 2007	2010	2008, 2009, 2010
Period 3	2010	2008, 2009, 2010	2013	2010, 2011, 2012
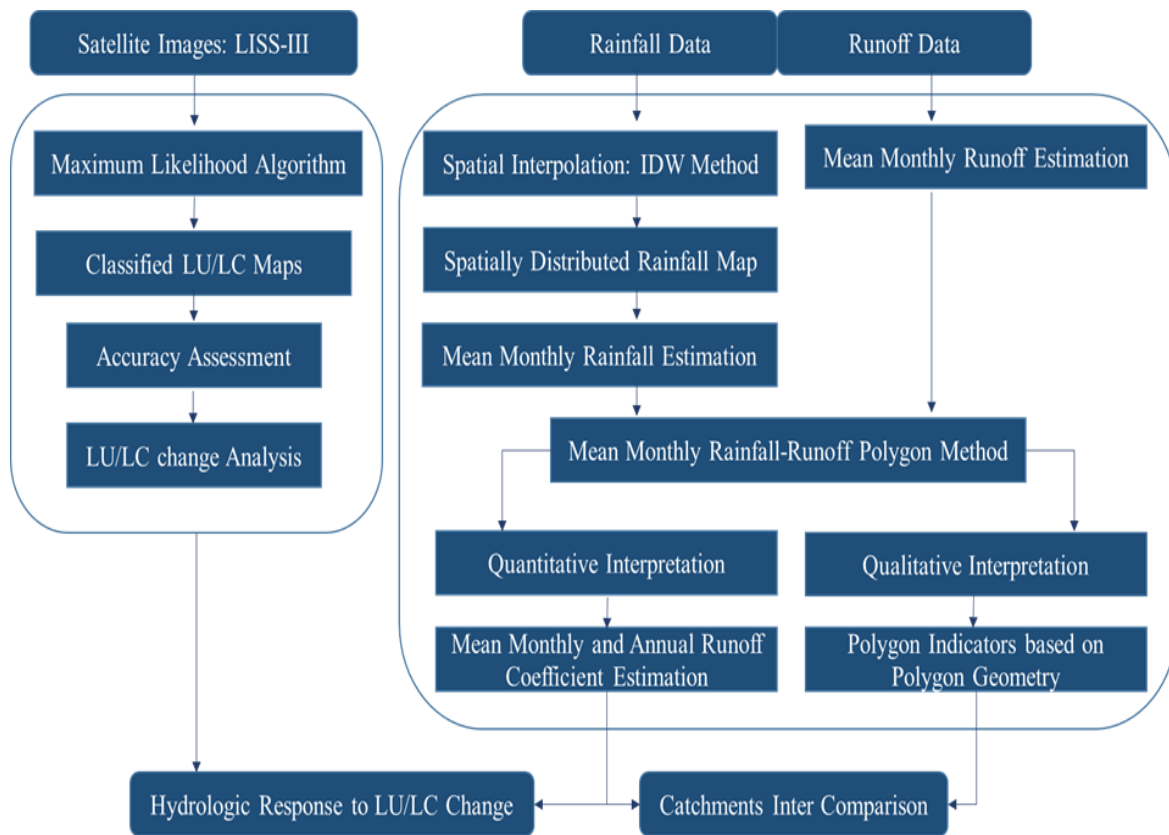
Figure 3.15 Methodology adopted to analyze hydrologic response to LU/LC change and catchment comparison

3.7.1 LU/LC Classification and Change Analysis

The satellite images of IRS-P6, LISS III multispectral sensor data collected from NRSC, Hyderabad, India were used for the preparation of LU/LC maps for the years 2005, 2007 and 2010 of Netravati river basin and the years 2007, 2010 and 2013 of Harangi catchment. The previously classified LU/LC maps of both the study areas were used here for analysing the hydrologic response to LU/LC change.

3.7.2 Spatial Interpolation of Rainfall

The measured rainfall data was available for raingauge stations distributed uniformly over the study areas. A well-known spatial interpolation method namely Inverse Distance Weighting (IDW) method was used to obtain the average areal rainfall in the study catchments. Then the mean monthly rainfall and runoff were estimated for the study periods.

3.7.3 Mean Rainfall-Runoff Polygon Method

The rainfall-runoff polygon is constructed on a cartesian co-ordinate system by plotting rainfall v/s runoff and connecting each point by drawing line on a month to month basis (Kadioglu and Sen 2001; Nazir et al., 2015; Ali et al., 2014). The hydrological response characteristics of two contrasting study areas were expressed and interpreted through quantitative and qualitative approaches.

i. *Quantitative Interpretation*

The runoff coefficient is one of the important factors representing the hydrological response of any watershed which is calculated as the ratio of runoff to precipitation. In the present research work, the mean monthly runoff coefficient was estimated as the arithmetic average of the preceding and current month's runoff coefficients (Kadioglu and Sen 2001; Nazir et al., 2015).

$$RC_m = \frac{\sum (R_{rc} + R_{rp})}{2}$$

(3.22)

where, RC_m is mean monthly runoff coefficient

R_{rc} is runoff to rainfall ratio of current month

R_{rp} is runoff to rainfall ratio of preceding month

The average annual runoff coefficient was calculated as the arithmetic average of 12 months coefficient values.

$$RC_a = \frac{\sum RC_m}{12}$$

(3.23)

where, RC_a is the average annual runoff coefficient.

ii. Qualitative Analysis

The qualitative interpretation of monthly runoff coefficients was carried out based on the features of polygon geometry, as shown in Figure 3.16 (Nazir et al., 2015). The detailed interpretation is as follows:

1. Variability of annual hydrological cycle

    Polygon criterion: Polygonal side

    The polygon sides represent the change in average values of precipitation or runoff for preceding months. All sides connected together form a closed polygon representing the natural balance between precipitation runoff conversions in a year. The end point of polygon is the mean runoff coefficient for a particular month.

2. Seasonality behavior of mean rainfall and runoff

    Polygon criterion: order of polygon side

    Each polygon consists of rising order of sides as well as falling order. Normally, the runoff coefficient associated with rising order is higher in comparison with falling order. This indicates the seasonality in the mean monthly runoff coefficient. During rising sequence, the catchment becomes wetter with time, whereas along the falling sequence the same catchment becomes drier. This explains one of the important

natural processes namely precipitation is the main contributor for runoff generation during rising order, whereas falling order symbolizes more contribution from groundwater flow and baseflow to runoff than precipitation. It is important to consider the direction of time around the polygons to advise about inter-annual variation in the monthly runoff coefficient (Ali et al., 2014).
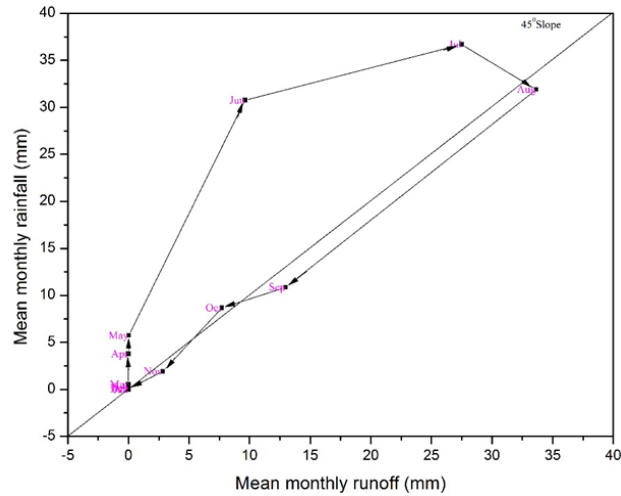
Figure 3.16 Mean monthly rainfall-runoff polygon

3.   Temporal trend detection

Polygon criterion: size and shape of polygon

This is one of the important criterions to explain about the linearity and nonlinearity of the relationship between rainfall and runoff. A narrow polygon constitutes smaller polygonal area indicating the consistency of the monthly rainfall and runoff coefficients. The narrow polygon represents the uniformity of representative runoff coefficient for the catchment under study. Wider polygon implies the temporal heterogeneity of the runoff coefficient in the catchment due to the influence of factors such as evapotranspiration, retention, infiltration contributing to baseflow and groundwater storage. Mainly it explains the temporal trends of rainfall and runoff over a given period. The closeness of the slope of each side vertically or horizontally

indicates the relative amount of the rainfall and runoff in composing the numerical value of the monthly runoff coefficient.

4.   Rainfall-runoff conversion mechanism

Polygon criterion: length of polygonal peripheral and slope of overall polygon

The length of polygon side specifies the magnitude of the change in average values for consecutive months. The total amount of rainfall and runoff in any catchment under study can be estimated by adding the length of polygon peripheral. It also acts as an indicator for identifying seasonal effects on the annual hydrological cycle of the catchment. The present study considers that more precipitation is converted into runoff when the overall slope of the polygon with respect to the horizontal axis is smaller.

5.   Groundwater, baseflow contribution and evapotranspiration (ET)

Polygon criterion: slope of each polygon sides

A steep slope signifies that the volume of runoff not only depends on rainfall contribution but also have significant influence of ground water recharge, baseflow pattern and evapotranspiration. In addition, the steep slope of the polygon side of a month is considered as the dry month that is influenced by groundwater recharge and ET (Nazir et al., 2015).

3.8 SUMMARY

This chapter presented the detailed course of action adopted to address the research objectives under four different sections including LU/LC change analysis and prediction, estimation of actual ET using satellite images, studying the applicability of semi distributed model for streamflow estimation and comparison of hydrologic response characteristics of humid and sub-humid catchments to LU/LC change. The results obtained by adopting these methodologies will be provided and discussed in Chapter 4-Results and Discussion.

4.1 GENERAL

The increase in population growth and urbanization are leading to the conversion of vegetation rich areas into human settlements and infrastructure development hotspots, which restricts the sustainable development of regional environment. This will significantly vary the hydrological fluxes of the river basin, which in turn decreases the infiltration, canopy storage and water storage of basin. The change in vegetation cover influences the different hydrological processes including runoff, Evapotranspiration (ET), and baseflow. Hence, the present research work intends to carry out a detailed analysis to ascertain the hydrological response to spatio-temporal changes taking place in humid and sub-humid catchments of Karnataka state, India. The chapter presents the results of analysis described in methodology chapter. This chapter also consists of four different themes discussed under following sections:

- Prediction of future trends in LU/LC pattern of Netravati river basin and Harangi catchment.

- Actual ET and Land Surface Temperature (LST) estimation using satellite images

- Streamflow estimation using continuous hydrologic modelling

- Comparison of hydrologic response characteristics of two contrasting catchments

4.2 PREDICTION OF FUTURE TRENDS IN LU/LC PATTERN

4.2.1 LU/LC Dynamics in Netravati River Basin

The LU/LC changes of the study area for the years 2005, 2007 and 2010 were studied and LU/LC maps and area changes are as shown in Figure 4.1 (a), (b) and (c) and Table 4.1, respectively. The study has classified the satellite images using three classification algorithms - Maximum likelihood algorithm, Minimum distance to

mean algorithm and Parallelepiped algorithm. The detailed accuracy assessment of classified maps by all the three algorithms was done for satellite images of Harangi catchment. Therefore, the accuracy of the classified maps of Netravati river basin was evaluated only based on the Kappa value. It is observed that Kappa value with respect to the Maximum likelihood algorithm is 0.73, which is the highest compared to parallelepiped (0.58) and minimum distance to mean algorithm (0.55). All the three algorithms have come across confusion while classifying land with or without scrub, built-up land, and fallow land, because more or less similar signatures characterize these three classes. Also, algorithms failed to discriminate among plantation and forest area because their reflectance values are close to each other. Therefore, the classification accuracy can be improved by considering more representative signatures, using high spectral resolution images etc.,
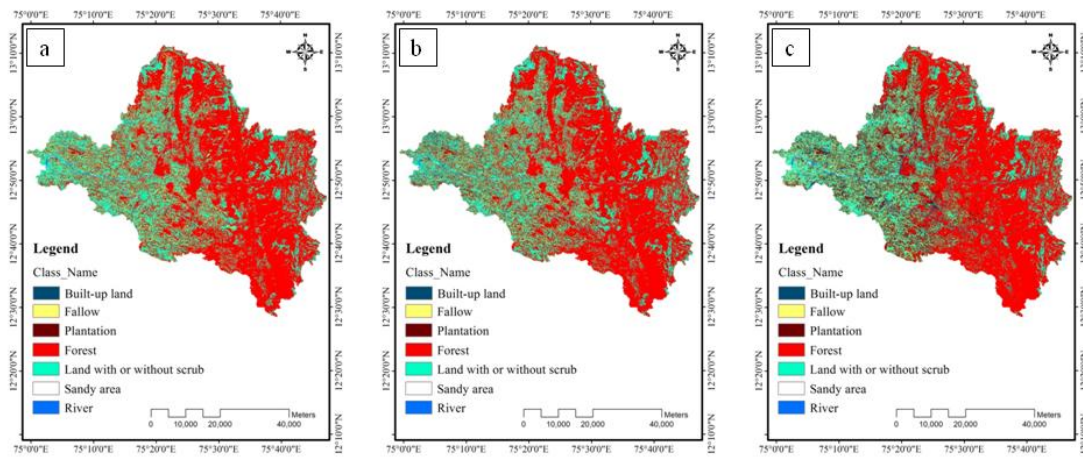
Figure 4.1 LU/LC maps for the years a) 2005, b) 2007 and c) 2010 of Netravati river basin

Table 4.1 LU/LC distribution in Netravati river basin for the years 2005, 2007 and 2010 and change in area

LULC class	Year			Change in Area (sq. km)	
	2005 (sq. km)	2007 (sq. km)	2010 (sq. km)	2005-2007	2007-2010
Built-up land	74.16	146.80	**200.94**	72.64	54.13
Fallow	377.55	374.21	358.63	-3.34	-15.57
Plantation	203.59	293.75	**445.47**	90.16	151.71
Forest	1801.18	1695.84	1603.56	-105.34	-92.28
Land with or without scrub	793.89	735.56	639.36	-58.33	-96.19
Sandy area	9.63	19.99	16.66	10.36	-3.32
River	28.25	22.15	23.68	-6.1	1.54
Total	**3288.3**	**3288.3**	**3288.3**	**0**	**0**

i. Change Detection Analysis during 2005-2010

The post classification change detection technique has been adopted to analyze the LU/LC change between the years 2005 and 2010 (Table 4.1). Based on the results of accuracy assessment process, the LU/LC statistics obtained using Maximum likelihood algorithm, which gave better accuracy with 0.73 Kappa value, has been utilized for further analysis in the study.

LU/LC change during 2005 – 2007

The results show that, the built-up land and plantation are increased from 74.16-146.80 sq.km, 203.59-293.75 sq. km respectively. The fallow land, forest area, and land with or without scrub are decreased from 377.55-374.21 sq.km, 1801.18-1695.84 sq.km, and 793.89-735.56 sq.km respectively. The increase in the population growth and industrial expansion has led to the conversion of land with or without scrub into built-up land. In the process of improving the agricultural productivity, most of the forest areas are converted into plantations.

LU/LC change during 2007 - 2010

The noteworthy change is observed under classes such as built-up land, plantation, forest area, fallow land and land with or without scrub. In specific, built-up land and plantation are drastically increased from 146.80-200.94 sq.km and 293.75-445.47 sq.km, respectively. In contrast, the fallow land, forest area, and land with or without scrub have shown a decreasing trend of 374.21-358.63 sq.km, 1695.84-1603.56 sq.km

and 735.56-639.36 sq.km respectively. There is a slight variation in the water body and sandy area also.

LU/LC change during 2005 - 2010

The LU/LC change detection results for the years 2005 and 2010 indicated a drastic change in forest area, plantation and built-up land among all other classes (Table 4.4). Forest area is found to be the most dominant class among other classes in 2005 and has decreased drastically during 2010 from 1801.18 sq.km to 1603.56 sq.km. Eventually, there is an abrupt increase in built-up land from 74.16 sq.km to 200.94 sq.km and plantation from 203.59 sq.km to 445.47 sq.km during 2005 and 2010, respectively. This may be because most of the forest and land with or without scrub have been converted to plantation. The result shows an increase in population and built-up land expansion, promoting the conversion of land with or without scrub to built-up land. The changes in water and sandy area are interdependent, as when water spread area increases, the amount of sandy area decreases and vice versa. This relationship is valid for the present study also, as per the values provided in Table 4.1.

4.2.2 LU/LC Dynamics in Harangi Catchment

A spatio-temporal quantification of changes in the land use pattern of Harangi catchment during 2007-2013 was performed using three classification algorithms. The classified LU/LC maps and graphical representation of area changes for the years 2007, 2010, and 2013 are shown in Figure 4.2 and 4.3, 4.4 and 4.5, 4.6 and 4.7 respectively. The classification was carried out using three different methods - Maximum likelihood algorithm, Minimum distance to mean algorithm and Parallelopiped algorithm and the classified area of different LU/LC classes are given in Table 4.2.

Figure 4.2 Classified images of Harangi catchment using Maximum Likelihood Algorithm for years a) 2007, b) 2010 and c) 2013

Figure 4.3 Graph of LULC change for years 2007, 2010 and 2013 in Harangi catchment using Maximum Likelihood Algorithm
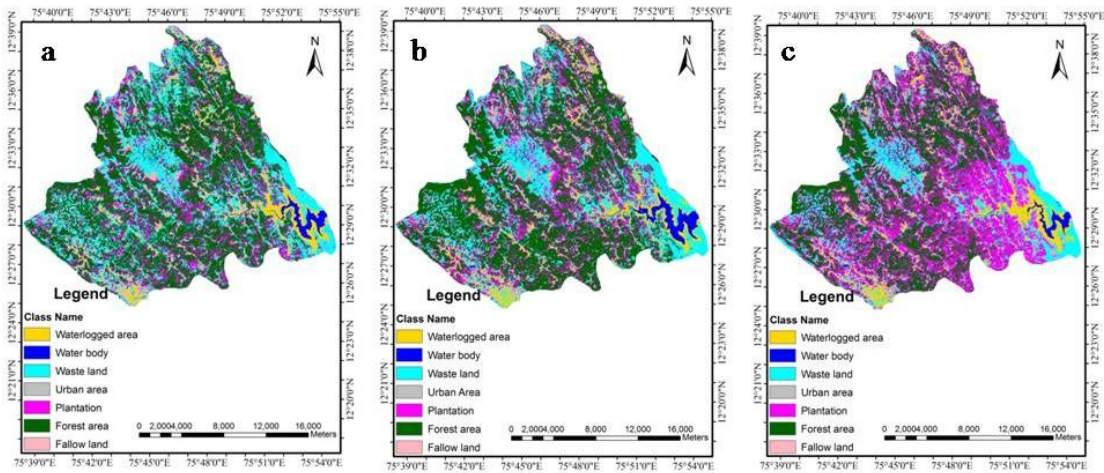
Figure 4.4 Classified images of Harangi catchment using Parallelepiped Algorithm for years a) 2007, b) 2010 and c) 2013
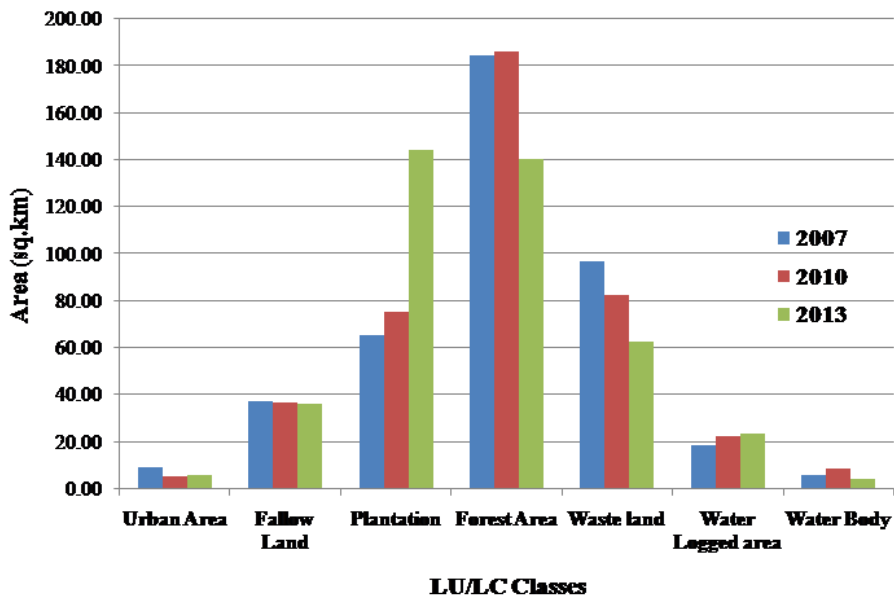
Figure 4.5 Graph of LULC change for years 2007, 2010 and 2013 in Harangi catchment using Parallelepiped Algorithm
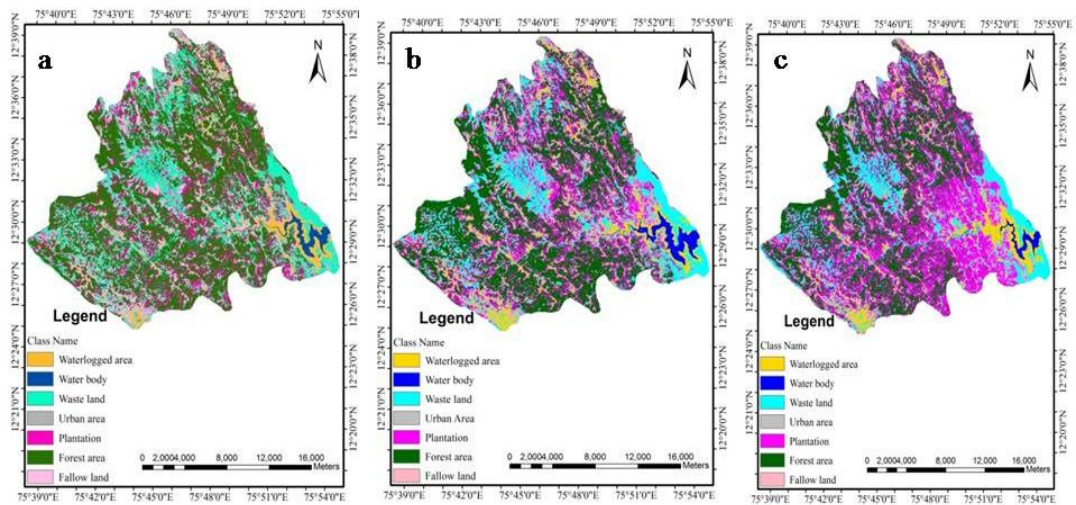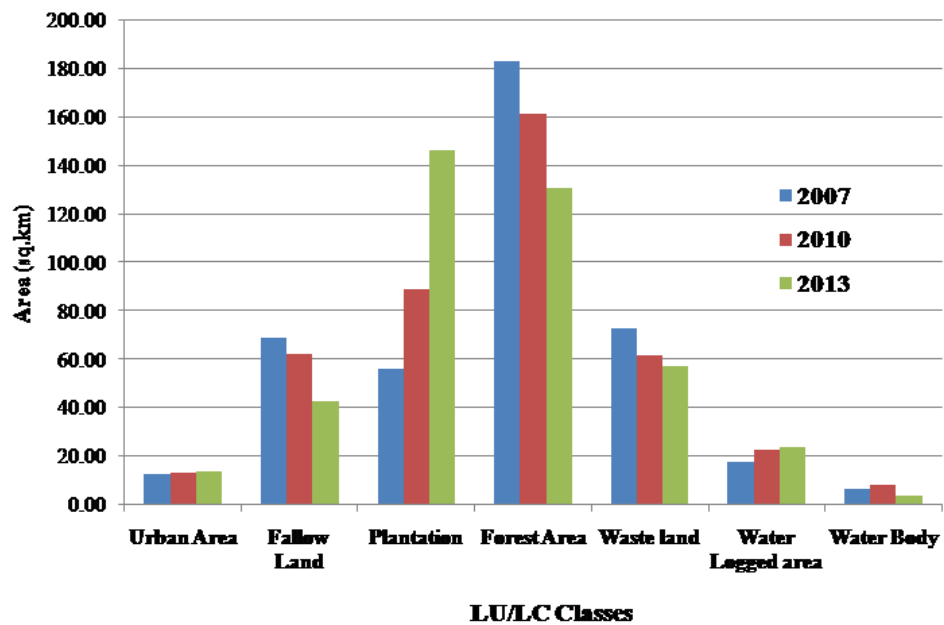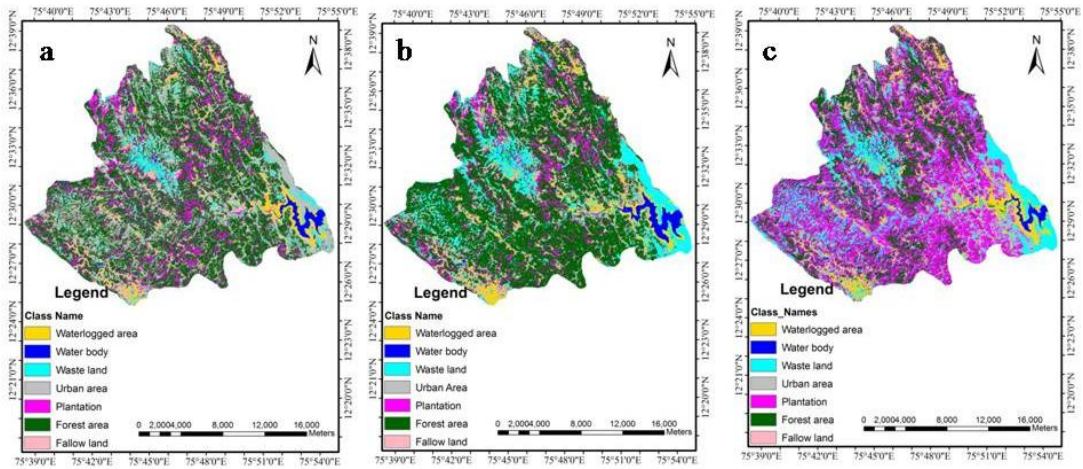
Figure 4.6 Classified images of Harangi catchment using Minimum Distance to Mean Algorithm for years a) 2007, b) 2010 and c) 2013
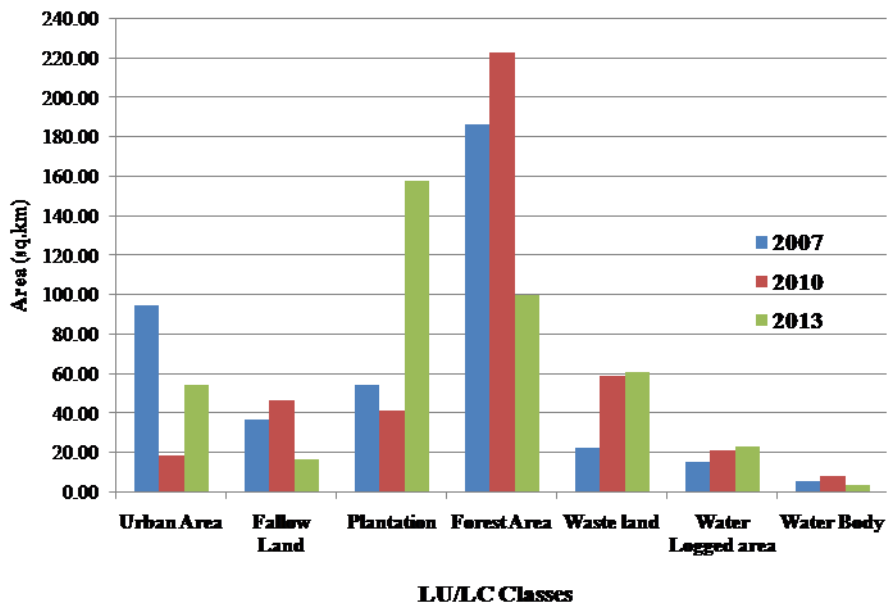
Figure 4.7 Graph of LULC change for years 2007, 2010 and 2013 in Harangi catchment using Minimum Distance to Mean Algorithm

Table 4.2 Results of LU/LC classification of Harangi catchment using Maximum likelihood, Parallelepiped and Minimum distance to mean algorithm

Methods & Year / LU/LC Classes	Maximum Likelihood Algorithm (km²)			Parallelepiped Algorithm (km²)			Minimum Distance to Mean Algorithm (km²)		
	2007	2010	2013	2007	2010	2013	2007	2010	2013
Urban Area	13.07	13.35	13.72	9.39	5.76	6.15	95.07	18.59	54.92
Fallow Land	68.90	62.38	42.63	37.38	37.19	36.49	37.14	46.95	17.16
Plantation	56.07	88.91	146.55	65.34	75.64	144.11	54.92	41.50	158.16
Forest Area	183.12	161.37	131.02	184.77	186.48	140.53	186.98	222.81	99.95
Waste land	72.86	62.00	57.15	97.00	82.41	63.07	22.77	59.35	61.28
Water Logged area	17.99	22.56	23.81	18.72	22.37	23.93	15.70	21.36	23.21
Water Body	6.71	8.14	3.83	6.11	8.86	4.43	6.14	8.16	4.03
Total	418.71	418.71	418.71	418.71	418.71	418.71	418.71	418.71	418.71

The detailed accuracy assessment of classified maps was carried out by estimating the Kappa value and overall accuracy. The results of accuracy assessment is as given in Table 4.3. It is observed that Kappa value with respect to the Maximum likelihood algorithm is 0.81 which is the highest value compared to parallelepiped (0.71) and minimum distance to mean algorithm (0.68). A Kappa value of 0.75 or greater indicates a good degree of classification. There is no simple way to evaluate the errors in the classification associated with change detection. In addition to the errors generated in the classification of single date satellite image, the analyst must contend with the propagation of errors in the classification of second-date satellite image, the change-detection algorithm, registration and radiometric differences between the images of different dates. In the present research work, the accuracy was assessed based on overall accuracy and Kappa coefficient. Overall accuracy refers to the proportion of agreement between a classification result and the reference data at certain specific locations. Kappa coefficient is a more discerning statistical parameter for comparing the accuracy of different classifiers and offers better interclass discrimination than the overall accuracy measure. The results of accuracy assessment process shows that, the overall accuracy and kappa coefficient for Maximum

likelihood algorithm, Parallelepiped algorithm and Minimum distance to mean algorithm are 89.36%, 81.47% and 78.67% and 0.81, 0.71 and 0.68 respectively (Table 4.3). The graphical representation of the results obtained from three classification algorithm shows that the area distribution under different land use categories varies drastically from one algorithm to another algorithm (Figure 4.3, 4.5 and 4.7). Hence, accuracy assessment process was used to take decision regarding the selection of efficient classification algorithm. Results indicate a decrease in Kappa value from the Maximum likelihood algorithm to the Parallelepiped algorithm, and from the Parallelepiped algorithm to the Minimum distance to mean algorithm. This general trend indicates that the Maximum likelihood algorithm is the most accurate, followed by the Parallelepiped algorithm and the least accurate method would be the Minimum distance to mean algorithm.

Table 4.3 Kappa values and overall classification accuracy of three different classification algorithms for the LU/LC maps of the year 2013 in Harangi catchment

2013 LU/LC map Methods	Kappa Value	Overall Classification Accuracy [%]
Maximum Likelihood Algorithm	0.81	89.36
Parallelepiped Algorithm	0.71	81.47
Minimum Distance to Mean Algorithm	0.68	78.67

Minimum distance to mean algorithm provided less accurate classification results. Because, it has misclassified four LULC classes such as urban area, plantation, fallow land and forest area. It can be observed clearly in the LU/LC maps and graph of Minimum distance to mean algorithm (Figure 4.6 and 4.7). The result of Parallelepiped algorithm also shows less efficiency compared to Maximum likelihood algorithm, because of misclassification of three land use classes such as urban area, plantation and forest area (Figure 4.4 and 4.5). Even though Maximum likelihood algorithm provided classified LU/LC maps with 89.36 % accuracy, it has failed to represent spatial distribution of urban area and it has misclassified waste land and fallow land as urban area (Figure 4.2). All the three algorithms have come across confusion while classifying waste land, urban area, fallow land and waterlogged area.

The major reason for misclassification that has been done by these algorithms is due to poor performance of algorithms in distinguishing waste land, fallow land and urban area. Since, these three classes are characterized by more or less similar signatures. Similarly, algorithms failed to distinguish between forest area and plantation as they are represented by similar tones of red in False Colour Composite (FCC) image. The accuracy of classification can be improved by including more number of representative signatures for each class, using high resolution satellite images, using secondary data such as study area knowledge from field survey and Google Earth maps etc.,

i. Change Detection Analysis during 2007-2013

The postclassification change detection technique was adopted to analyse the LU/LC change between the years 2007 and 2013 (Table 4.4). Based on the results of accuracy assessment process, the LU/LC statistics obtained using Maximum likelihood classifier, which gave better accuracy with 0.81 Kappa value, was utilized for studying the change. The forest land, fallow land and plantation are the land cover types occupying highest percentage of area in the study region, covering about 70% of the total area.

Table 4.4 Results of change detection between 2007 and 2013 in Harangi catchment using Maximum likelihood algorithm

Sl.No	LU/LC Class Name	% area			Changes in area (%)		
		2007	2010	2013	2007-2010	2010-2013	2007-2013
1	Urban Area	3.12	3.19	3.28	0.07	0.09	0.16
2	Fallow Land	16.45	14.90	10.18	-1.56	-4.72	-6.27
3	Plantation	13.39	21.23	35.00	7.84	13.77	21.61
4	Forest Area	43.74	38.54	31.29	-5.19	-7.25	-12.44
5	Waste land	17.40	14.81	13.65	-2.59	-1.16	-3.76
6	Water Logged area	4.30	5.39	5.69	1.09	0.30	1.39
7	Water Body	1.60	1.94	0.91	0.34	-1.03	-0.69
	Total	**100**	**100**	**100**	**0**	**0**	**0**

LU/LC change during 2007 - 2010

The results show that, mainly the plantation, water logged area, urban area and water body are increased from 56.07 sq.km to 88.91 sq.km, 17.99 sq. km to 22.56 sq.km, 13.07 to 13.35 sq. km and 6.71 sq. km to 8.14 sq. km respectively. The forest area, fallow land and waste land are reduced from 183.12 sq.km to 161.37 sq.km, 68.90 sq.km to 62.38 sq.km and 72.86 sq. km to 62 sq.km respectively. The major occupation of the population in Harangi catchment is agriculture. In the course of increasing the agriculture-based income, people are converting waste land, fallow land and forest area into plantation. The coffee plantation is the dominant plantation type prevailing in harangi catchment.

LU/LC change during 2010 - 2013

The notable change is observed under classes such as plantation, forest area, fallow land and waste land. In particular, a drastic increase in plantation from 88.91 sq.km to 146.55 sq.km is observed. In contrast, the forest area, waste land and fallow land have shown a decreasing trend of 161.37 sq. km to 131.02 sq. km, 62 sq. km to 57.15 sq. km and 62.38 sq. km to 42.63 sq. km. There is a slight variation in the water logged area and urban area of about 22.56 sq.km and 23.81 sq.km and 13.35 sq. km to 13.72 sq. km respectively. Harangi reservoir is located near the catchment outlet, which is the major water storage system providing water for drinking and agricultural activities in the downstream. This will have the influence on the variation of water spread area and water logged area.

LU/LC change during 2007 - 2013

The LU/LC change detection results for the years 2007 and 2013 indicated a drastic change in forest area, plantation and waste land among all other classes (Table 4.4). The forest area decreased dramatically from 183.12 sq. km to 131.02 sq. km. The waste land is decreased from 72.86 sq. km to 57.15 sq. km. Also, fallow land and water body are decreased from 68.90 sq. km to 42.63 sq. km and 6.71 sq. km to 3.83 sq. km respectively. In contrast, plantation and waterlogged area are observed to have an increasing trend of about 56.07 sq. km to 146.55 sq. km and 17.99 sq. km to 23.81 sq. km. The urban area has been increased from 13.07 sq. km to 13.72 sq. km.

The results indicate that increase in urban area from year 2007 to 2013 is because of improved living style of people in this region. As study area is a rural catchment, the main occupation is agriculture. Hence, it is observed that forest area and waste land has been decreased drastically, which have been utilized for agricultural activity specially coffee plantation. Also, there is a fluctuation in the water body and waterlogged area because of change in water level from year to year in the Harangi reservoir. Harangi reservoir is one of the important water sources for drinking and agricultural activity in the region. Overall, there is a drastic change in all LU/LC classes of the study area.

4.2.3 Land Change Modeler (LCM)

i. Application to Netravati River Basin

Land use maps for the year 2005 and 2007 were given as the input maps to calibrate the LCM model to analyse LU/LC dynamics in Netravati river basin. The gains and losses experienced by each class in terms of cells are as shown in Figure 4.8 (a) and (b). Built-up land and plantation is increased which means forest and land with or without scrub might have converted to built-up land. From the graph, it is clear that the increase in plantation is mainly due to the conversion of forest. A portion of fallow land has been used for cultivation, thereby increasing the area of plantation (Figure 4.8 (b)). The spatial pattern in the exchange between fallow land and plantation and urban and plantation classes in Netravati river basin is as shown in Figure 4.9 (a) and (b). The transition sub models were selected based on the major transitions, which are found to be useful for the prediction of future changes. The sub models and the corresponding transition probability matrix used for Netravati river basin are as shown in Table 4.5 and Figure 4.10 respectively.

Figure 4.8 a) Gains and Losses experienced by each classe and b) contributors to net change in plantation for Netravati river basin from 2005 to 2007

Figure 4.9 The exchanges between a) fallow land and plantation and b) urban and plantation for Netravati

Table 4.5 Transition sub models used in LCM for Netravati river basin

From	To	Sub-Model Name
Sandy area	River	From sandy area
Plantation	Built-up land	From plantation
Plantation	Fallow land	
Land with or without scrub	Plantation	From land with or without scrub
Land with or without scrub	Forest	
Land with or without scrub	Built-up land	
Land with or without scrub	River	
River	Land with or without scrub	From River
River	Sandy area	

Figure 4.10 Transition probability matrix for Netravati catchment derived from LCM

ii. Application to Harangi Catchment

Land use maps for the year 2007 and 2010 were given as the input maps to calibrate the LCM model to analyse LU/LC dynamics in Harangi catchment. The gains and losses experienced by each class in terms of cells are shown in Figure 4.11 (a). Forest and wasteland are experiencing a decreasing trend where as plantation and waterlogged areas had increased abruptly. Fallow land also shows a decreasing trend but the rate of reduction is very less. Figure 4.11 (b) shows the contributions to the net change experienced by plantation in Harangi catchment. The conversion of fallow land to plantation is more compared to plantation to fallow land. The spatial pattern in the exchange between fallow land and plantation and urban and plantation classes in Harangi catchment are shown in Figure 4.12 (a) and (b).

The transition sub models were selected based on the major transitions, which are found to be useful for the prediction of future changes. The sub models and the corresponding transition probability matrix used for Netravati river basin and Harangi catchment are shown in Table 4.6 and Figure 4.13, respectively.
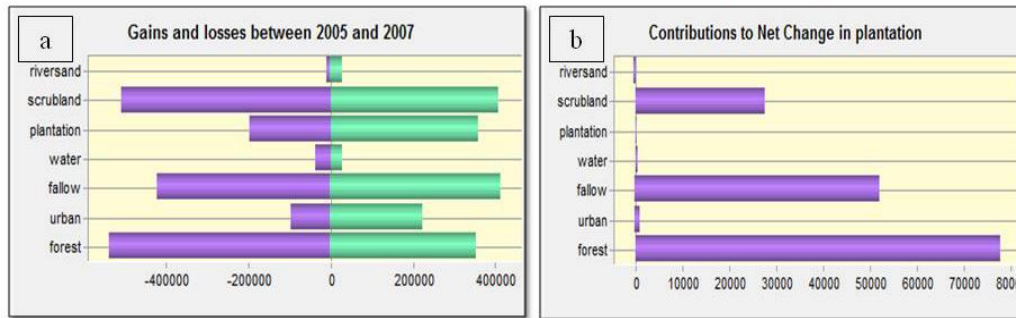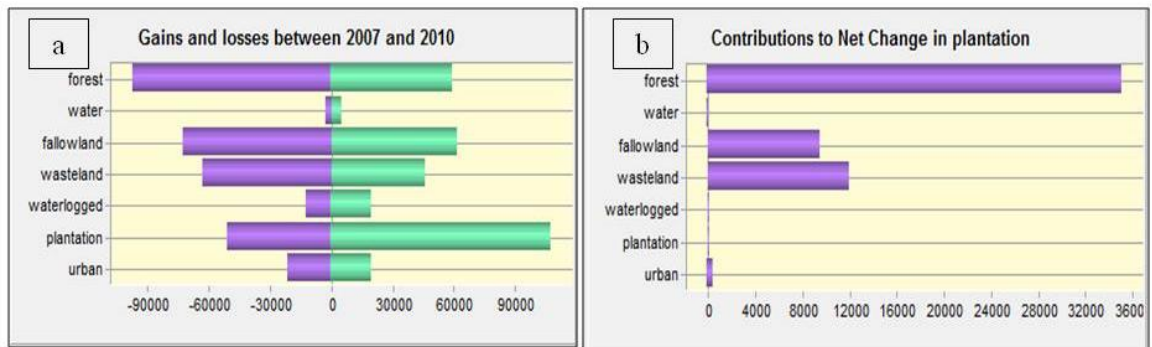
Figure 4.11 a) Gains and Losses experienced by each classes and b) contributors to net change in plantation for Harangi from 2007 to 2010
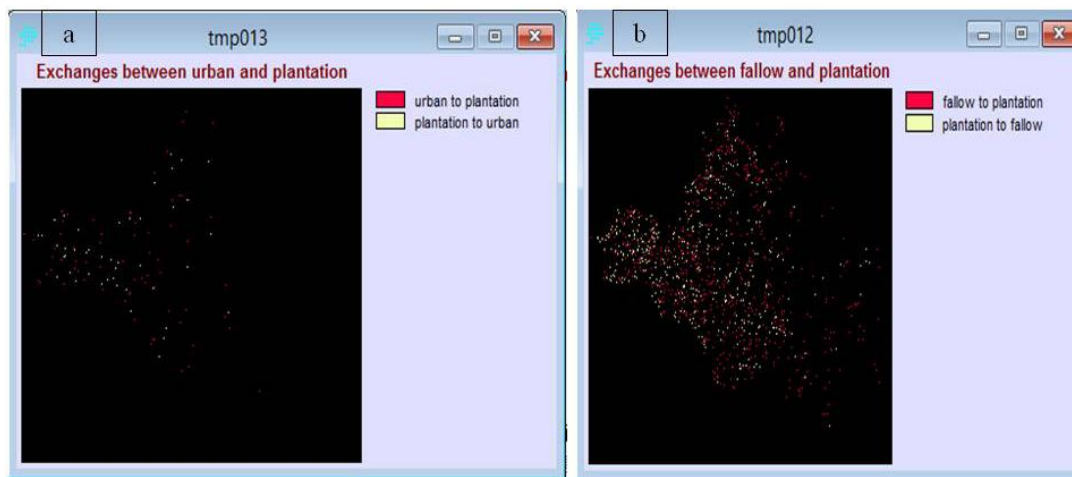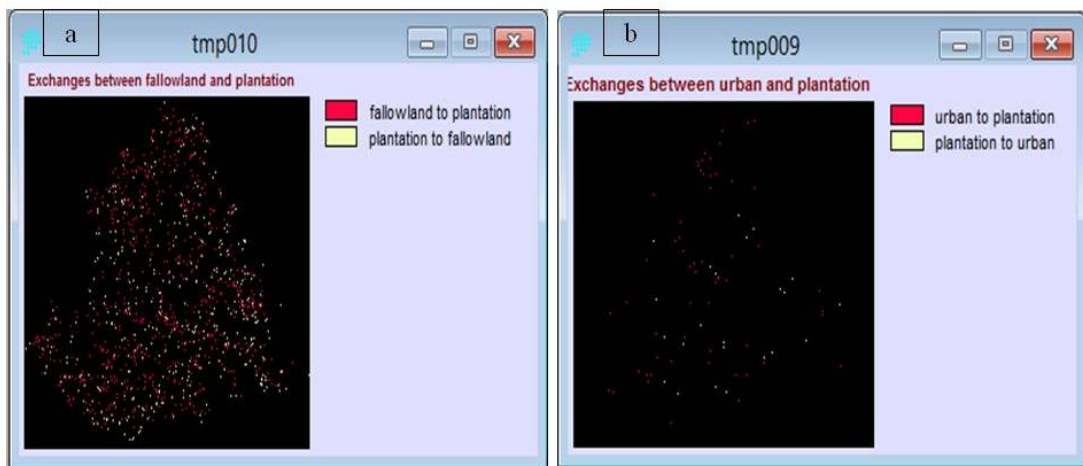

Figure 4.12 The exchanges between a) fallow land and plantation and b) urban and plantation for Harangi.

Table 4.6 Transition sub models used in LCM for Harangi catchment

From	To	Sub-Model Name
Forest	Plantation	Forest transitions
Forest	Urban	
Fallow land	Urban	Fallow land transitions
Fallow land	Plantation	
Fallow land	Wasteland	
Waste land	Plantation	Wasteland transitions
Waste land	Urban	
Water logged	Water	Waterlogged transitions

Figure 4.13 Transition probability matrix for Harangi catchment derived from LCM

4.2.4 CA-Markov Model

The generated transition probability matrix and transition area matrix by using CA-Markov model for Netravati river basin and Harangi catchment are given in Table 4.7, 4.8 and Table 4.9, 4.10, respectively. CA–Markov model used transition area matrix obtained from Markov chain analysis to predict the changes in LU/LC of the year 2010 and 2013 in Netravati and Harangi catchment, respectively.

Table 4.7 Transition probability matrix for the year 2005 and 2007 for Netravati river basin

	Forest	Urban	Fallow land	Water	Plantation	Scrubland	River sand
Forest	0.649	0.022	0.085	0.006	0.107	0.127	0.001
Urban	0.213	0.113	0.258	0.011	0.119	0.274	0.007
Fallow land	0.236	0.087	0.217	0.005	0.194	0.251	0.007
Water	0.216	0.117	0.125	0.086	0.046	0.397	0.010
Plantation	0.377	0.040	0.208	0.003	0.260	0.106	0.003
Scrubland	0.154	0.113	0.184	0.009	0.067	0.447	0.022
River sand	0.036	0.078	0.081	0.025	0.019	0.622	0.136

Table 4.8 Transition area matrix for the year 2005 and 2007 for Nethravathi river basin

	Forest	Urban	Fallow land	Water	Plantation	Scrubland	River sand
Forest	1674744	168005	201659	10140	451960	302723	6341
Urban	48823	32124	76502	3776	59527	128563	3912
Fallow land	136704	68178	107629	3627	150908	159412	4371
Water	11540	3699	5235	4691	4446	11296	741
Plantation	271970	65300	130861	2409	197734	112095	2884
Scrubland	271787	90999	206612	18074	166316	358944	11787
River sand	3548	2132	5634	501	3529	13094	818

Table 4.9 Transition probability matrix for the year 2007 and 2010 for Harangi river basin

	Urban	Plantation	Water logged	Waste land	Fallow land	Water	Forest
Urban	0.051	0.056	0.022	0.605	0.220	0.001	0.042
Plantation	0.009	0.405	0.003	0.018	0.144	0	0.418
Water logged	0.057	0.008	0.515	0.149	0.095	0.172	0.001
Waste land	0.046	0.122	0.040	0.427	0.224	0.004	0.133
Fallow land	0.106	0.200	0.131	0.156	0.333	0.001	0.068
water	0.005	0.005	0.048	0.183	0.026	0.660	0.070
forest	0.004	0.299	0.001	0.034	0.070	0.000	0.589

Table 4.10 Transition area matrix for the year 2007 and 2010 for Harangi river basin

	Urban	Plantation	Water logged	Waste land	Fallow land	Water	Forest
Urban	1104	1219	471	12988	4734	17	903
Plantation	1444	62573	485	2866	22326	2	64623
Water logged	2238	344	20190	5869	3728	6747	51
Waste land	5110	13422	4435	46724	24552	468	14638
Fallow land	11532	21727	14215	16960	36161	209	7464
water	76	76	687	2596	375	9333	993
forest	1216	83831	391	9787	19671	18	165170

4.2.5 Prediction and Validation

LCM and CA-Markov model were used to predict land use changes in Netravati river basin and Harangi catchment for the year 2010 and 2016. Validation was carried out by using the module 'validate', which compares the output image with the reference image and calculates the accuracy. For Netravati river basin, CA-Markov and LCM provided 82.13% and 80.1% accuracy respectively, where as for Harangi catchment, an accuracy of 86.6% and 80% are given by LCM and CA-Markov model respectively. The validation results show that CA-Markov model is better for future prediction in Netravati river basin (Figure 4.14 and 4.15), whereas LCM is good in predicting future changes for Harangi basin (Figure 4.16 and 4.17), because, Harangi catchment is characterized by steep slope compared to Netravati river basin and CA-Markov model is more sensitive to spatial transitions based on slope in comparison with LCM. The result of land change prediction in Netravati river basin for the year 2016 by CA-Markov model shows a decrease in forest, fallow land and land with or without scrub land between 2010 and 2016, contributing to an increase in built-up land and plantation. LCM is found to be good in predicting changes in forest and land with or without scrub, whereas all other classes are well predicted by CA-Markov model in Netravati river basin.

The predicted map for the year 2010 and 2016 in Netravati river basin (Figure 4.14 and 4.15) shows that forest area, fallow land, scrub land is decreased from 1603.59 to 1375.59 sq.km, 453.54 to 420.01 sq.km, and 639.44 to 617.61 sq.km respectively, which have contributed to the increase in plantation and urban area from 445.38 to 588.21 sq.km and 200.85 to 244.76 sq.km respectively. The projections for the year 2013 and 2016 in Harangi catchment (Figure 4.16 and 4.17) indicates that forest area, fallow land, and waste land are reduced from 129.7 to 81 sq.km, 40.23 to 25 sq.km and 44.41 to 42 sq.km respectively. This decrease in area has contributed to the increase of plantation and urban area from 175.77 to 220 sq.km and 13.7 to 18 sq.km respectively.
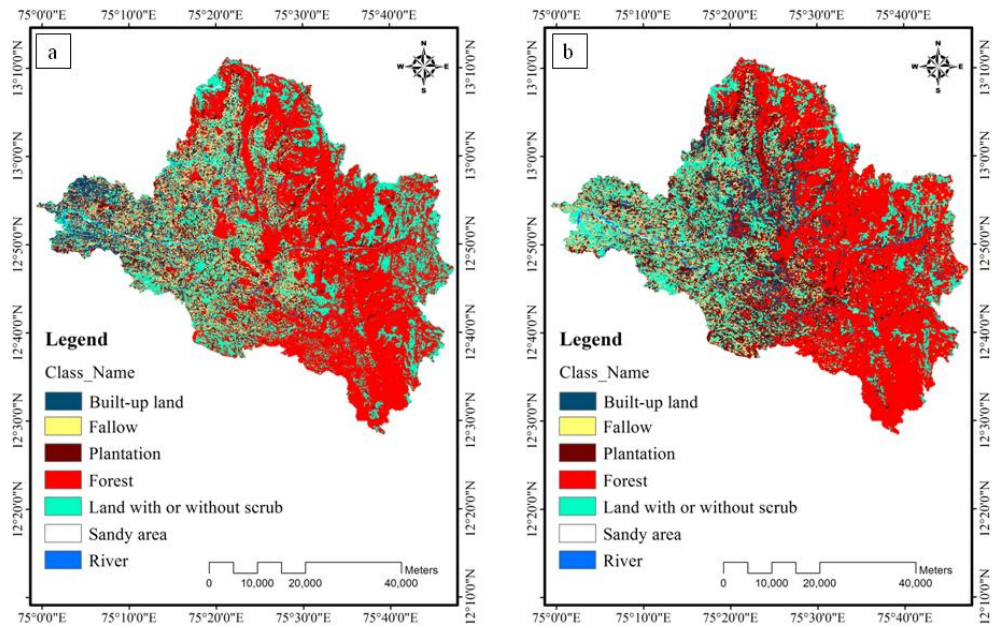
Figure 4.14 Predicted LU/LC map for a) 2010 and b) 2016 using CA-Markov model in Netravati river basin
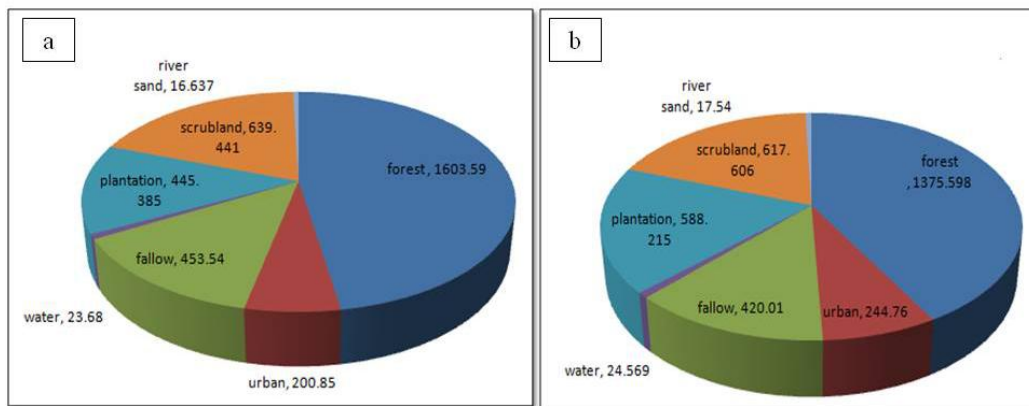
Figure 4.15 Predicted scenarios of LU/LC area for the years a) 2010 and b) 2016 using CA-Markov model in Netravati river basin
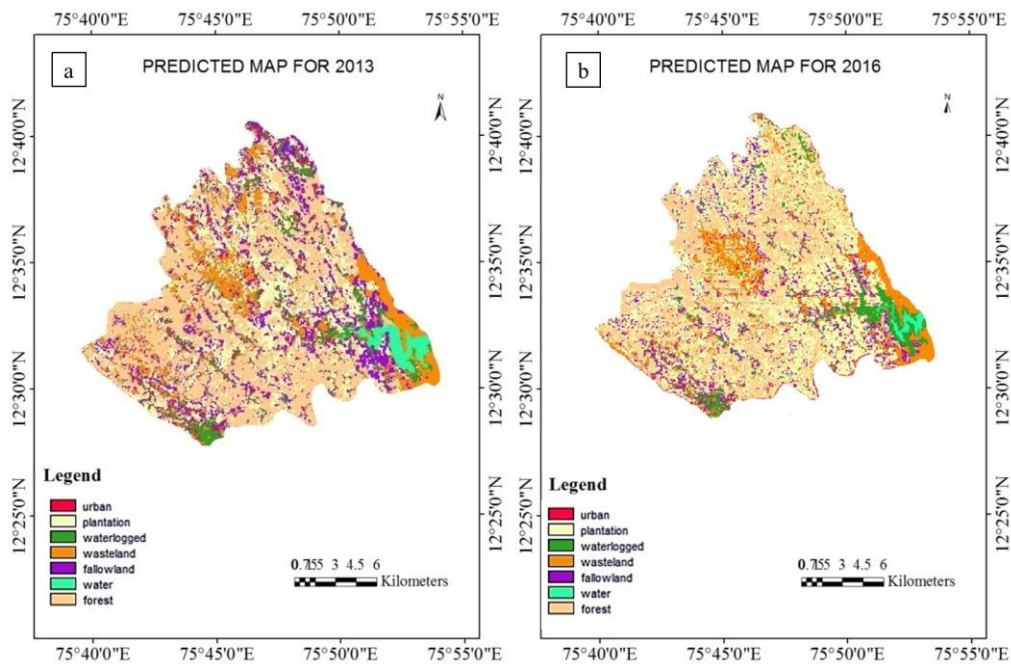
Figure 4.16 Predicted LU/LC map for a) 2013 and b) 2016 using LCM model in Harangi catchment
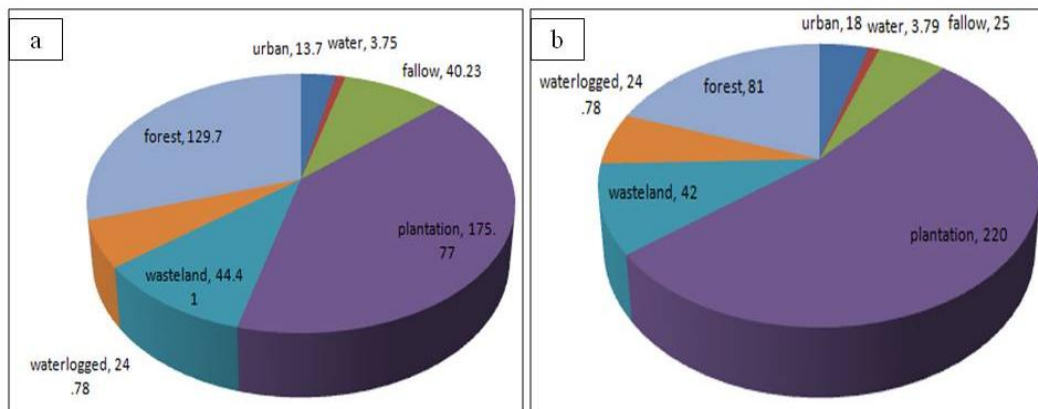
Figure 4.17 Predicted scenarios of LU/LC area for the years a) 2013 and b) 2016 using LCM in Harangi catchment

Depending upon the topographic features of the study area, the accuracy of different models varies accordingly, since slope is considered as one of the important factors causing the change. For instance, forest area with slope < 15% has been converted to built-up land and plantation. Based on the accuracy value alone, it cannot be concluded as to which model is the best. One model works better in one study area, while the other will give appropriate results in some other area with different

106

biophysical factors. The prediction accuracy is mainly dependent on the classified images which are used as base maps. In this study, there is a chance for misclassification between sandy area and land with or without scrub, forest area and plantation. The use of more driver variables can improve the accuracy of the results to some extent. Also, models which can take up several different time period LU/LC images, instead of considering only two time period LU/LC images, can improve the accuracy of model prediction. The major benefit of applying LU/LC dynamic models to predict possible future changes is that they provide better alternatives to define suitable weightages based on multi criteria evaluation.

The constraints and drivers are the criteria that define the changes in the particular LU/LC class. In this study, built-up land expansion is restricted in river, sandy area, less distance to river network, and forest cover with steep slope. The drivers used in this study are soil data, road and river network, distance to road and river and slope map. Distance between 20 to 500m is most suitable for built-up land and beyond 500m is not suitable, and hence such areas near existing built-up land have been converted to plantation and new built-up land. Such areas of forest and land with or without scrub have been converted to built-up land. Slope is also considered as an important factor causing these changes.

4.3 ESTIMATION OF ACTUAL EVAPOTRANSPIRATION (AET) USING SATELLITE IMAGES

The present research work estimated the AET by using Priestley Taylor (PT) method in Netravati river basin and Harangi catchment for the years 1997, 1999, 2011 and 2015. LST is one of the major inputs for the estimation of AET calculated using Split Window algorithm. The Fractional Vegetation Cover (FVC) and Land Surface Temperature (LST) were estimated and analysed for Netravati river basin and Harangi catchment during February month of the years 1997, 1999, 2003, 2011 and 2015 and are shown in Figure 4.18, 4.20 and Figure 4.19, 4.21, respectively. The estimated LST in Netravati river basin during February month of the years 1997, 1999, 2003, 2011 and 2015 are in the range of 237.12-332.29 Kelvin, 196.61-338.30 Kelvin, 258.13-303.90 Kelvin, 281.18-318 Kelvin, and 260.81-362.02 Kelvin respectively (Figure 4.20). The LST in Harangi catchment during February month of the years 1997, 1999,

2003, 2011 and 2015 ranges from 228.62-312.23 Kelvin, 188.77-324.70 Kelvin, 261.04-295.07 Kelvin, 269.65-300.20 Kelvin and 256.29-351.39 Kelvin respectively (Figure 4.21). From the results, it is observed that the estimated LST value contain outliers (extreme values). The presences of outliers in all the analysed images are due to cloud cover and scan line errors that were present in the satellite image. The area covered by outliers is very less; therefore its effect on the overall result is negligible. The LST shows an increasing trend, whereas FVC indicates a decreasing trend during study period. The variation in LST can be attributed towards the change in vegetation pattern of the study areas, which is influenced by urbanization and industrialization. The comparison between LST and FVC maps indicate that the LST is low in vegetation dense area like Western Ghat region in comparison with the areas which experiences continuous land surface change (Figure 4.18, 4.20 and Figure 4.19, 4.21). It can be concluded that the decrease in vegetation fraction and increase in land degradation increased the LST. The accuracy of estimated LST and FVC depends mainly on the quality of satellite images used as input for the analysis. It is observed that FVC value is low in some areas that is supposed to have higher value of FVC (Figure 4.19 (a) and (c)). This is because of the presence of cloud cover in the satellite image. Due to lack of measured LST data, validation of estimated LST values could not be carried out. However, it is verified with the weather forecast website:

(http://www.accuweather.com/en/in/mangalore/188760/weather-forecast).

108
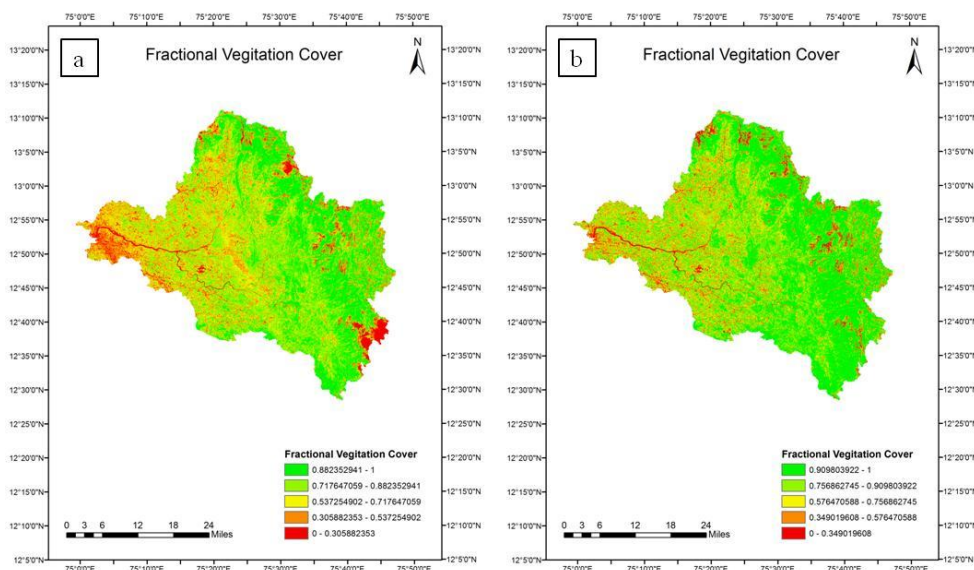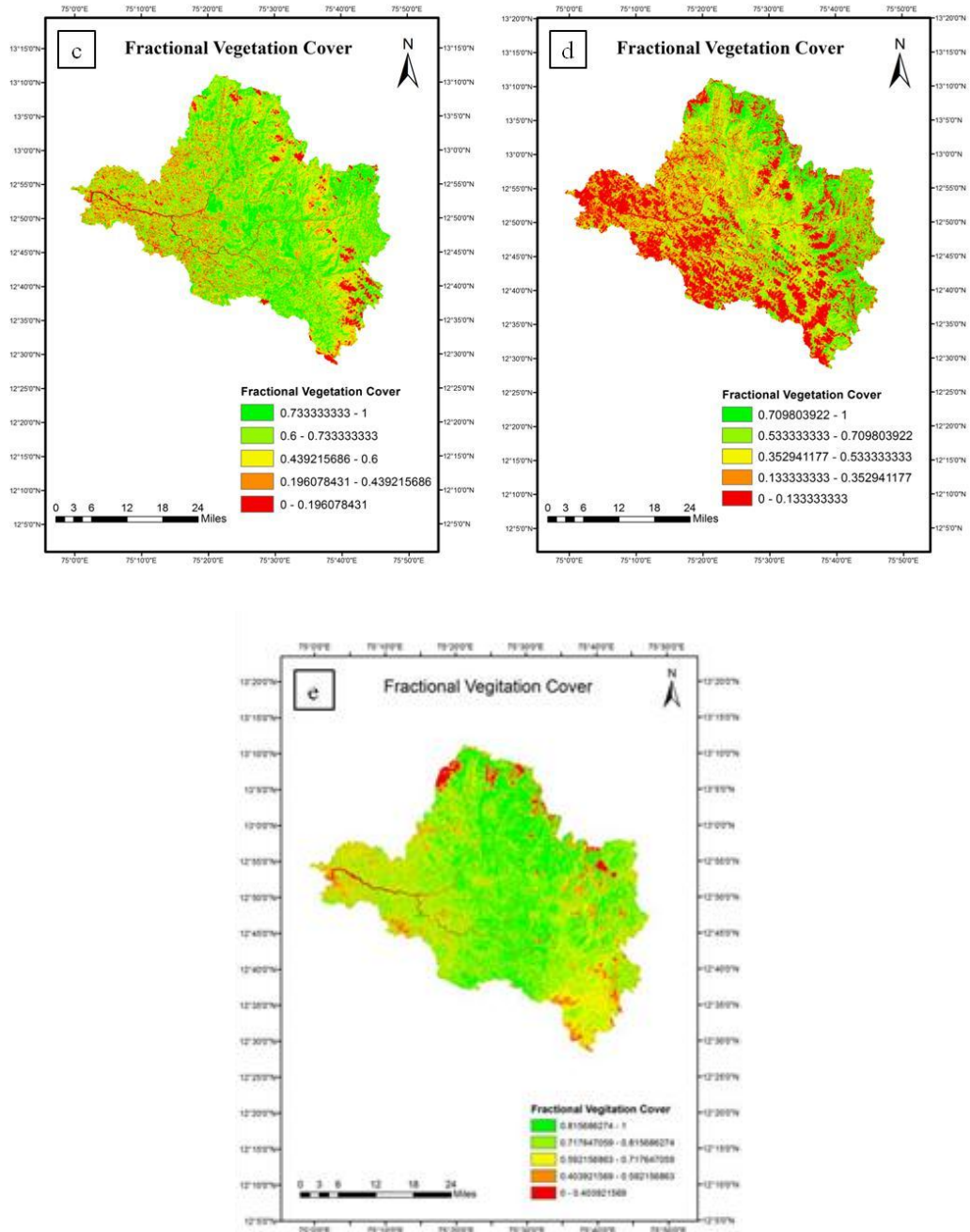
Figure 4.18 The FVC maps of Netravati river basin during February month of the years a) 1997, b) 1999, c) 2003, d) 2011 and e) 2015
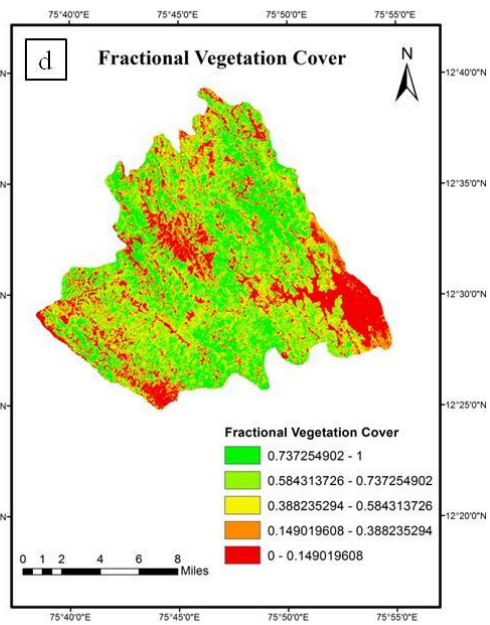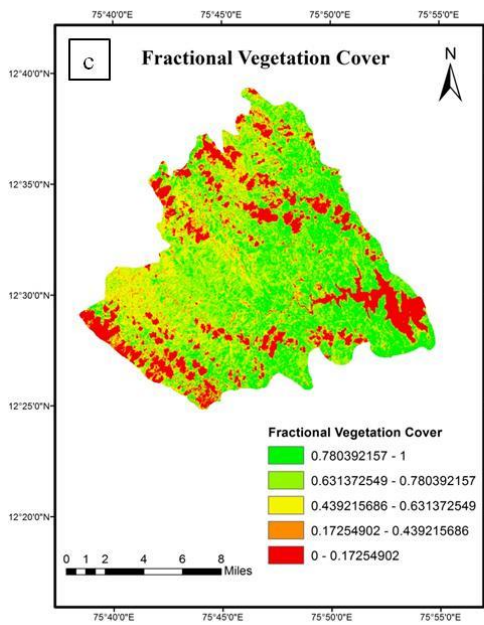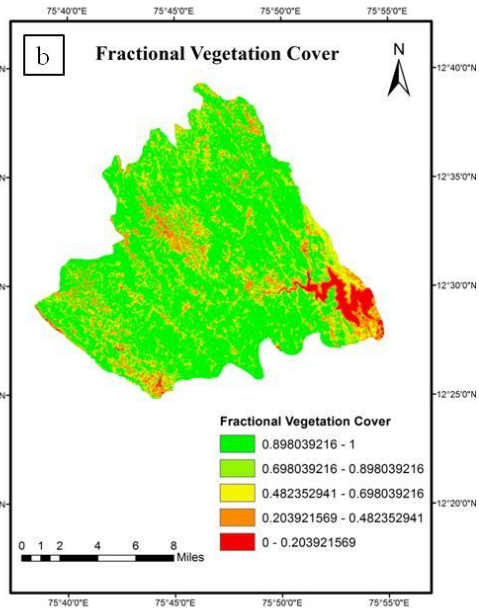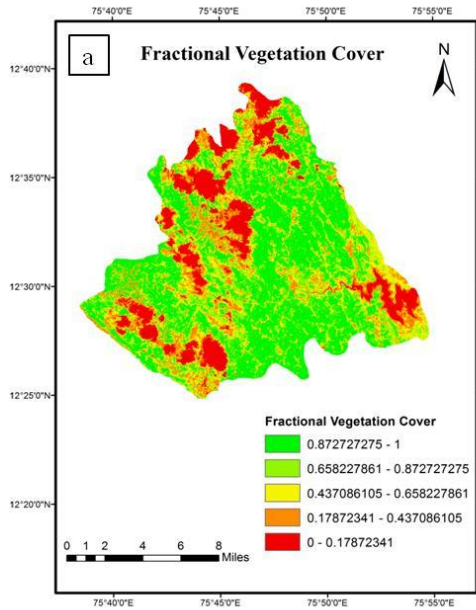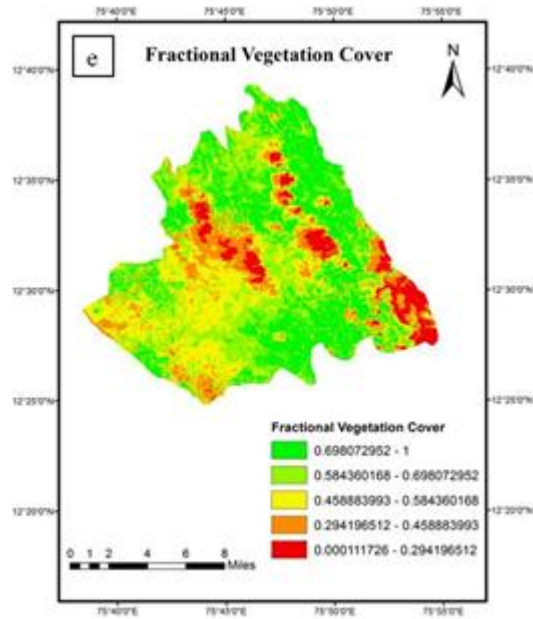
Figure 4.19 The FVC maps of Harangi catchment during February month of the years a) 1997, b) 1999, c) 2003, d) 2011 and e) 2015
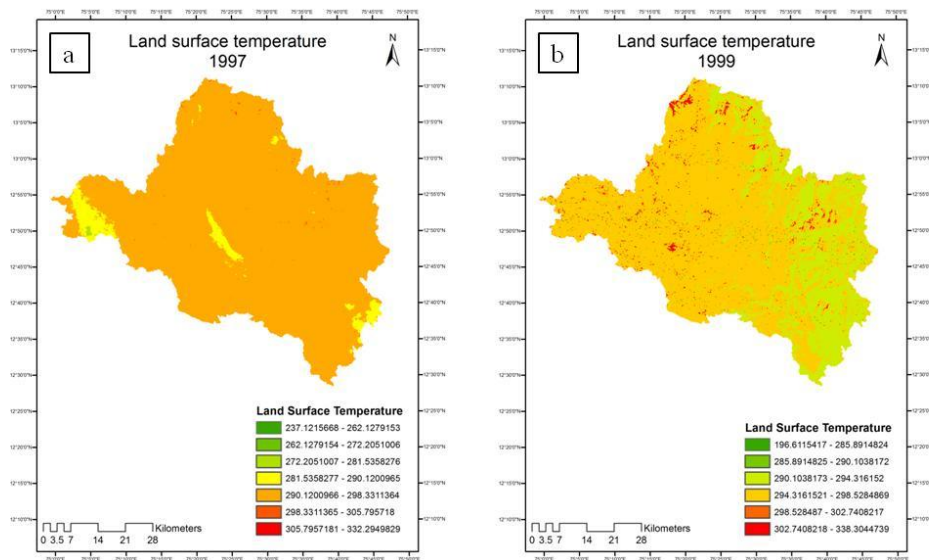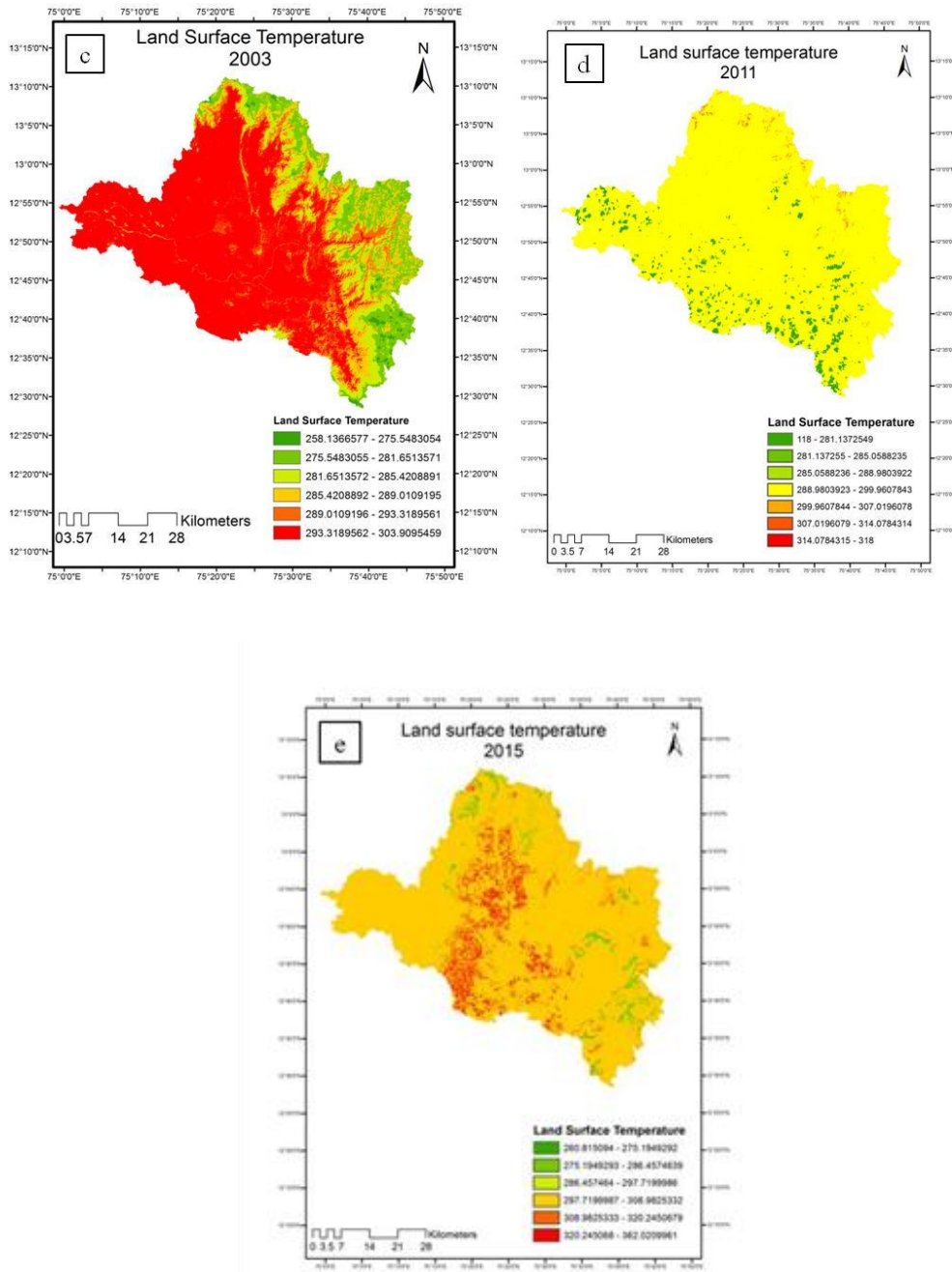
Figure 4.20 The LST maps of Netravati river basin during February month of the years a) 1997, b) 1999, c) 2003, d) 2011 and e) 2015
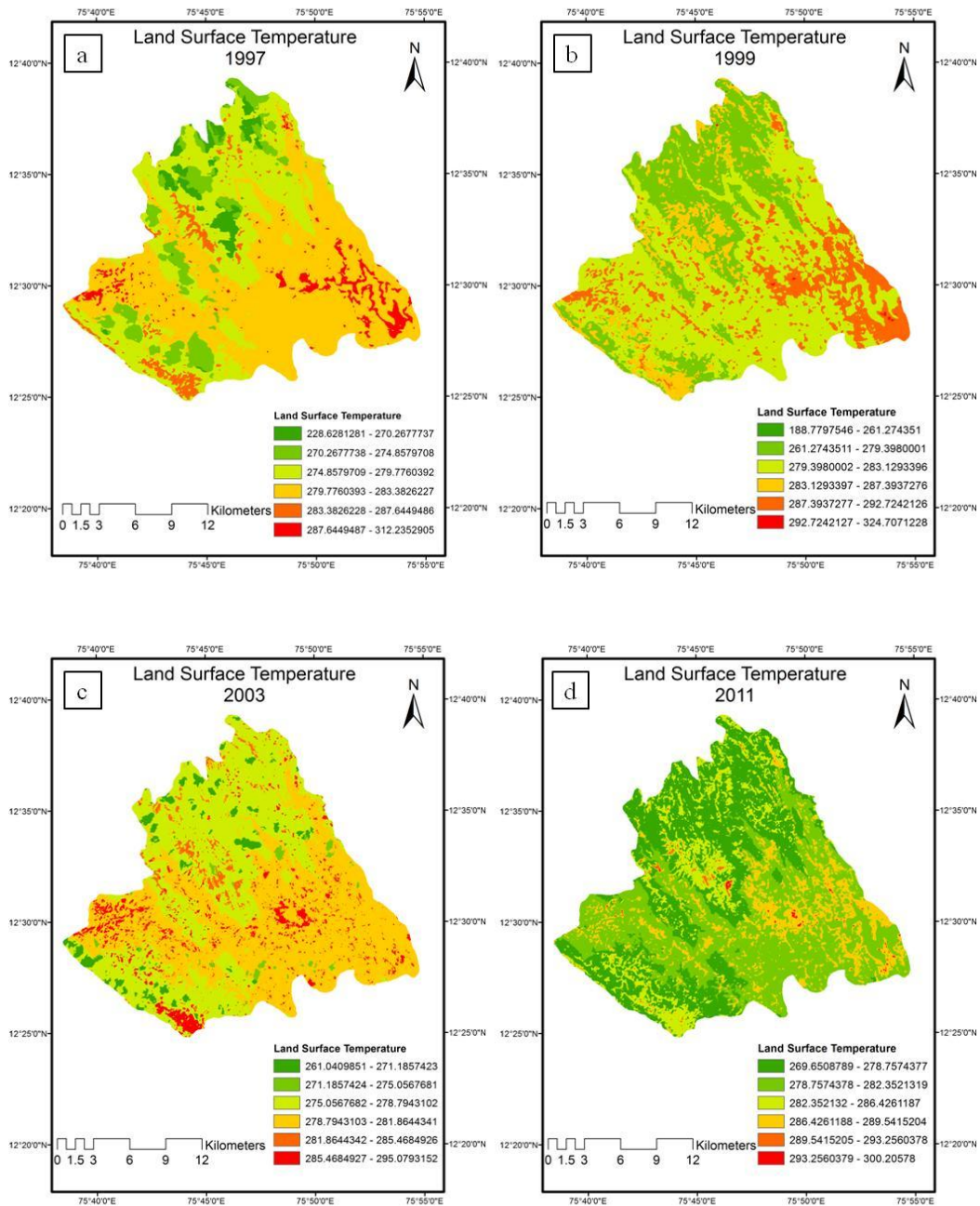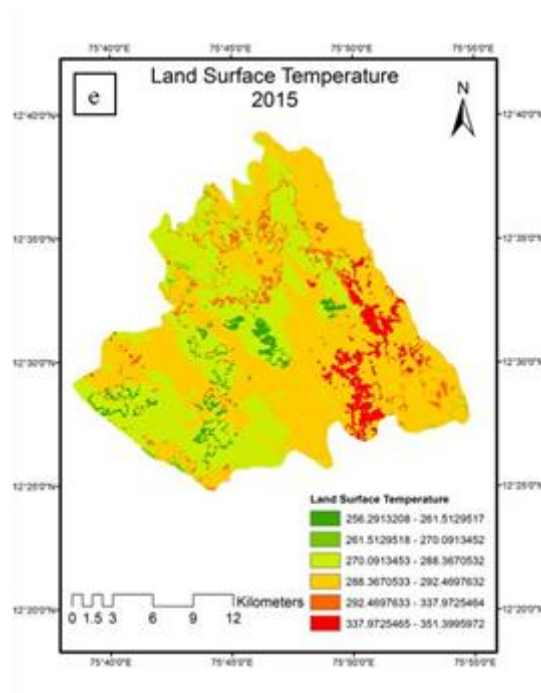
Figure 4.21 The LST maps of Harangi catchment during February month the years a) 1997, b) 1999, c) 2003, d) 2011 and e) 2015

The actual ET estimated by using Priestley Taylor method in Netravati river basin for the years 1997, 1999, 2011, and 2015 are in the range of 0.22-2.27 mm/day, 2.14-4.98 mm/day, 1.07-1.92 mm/day, and 2.22-7.39 mm/day respectively (Figure 4.22). Result shows that AET has been increased during the study period of 1997-2015. The AET in Harangi catchment during 1997, 1999, 2011, and 2015 are in the range of 1.04-2.14 mm/day, 2.33-4.28 mm/day, 1.25-1.92 mm/day and 0.92-2.96 mm/day respectively (Figure 4.23). The results indicate that the increase in LST and decrease in fractional vegetation cover has led to increase in AET. This is because, the Priestley Taylor method is based on brightness temperature and fractional vegetation cover, which have great influence on the estimated AET. The AET is observed to be high in the regions where vegetation fraction is high, eg., Western Ghat region, plantations. This is due to the fact that, forest canopies capture highest percentage of precipitation leading to high rate of AET. Also, the rate of transpiration is much higher from the vegetation rich areas, where plants uptake water from root zone. The estimated AET could not be validated due to lack of measured AET data in the study area. However, Laxmi (2015) validated the adopted methodology for Netravati river basin which is also based on Priestley Taylor method.

114
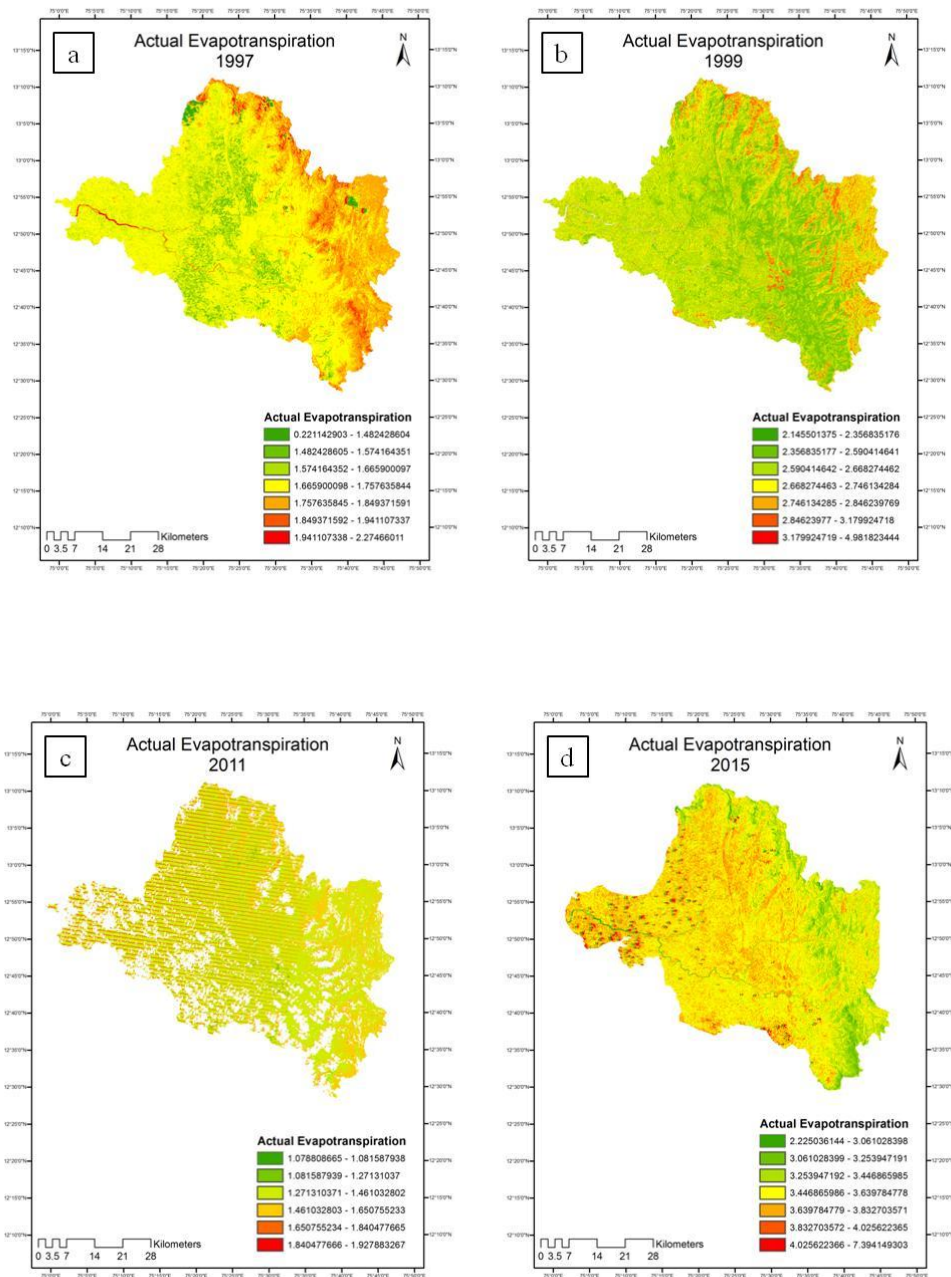
Figure 4.22 AET map of Netravati river basin during February month of the years a) 1997, b) 1999, c) 2011 and d) 2015
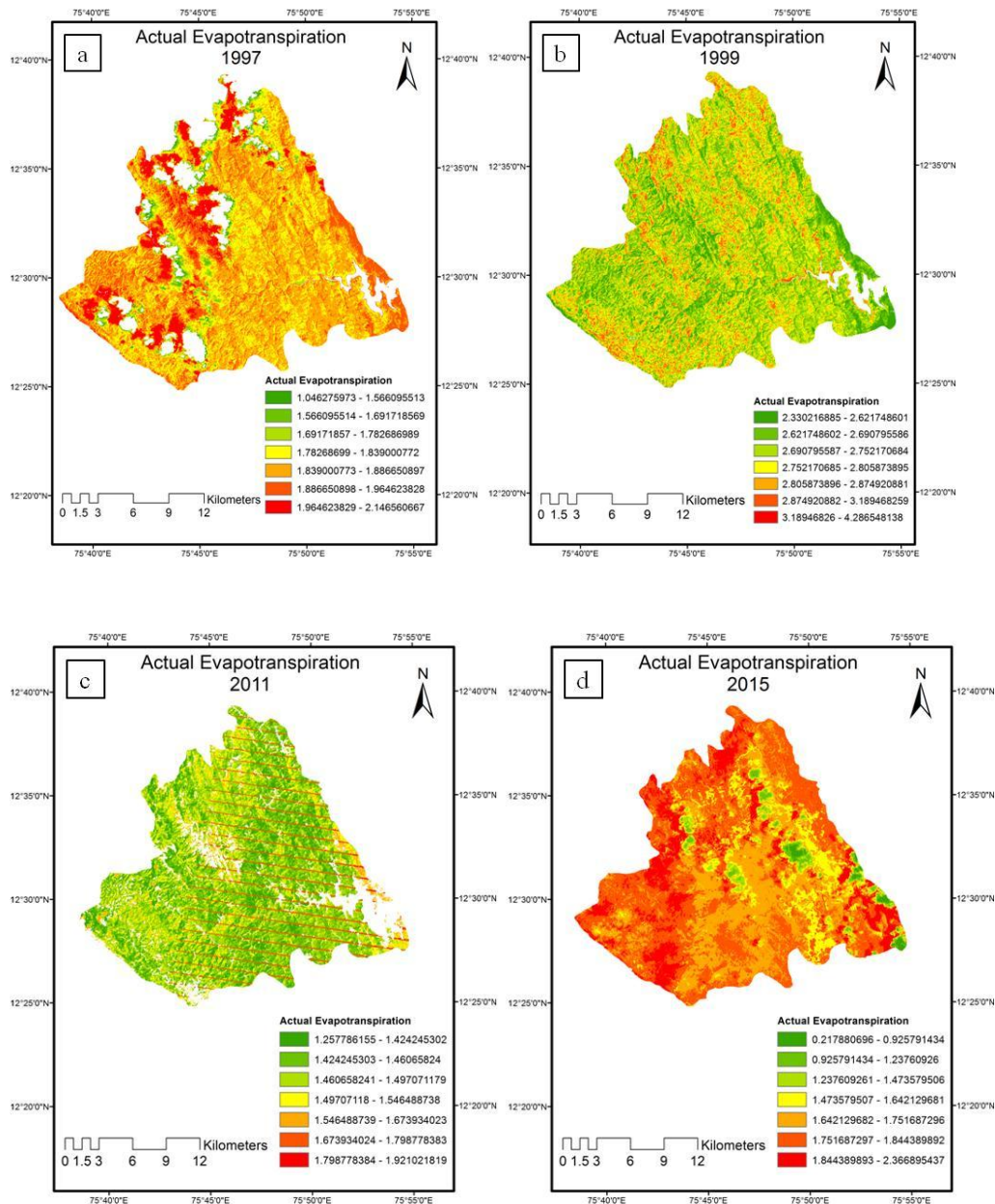
Figure 4.23 AET map of Harangi catchment during February month of the years a) 1997, b) 1999, c) 2011 and d) 2015

The presence of cloud cover in satellite images is the major reason for obtaining very low and very high strange values in AET maps. Therefore, it is suggested to apply Digital Image Processing technique to remove cloud cover in the satellite image before utilizing for the analysis. The principal advantage of this method is that they require only satellite data, easy to implement and ET estimates are possible in areas

without field measured data. However, the disadvantage is that this method requires many input parameters, which made the method data intensive.

4.4 STREAMFLOW ESTIMATION USING CONTINUOUS HYDROLOGIC MODELLING

The Hydrological-modeling framework in HEC-HMS involves the preparation of basin and meteorological model for simulation of streamflow. The basin model was prepared using DEM, which indicates the physical characteristics of the river basin. The meteorological model was prepared by considering daily rainfall data of seven rain gauge stations and daily evapotranspiration (ET), which is estimated using Hargreaves method. The Figures 4.24 and 4.25 shows the temporal variation in rainfall and ET respectively. The SMA model parameters were estimated based on the soil physical and hydraulic properties measured in the laboratory.
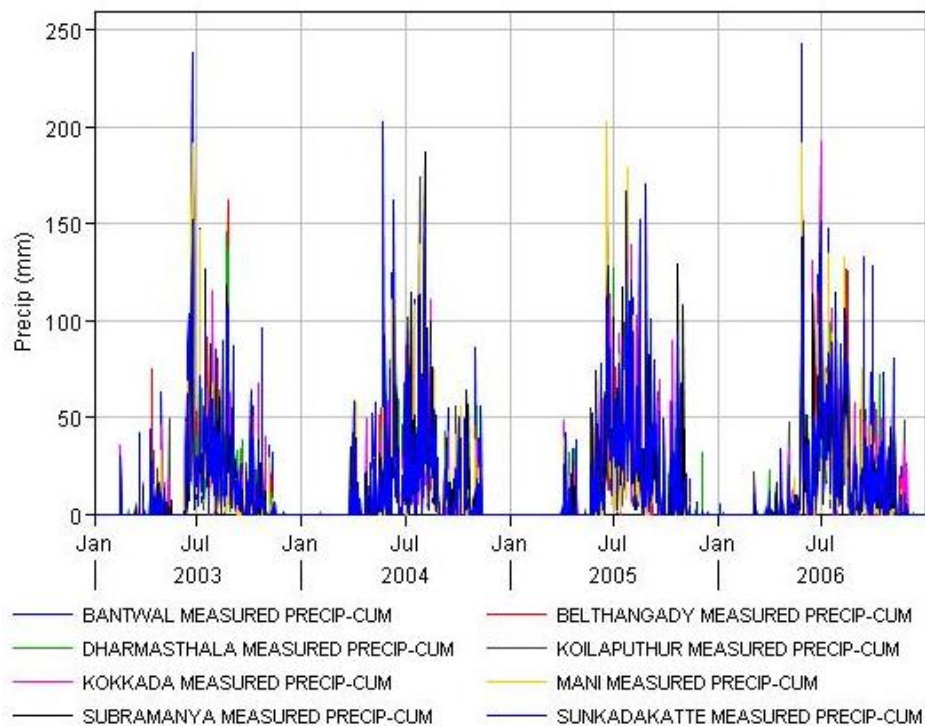
Figure 4.24 The temporal variation in rainfall
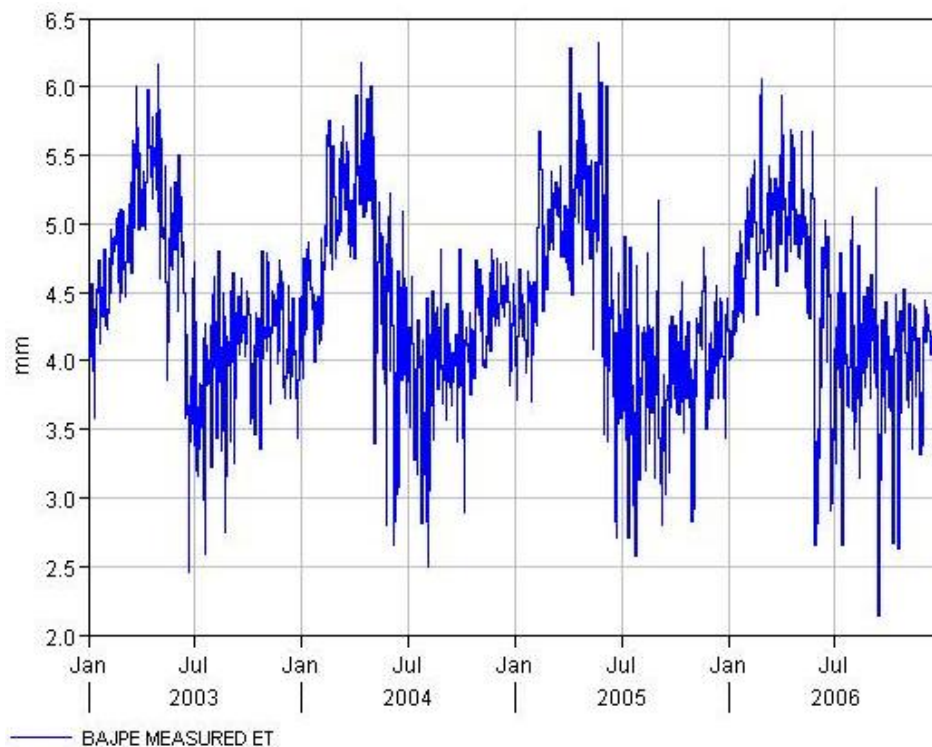
Figure 4.25 The temporal variation in ET

4.4.1 Assessment of Spatial Variability of Soil Physical and Hydraulic Properties

i. Laboratory Analysis of Soil Properties

The soil physical properties such as particle size distribution (% of gravel, sand, silt and clay), bulk density and soil hydraulic property i.e., saturated hydraulic conductivity were measured in laboratory for 38 soil samples collected at 0-50cm soil layer and 50-100 cm soil layer in spatially well distributed 19 sampling locations in Netravati river basin. The wet and dry sieve analysis was done to determine the soil particle size distribution for each soil sample. The descriptive statistics of soil properties in 0-50cm and 50-100cm soil layers are given in Table 4.11 and Table 4.12.

Table 4.11 Descriptive statistics of soil properties for (0-50 cm) soil layer

Soil Properties	Min	Max	SD	Skewness	Kurtosis
%Sand	23.33	68.53	15.50	-0.55	-1.02
%Silt	28.94	75.51	12.26	1.18	1.16
%Clay	0.54	26.50	7.00	1.43	2.14
Saturated Hydraulic conductivity (cm/sec)	1.5E-05	0.006	0.0017	2.07	4.35
Organic Matter (%)	0.27	5.45	1.43	0.78	-0.14
Bulk density (gm/cc)	1.24	2.04	0.27	0.16	-1.31

Table 4.12 Descriptive statistics of soil properties for (50-100 cm) soil layer

Soil Properties	Min	Max	SD	Skewness	Kurtosis
%Sand	7.35	66.30	16.08	-0.20	-0.68
%Silt	33.15	76.92	13.27	0.58	-0.88
%Clay	0	32.35	8.82	0.62	0.21
Saturated Hydraulic Conductivity (cm/sec)	5.83E-06	0.02	0.006	2.13	3.73
Organic Matter Content (%)	0.16	3.13	0.93	0.53	-0.94
Bulk density (gm/cc)	1.24	2.12	0.22	0.55	0.17

ii. Spatial Variability Analysis of Soil physical and Hydraulic Properties

The study attempted to interpolate soil properties such as sand, silt, clay, saturated hydraulic conductivity, organic matter content and bulk density spatially. In order to check the accuracy of different interpolation techniques, the soil data was divided into training data set (12 sample points) and validation data set (7 sample points).

For carrying out geospatial analysis for surface (0-50cm) soil layer, firstly appropriate method was chosen based on validation statistics. The details of interpolation techniques are given Table 4.13. The error associated with the interpolated map by using three models is as given in Table 4.15. For sand, silt, clay and saturated hydraulic conductivity, OK is found to be the best with less error. Whereas for organic matter content and bulk density, IDW and RBF techniques are found to be more accurate with similar error factor of 1.08%, 1.09% and 1.05g/cc, 1.04g/cc respectively. The degree of spatial dependence of these soil parameters was computed by finding percentage ratio of nugget to sill value of semivariogram. If this

percentage ratio is less than 25%, it was considered as the indicator of strong dependence and if it is between 26-75%, it was indicator of medium spatial dependence. Results indicate that sand, silt, clay, saturated hydraulic conductivity and bulk density showed medium spatial dependence, whereas organic matter content showed strong spatial dependence. The spatial interpolation maps obtained by technique that proved best for respective soil property (0-50cm soil layer) are shown in Figure 4.26.

Similarly, for subsurface (50-100cm), spatial interpolation was carried out for all soil properties (Table 4.14). Result shows that, IDW technique is best for predicting sand and silt with error of 6.62% and 5.01%. OK is the better technique for clay, saturated hydraulic conductivity and organic matter content with error of 0.12%, 0.002 cm/sec and 0.26% respectively (Table 4.15). Bulk density was predicted more accurately by IDW and RBF techniques. The results of spatial dependency shows that sand, silt, clay, saturated hydraulic conductivity and bulk density have showed medium spatial dependence, whereas organic matter content has showed strong spatial dependence. The spatial interpolation maps obtained by technique that proved best for respective soil property (50-100cm soil layer) are shown in Figure 4.27.
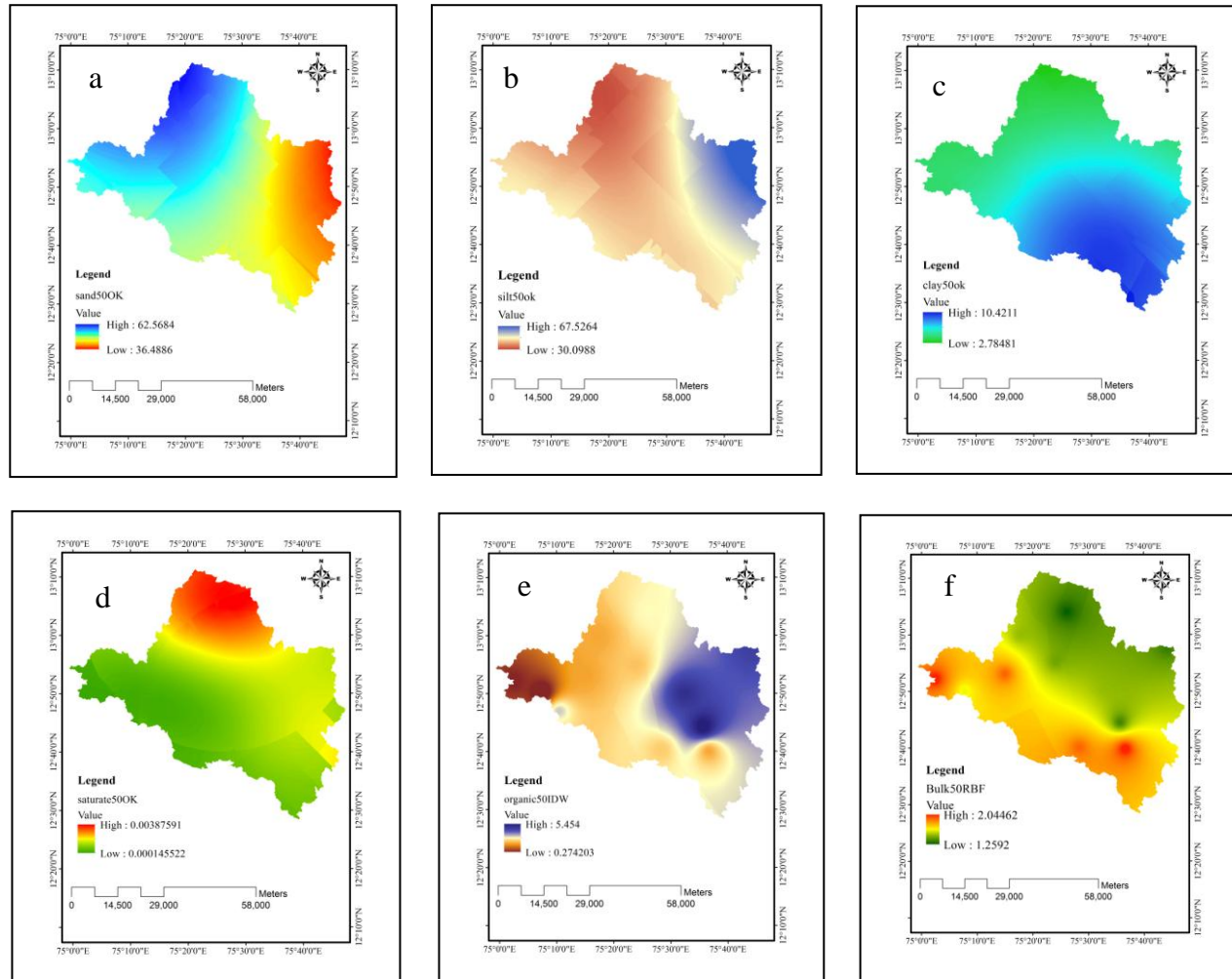
Figure 4.26 Spatial interpolation map of soil properties (0-50cm) a. Sand, b. Silt, c. Clay, d. Saturated hydraulic conductivity, e. Organic matter content, f. Bulk density

121
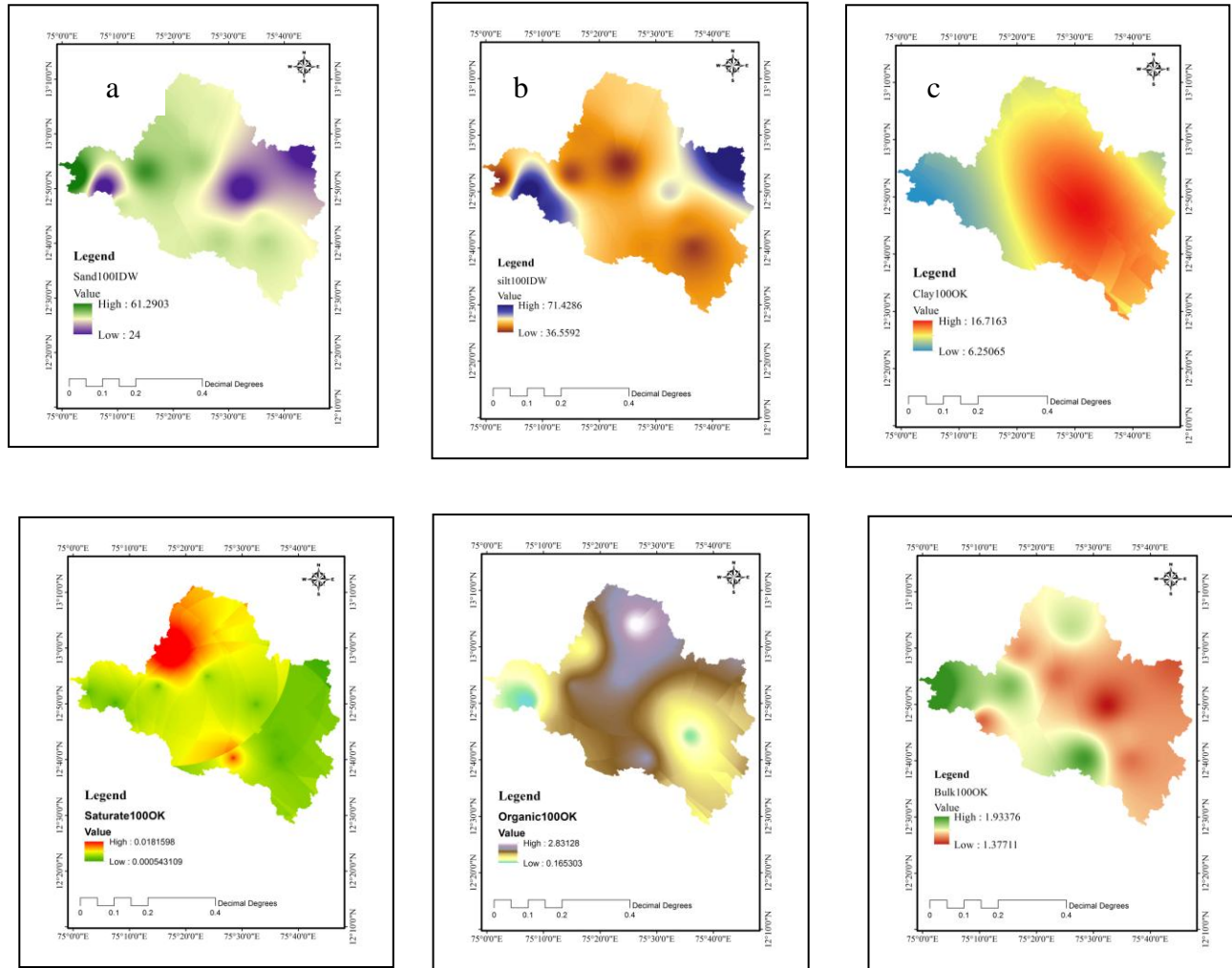
Figure 4. 27 Spatial interpolation map of soil properties (50-100cm) a. Sand, b. Silt, c. Clay, d. Saturated hydraulic conductivity, e. Organic matter content, f. Bulk density

Table 4.13 Model Structure of Ordinary Kriging Interpolation Technique for Soil Parameters for (0-50 Cm) Soil Layer

	Semivariogram Model	Lag size/No. of Lags	Sector type	Nugget (c0)	Partial Sill (c)	c0/(c0+c) (%)	Spatial dependence
Sand	Stable	8587.00/12	4 & 45°	104.74	281.78	27	Medium
Silt	Stable	8587.00/12	4 & 45°	45.64	258.55	15	Strong
Clay	Stable	8357.36/12	4 & 45°	14.61	16.41	47	Medium
Saturated Hydraulic Conductivity (cm/sec)	Stable	5508/12	4 & 45°	2.78e006	2.63e006	51.3	Medium
Organic Matter Content (%)	Stable	8587.00/12	4 & 45°	1.59	2.34	40.4	Medium
Bulk Density (g/cc)	Stable	8587.00/12	4 & 45°	0.053	0.083	38.9	Medium

Table 4.14 Model structure of Ordinary Kriging Interpolation Technique for soil parameters for (50-100 cm) soil layer

	Semivariogram Model	Lag size/No. of Lags	Sector type	Nugget (c0)	Partial Sill (c)	c0/(c0+c) (%)	Spatial dependence
Sand	Stable	8587.00/12	4 & 45°	114.03	41.38	73.3	Medium
Silt	Stable	5389.98/12	4 & 45°	54.95	94.17	36.84	Medium
Clay	Stable	5909.73/12	4 & 45°	32.99	33	49.99	Medium
Saturated Hydraulic Conductivity (cm/sec)	Stable	4435.28/12	4 & 45°	6.13	4.01	60.45	Medium
Organic Matter Content (%)	Stable	4507.93/12	4 & 45°	0	0.81	0	Strong
Bulk Density (g/cc)	Stable	8587.00/12	4 & 45°	0.021	0.021	50	Medium

Table 4.15 Error Associated in Spatial Interpolation of Soil Properties by Three Techniques

Soil Properties	Ordinary Kriging (Error)		IDW (Error)		RBF (Error)	
	50cm	100cm	50cm	100cm	50cm	100cm
Sand (%)	0.07	8.54	2.65	6.62	1.08	7.47
Silt (%)	3.27	6.34	5.00	5.01	4.36	5.11
Clay (%)	1.44	0.12	2.34	1.61	2.12	1.22
Saturated Hydraulic Conductivity (cm/sec)	0.00002	0.0025	0.0003	0.0028	0.0002	0.0027
Organic Matter Content (%)	1.14	0.26	1.08	0.27	1.09	0.29
Bulk Density (g/cc)	0.06	0.08	0.05	0.07	0.04	0.07

4.4.2 Model Calibration

The data set used for model calibration of four years, between 01/01/2003 to 31/12/2006. Due to insufficient availability of measured data, calibration could be done only at one stream gauging location, ie., Bantwal station, which is situated at the outlet of Netravati river basin. HEC-HMS offers automatic calibration facility, which is an iterative process to minimize the objective function. However, the optimized values obtained by HEC-HMS are not always realistic, due to default constraints set by the software. Therefore, the present study adopted the manual calibration procedure, which helps to find and assign practical range of values for parameters. The model calibration was carried out by fitting the outflow and the hydrograph shape between estimated outflow and the measured flow data at stream gauge location (Figure 4.28). During calibration, the SMA model parameters - soil storage, tension zone storage, soil percolation rate, GW 1 and 2 storage and the respective storage coefficients, GW 1 and 2 percolation rate were modified to reduce the objective function. The result of simulation run for the calibration period shows that the model is underestimating peak flows during monsoon and overestimating low flows during summer. The Nash Sutcliffe Efficiency obtained for calibration period is 0.251, which indicates that the model prediction efficiency is very much low. The lack of available observed data at different sub basins is the major reason for obtaining lower model efficiency. This indicates that the model is data intensive to apply in data scarce catchments. Therefore, the present research work necessitates the development of

simple methodology to study hydrologic response characteristics of study areas. The next section of this chapter presents details about the simple approach to compare and analyse the hydrologic response characteristics to LU/LC changes.
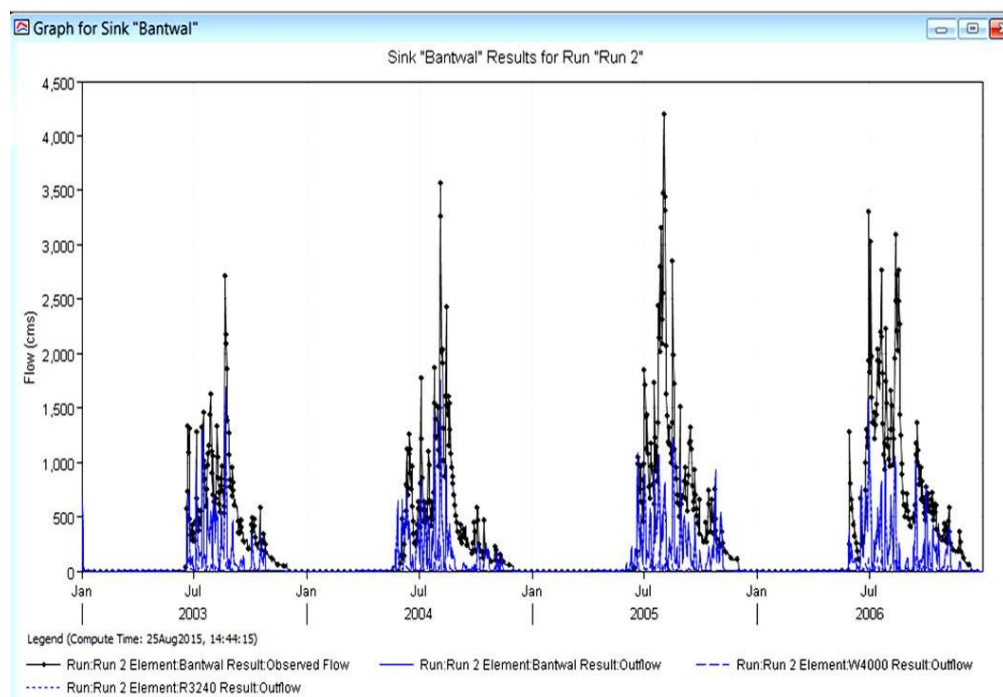
Figure 4.28 The goodness of fit between predicted and observed streamflow

4.5 HYDROLOGIC RESPONSE CHARACTERISTICS TO LU/LC CHANGE IN HUMID AND SUB-HUMID CATCHMENTS

4.5.1 Analysis based on Runoff Coefficient (RC) and Rainfall-runoff polygons

The study determined the mean monthly and annual runoff coefficient at Netravati river basin and Harangi catchment for period 1, period 2 and period 3 (Table 3.7). Period 1 of Netravati river basin includes rainfall-runoff data of the years 2003, 2004, and 2005 and LU/LC map of the year 2005. Period 2 of Netravati river basin comprises rainfall-runoff data of the years 2005, 2006, and 2007 and LU/LC map of the year 2007. Period 3 of Netravati river basin comprises rainfall-runoff data of the years 2008, 2009, and 2010 and LU/LC map of the year 2010. Similarly, Period 1 of Harangi catchment covers rainfall-runoff data of the years 2005, 2006, and 2007 and LU/LC map of the year 2007. Period 2 of Harangi catchment covers rainfall-runoff data of the years 2008, 2009, and 2010 and LU/LC map of the year 2010. Period 3 of

125

Harangi catchment consists of rainfall-runoff data of the years 2010, 2011, and 2012 and LU/LC map of the year 2013. The LU/LC maps and the corresponding monthly rainfall-runoff polygons for Netravati river basin and Harangi catchment are provided in Figure 4.29 and 4.30 respectively. Such polygons are capable of providing useful qualitative explanations about the rainfall-runoff transformation mechanism. At first look, the vertices of the polygon represent the ratio of runoff to rainfall, which is as shown in Figure 4.29 and 4.30. Runoff coefficient is usually calculated as the ratio of average of monthly runoff amount to the average of monthly rainfall depth. However, the present study calculated the mean monthly runoff coefficient as the arithmetic average of the preceding and current month's runoff coefficients as given in Table 4.16. The study also calculated the mean annual runoff coefficient (Table 4.16).

The annual runoff coefficient in Netravati river basin is observed to be small during period 1 with a value of 0.47, followed by 0.49 in the period 3 and the largest value of 0.57 is observed during period 2. The annual runoff coefficient during three different periods with varying LU/LC pattern in Harangi catchment shows different values, where largest runoff coefficient of 0.15 is observed during period 1 and period 3, followed by 0.14 during period 2. The variations in the estimated runoff coefficient value not only depends on rainfall and runoff value but also depends on physical characteristics of the catchment such as vegetation pattern, geological outcrops, and topography. Among them vegetation pattern is the significant one which undergoes spatio-temporal changes.
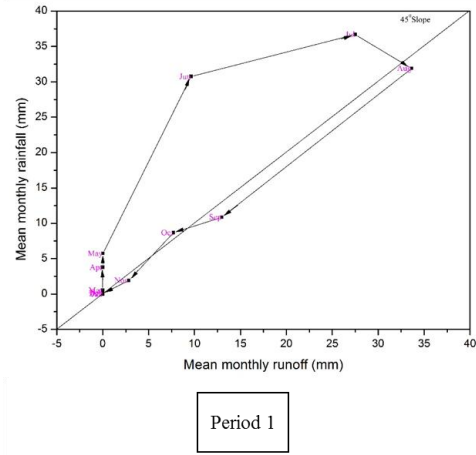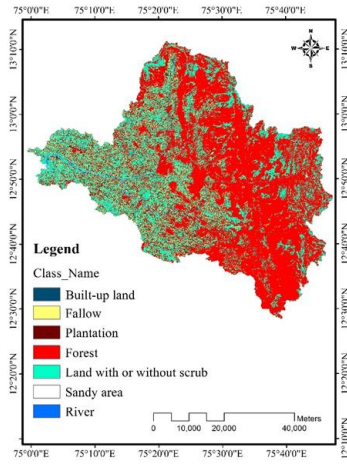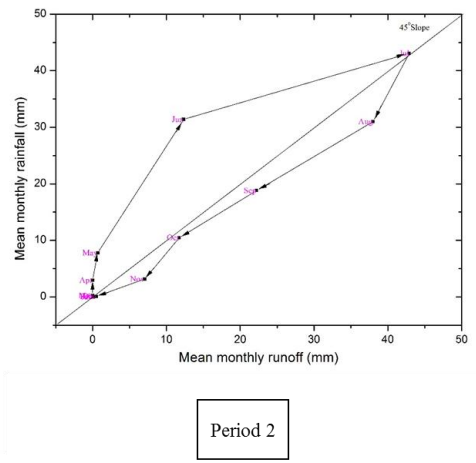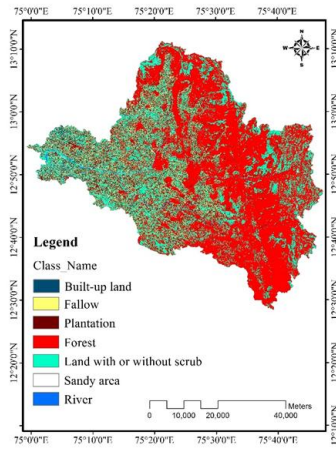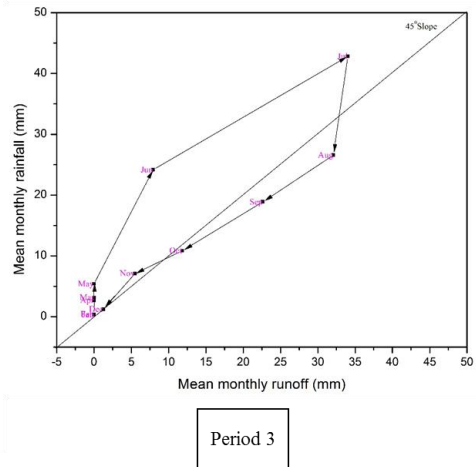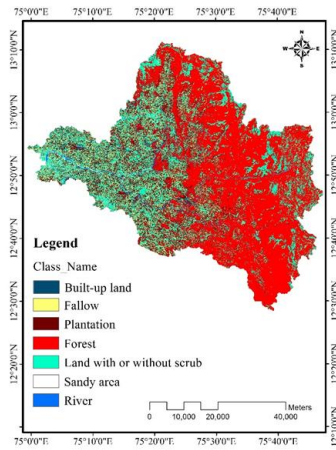
Figure 4.29 LU/LC maps and the corresponding monthly rainfall-runoff polygons for Period 1, 2 and 3 for Netravati river basin
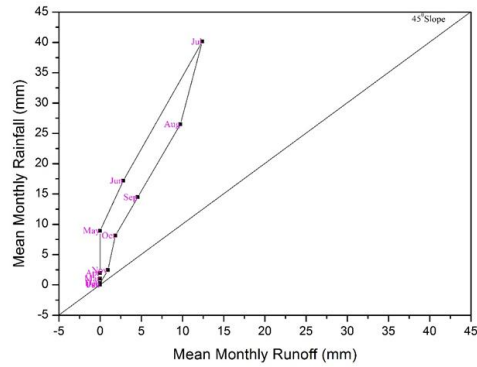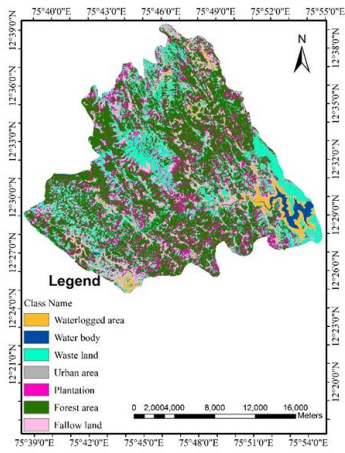
Figure 4.30 LU/LC maps and the corresponding monthly rainfall-runoff polygons for Period 1, 2 and 3 for Harangi catchment

Table 4.16 Mean monthly precipitation (P), runoff (Q), runoff coefficients (RC$_m$) and annual runoff coefficient (RC$_a$) for Netravati river basin and Harangi catchment

			Jan.	Feb.	Mar.	Apr.	May.	Jun.	Jul.	Aug.	Sep.	Oct.	Nov.	Dec.	(RC$_a$)
Netravati river basin	Period 1	Q	0.00	0.00	0.00	0.00	0.02	9.62	27.49	33.65	12.96	7.69	2.84	0.00	
		P	0.00	0.18	0.51	3.76	5.72	30.75	36.68	31.90	10.86	8.67	1.92	0.06	
		RC$_m$	0.00	0.00	0.00	0.00	0.00	0.16	0.53	0.90	1.12	1.04	1.19	0.74	0.47
	Period 2	Q	0.00	0.00	0.00	0.00	0.69	12.32	42.90	37.99	22.21	11.71	7.06	0.75	
		P	0.00	0.06	0.24	2.94	7.77	31.39	43.06	30.99	18.79	10.45	3.15	0.90	
		RC$_m$	0.00	0.00	0.00	0.00	0.04	0.24	0.69	1.11	1.20	1.15	1.68	0.83	0.57
	Period 3	Q	0.00	0.00	0.04	0.00	0.00	7.92	34.01	32.08	22.61	11.82	5.51	1.26	
		P	0.32	0.38	3.15	2.68	5.38	24.18	42.82	26.59	18.88	10.85	7.10	1.23	
		RC$_m$	0.00	0.00	0.01	0.01	0.00	0.16	0.56	1.00	1.20	1.14	0.93	0.90	0.49
Harangi catchment	Period 1	Q	0.00	0.00	0.00	0.00	0.00	2.80	12.39	9.74	4.56	1.84	0.94	0.00	
		P	0.01	0.00	1.03	1.96	8.93	17.16	40.11	26.49	14.45	8.12	2.43	0.26	
		RC$_m$	0.00	0.00	0.00	0.00	0.00	0.08	0.24	**0.34**	**0.34**	0.27	0.31	0.19	0.15
	Period 2	Q	0.00	0.00	0.00	0.00	0.00	1.29	7.16	5.93	3.38	1.85	1.24	0.27	
		P	0.00	0.09	3.04	1.39	2.12	11.22	32.52	20.80	11.91	6.23	3.56	1.00	
		RC$_m$	0.00	0.00	0.00	0.00	0.00	0.06	0.17	0.25	0.28	0.29	**0.32**	0.31	0.14
	Period 3	Q	0.00	0.00	0.00	0.00	0.00	2.26	5.33	5.76	4.18	1.69	1.66	0.41	
		P	0.01	0.41	0.98	4.56	3.29	22.73	36.69	32.25	17.85	7.12	7.21	0.49	
		RC$_m$	0.00	0.00	0.00	0.00	0.00	0.05	0.12	0.16	0.21	0.24	0.23	**0.84**	0.15

The seasonality being an important hydrological signature used effectively in catchment inter comparison studies. The seasonality in the rainfall and runoff pattern may produce different RC values. During Southwest monsoon, the rainfall occurs in high amount and intensity for long duration contributing high runoff, thus results in a large value of runoff coefficient. Result of the present study shows that the RC_m never exceeded '1'in Harangi catchment whereas it is exceeded during all three periods in Netravati river basin. These exceeded values indicate the contribution of baseflow and groundwater storage to runoff in addition to rainfall. In Netravati river basin, RC_m has exceeded in the months of September, October, November during period 1, whereas during period 2, it has exceeded more frequently in the months of August, September, October, and November. During period 3, it has exceeded in the months of August, September and October. In Harangi catchment, the highest RC_m values observed are 0.34 in September, 0.32 in November and 0.84 in December during period1, period 2 and period 3 respectively. This indicates that RC_m can efficiently represent seasonality existing between the months.

4.5.2 Relationship between LU/LC changes and hydrological response

The mean monthly surface runoff and rainfall values show a similar trend during all three periods in both the catchments. The mean monthly runoff polygon shows monthly variation in rainfall and runoff, which reflects the seasonal pattern. The monsoon, winter and summer seasons prevailing in the present study areas are between June-October, November-February and March-May respectively. The monthly RC was extracted for the LU/LC maps corresponding to month of satellite pass in both the study areas is as given in Table 4.17.

The result shows significant variation in annual runoff coefficient value between three periods of study in Netravati river basin reflected by wider polygon (Figure 4.29). Specifically, RCm values of Netravati river basin for the years 2005, 2007 and 2010 are showing an increasing trend (Table 4.17). This indicates that the changes in vegetation pattern from one period to another period have great influence on the rate of conversion of rainfall to runoff. In addition, the LU/LC change analysis shows dynamic changes over three study periods (Table 4.1). Especially, agricultural

area and built-up land shows increasing trend, whereas forest area shows decreasing trend.

The result of Harangi catchment shows, there is a correlation between monthly rainfall and runoff values represented by narrow polygon (Figure 4.30). Specially, RCm value of Harangi catchment for the years 2007, 2010 and 2013 (month of satellite pass) is showing an increasing trend (Table 4.17). In fact, the LU/LC change analysis shows a slight increase in urban area, but there is a major conversion from forest area to plantation (Table 4.4). Based on the analysis, it can be concluded that the influence of LU/LC change on rainfall-runoff conversion mechanism is predominant in Netravati river basin when compared to Harangi catchment.

Table 4.17 The RC$_m$ value corresponding to LU/LC map (month of satellite pass) of Netravati river basin and Harangi catchment

Period of Analysis	Netravati river basin			Harangi catchment		
	LU/LC Map	Month of Satellite Pass	RC$_m$	LU/LC Map	Month of Satellite Pass	RC$_m$
Period 1	2005	December	0.74	2007	December	0.19
Period 2	2007	December	0.83	2010	December	0.31
Period 3	2010	December	0.90	2013	December	0.84

4.5.3 Insights on Mean monthly rainfall runoff polygons and catchment behaviour

The graph of mean monthly rainfall versus mean monthly runoff were plotted and then the polygons were drawn and qualitative interpretation procedures were adopted to compare the hydrological dynamics prevailing in two contrasting catchments. The detailed interpretations of the polygons are as follows:

i. *Annual hydrological cycle features*

The polygon sides denote the linear variation in mean values of rainfall and runoff between consecutive months. During all the periods, the polygon sides from March to May are almost parallel to the y-axis in Netravati as well as Harangi catchment. This shows that soil moisture storage and antecedent moisture content is significantly low resulting in more infiltration and less runoff. For instance, during March-May months

of period 1, rainfall has increased from 0-6mm without any runoff in Netravati river basin (Figure 4.29). The sum of length of the polygonal peripheral represents the annual hydrological cycle. The length of peripheral is short from the month of April-May and March-April due to the consistency of the rainfall pattern as the rainfall amount on each event is low in Netravati and Harangi catchment respectively (Figure 4.29 and 4.30). More the length of polygon sides, more the variability of rainfall in contributing to runoff. There is a long peripheral length during May-September due to monsoon season, there is an increased rainfall frequency and amount in both Netravati and Harangi catchment. This increase in rainfall depth leads to the large surface runoff. The Harangi catchment polygon (Figure 4.30) has a least peripheral length compared to Netravati river basin (Figure 4.29), which shows that Harangi catchment does not take much time to complete its annual cycle of rainfall runoff conversion process.

ii. *Seasonality in catchment behavior*

The rising or falling order of the polygon sides indicates the seasonality in mean monthly runoff coefficient. The rising sequence represents wet season, indicated by increase in runoff coefficient value, whereas falling sequence represents dry season, indicated by decrease in runoff coefficient value. In Netravati river basin, wet and dry sequence is between May to August and August to April respectively (Figure 4.29). In Harangi catchment, wet and dry sequence is during May to July and July to April respectively (Figure 4.30). In the polygon diagram, the rising sequence has been observed due to increase in rainfall from month to month, which makes the ground surface wet by infiltrating more water into the ground contributing to soil and groundwater storage which in turn increases the antecedent soil moisture. Similarly, the falling sequence is noticed due to reduction in the amount of rainfall making the catchment drier that causes the runoff coefficient values to become smaller. It is observed in the polygon diagrams of both the catchments that even though the rainfall starts increasing from the month of March to May, there is negligible contribution to runoff generation. It shows the transition from dry season to wet season, during which rainfall amount will get lost in soil storage, infiltration, tension zone storage, ground water storage and ET.

iii. *Temporal trend detection based on size and shape of polygon*

The size and shape of polygon is one of the important indicators explaining the temporal variation in the catchment response to precipitation variation between months in a year. Netravati river basin is represented by the less steep and wider polygon which indicates that the catchment response to rainfall is variable in each month especially from May to September in all periods (Figure 4.29). Consider the polygon of Netravati river basin for period 1, it is observed that rainfall is increased by about 25mm between May to June contributing about 10mm runoff, whereas during June to July, the rainfall has increased about 5mm contributing about 17mm runoff. This implies that the rainfall occurring in the preceding months help in increasing the antecedent moisture content, saturation of soil storage and ground water storage. Therefore during successive months, even a small magnitude of increase in rainfall leads to heavy increment in runoff. This wider polygon constitutes larger polygonal area which implies high variability in the relationship between monthly rainfall and runoff coefficient.

Harangi catchment is characterized by more steep and narrow polygon which implies the consistent variation of catchment response to rainfall pattern in each month especially from end of June to the end of August during all the periods (Figure 4.30). The uniformity of the temporal variation of monthly runoff coefficients results in narrow polygons. The temporal variation of monthly runoff coefficient is uniform throughout the year resulting in narrow polygon.

iv. *Rainfall-runoff conversion mechanism*

The sum of length of polygon peripheral can provide an estimate of total amount of rainfall and runoff in any catchment. In the present study, the length of polygonal peripheral of Netravati river basin is more compared to Harangi catchment (Figure 4.29 and 4.30). Both the catchments are characterized by upward slope in the rainfall-runoff polygon. This is because; there is a consistent increase/decrease in runoff with the corresponding increase/decrease in rainfall.

Land use changes have significant impact on slope of runoff coefficient polygon by shifting its position, which tend to shift downwards. Smaller the overall slope of the polygon with respect to horizontal axis, larger the amount of rainfall converted into runoff by varying catchment characteristics. In this study, 45° slope line is drawn

as an indicator to measure the shift of the polygon. Netravati river basin is characterized by polygons of slope slightly lesser than $45^{°}$, indicates that more amount of rainfall is converted into runoff. It is observed that the polygon downward shifting is increased from period 1 to period 3. The LU/LC change analysis during period 1, 2 and 3 which shows that forest area has been decreased due to conversion of it to agricultural and urban area. This reduction in well-vegetated area has led to the generation of more surface runoff. The polygons of Harangi catchment do not show significant shift in their position during all three periods.

v. Characterization of ground water recharge and ET based on slope of each polygon side

During all the periods of LU/LC in both the catchments, the polygon sides in the month of March, April, and May are almost vertical. This steep slope indicates that contribution of rainfall to runoff is negligible but there is a significant ET, infiltration and GW recharge. In fact, Netravati river basin had a dry season from the months of September to April. After May, there is a significant contribution to runoff due to the onset of Southwest monsoon, which is represented by varying slopes.

4.6 SUMMARY

The main aim of the present research work was to carry out a detailed analysis for ascertaining the hydrological response to spatio-temporal changes taking place in Netravati river basin and Harangi catchment, Karnataka state, India. This chapter presented the results and the relevant discussion under four different themes namely prediction of future trends in LU/LC pattern of Netravati river basin and Harangi catchment, actual ET and Land Surface Temperature (LST) estimation using satellite images, streamflow estimation using continuous hydrologic modelling, and comparison of hydrologic response characteristic of two contrasting catchments. The obtained results facilitated in drawing the conclusions in relationship with objectives of the study and are provided in the Chapter 5.

SUMMARY AND CONCLUSIONS

5.1 GENERAL

The major focus of this dissertation was to study and compare the hydrologic response characteristics prevailing in two catchments namely Netravati river basin and Harangi catchment located in different hydro-climatic conditions. In the process of accomplishing this major objective, the present research work specifically addressed: a) LU/LC change analysis and prediction of future trends in LU/LC pattern by using LCM and CA-Markov model, b) the spatio-temporal pattern of AET in humid and sub-humid catchments by using remote sensing data, c) the applicability of semi-distributed model in continuous simulation of streamflow, and d) finally, hydrologic response characteristics were studied in two contrasting catchments using rainfall-runoff polygons.

This chapter provides summary and major conclusions drawn based on the results obtained. The summary is presented under above-mentioned four themes. In addition, limitations of the study and scope for further studies are enumerated.

5.2 SUMMARY

5.2.1 LU/LC Change Analysis and Prediction of Future Trends in LU/LC Pattern

The LCM and CA-Markov modeling approaches modeled the influence of spatial relationship between biophysical drivers and LU/LC changes in Netravati river basin and Harangi catchment, which is necessary to predict the impact on river basin environment. The major findings of the study are as follows:

1. The CA-Markov and LCM model gave 82.13% and 80.1% accuracy respectively in Netravati river basin.

2. An accuracy of 86.6% and 80% is obtained in Harangi catchment by using LCM and CA-Markov model respectively.

3. The validation results show that CA-Markov model is better for future prediction in Netravati river basin, whereas LCM is good in predicting future changes for Harangi catchment, because, Harangi catchment is characterized by steep slope compared to Netravati river basin and CA-Markov model is more sensitive to spatial transitions based on slope in comparison with LCM.

4. The prediction accuracy is mainly dependent on the classified images which were used as base maps, since there is a chance for misclassification between sandy area and land with or without scrub, forest area and plantation.

5. It is observed that the forest area and scrub land has decreased in 2016 leading to an increase in plantation and built-up land in Netravati river basin. Predicted map of Harangi catchment for the year 2016 shows that the plantation is increasing from 175.77 to 220 sq.km area, but forest, fallow and wasteland are showing a decreasing trend.

5.2.2 The Spatio-temporal Pattern of AET in Humid and Sub-humid Catchments

The present research work estimated the AET in Netravati and Harangi catchment by using Priestley Taylor method and the outcomes are as follows:

1. The comparison between LST and FVC maps indicate that the LST is low in vegetation dense area in comparison to the areas which experiences continuous land surface change. It can be concluded that the decrease in vegetation fraction and increase in land degradation will increase LST.

2. The actual ET estimated by using Priestley Taylor method in Netravati river basin during February month the years 1997, 1999, 2011, and 2015 are in the range of 0.22-2.27 mm/day, 2.14-4.98 mm/day, 1.07-1.92 mm/day, and 2.22-7.39 mm/day respectively. The AET in Harangi catchment during 1997, 1999, 2011, and 2015 are in the range of 1.04-2.14 mm/day, 2.33-4.28 mm/day, 1.25-1.92 mm/day and 0.92-2.96 mm/day respectively.

3. Results show that AET has been increased during the study period of 1997-2015. Since the AET estimation method is based on brightness temperature and

fractional vegetation cover, the increase in LST and decrease in fractional vegetation cover has lead to increase in AET.

4. The AET is observed to be high in the regions where vegetation fraction is high, eg., Western Ghat region, and agricultural plantations. This is due to the fact that, forest canopies capture highest percentage of precipitation leading to high rate of AET. Also, the rate of transpiration is much higher from the vegetation rich areas, where plants uptake water from root zone.

5. The presence of cloud cover in satellite images is the major reason for obtaining very low and very high strange values in AET maps.

6. The study shows that satellite data can be efficiently used for estimation of ET in any river basin which is lacking in measured data.

5.2.3 The Applicability of Semi-Distributed Model in Continuous Simulation of Streamflow

Aim of the study was to calibrate the hydrological model based on SMA model for estimating streamflow in Netravati river basin. The following inferences are drawn:

1. The Nash Sutcliffe Efficiency and Mean absolute error obtained for calibration period are 0.251 and 244.4 m3/sec respectively, which indicates that the model prediction efficiency is lower for daily stream flow prediction.

2. The lack of available observed data at different sub basins is the major reason for obtaining lower model efficiency.

5.2.4 Rainfall-Runoff Polygon Method to Study Hydrologic Response Characteristics

The hydrological responses of two contrasting catchments were compared through qualitative and quantitative interpretation of rainfall-runoff polygons. The following inferences are listed based on the analysis:

1. The Netravati river basin is characterized by high temporal variability of monthly runoff coefficient indicated by wider polygon, whereas Harangi catchment is characterized by uniform temporal variability of monthly runoff coefficient throughout the year resulting in narrow polygon.

2. The mean monthly runoff polygon method can be used as efficient tool to study the seasonality behavior of catchments.

3. Results of the study show that rainfall-runoff polygon in combination with LU/LC change analysis is capable of explaining hydrologic response in a better way.

5.3 CONCLUSIONS

1. The results of the study show that CA-Markov model is better for future prediction in Netravati river basin, whereas LCM is good in predicting future changes for Harangi catchment, because Harangi catchment is characterized by steep slope compared to Netravati river basin and CA-Markov model is more sensitive to spatial transitions based on slope in comparison with LCM.

2. The accuracy of prediction is mostly dependent on the classified images, which were used as base maps and the selected driving factors, since there is a chance for misclassification between sandy area and land with or without scrub, forest area and plantation.

3. The qualitative assessment of LST and FVC maps shows that the decrease in vegetation fraction and increase in land degradation has increased LST.

4. The AET is observed to be high in the regions where vegetation fraction is high, eg., Western Ghat region, and agricultural plantations. Based on the analysis, it can be concluded that high rate of AET takes place from forest canopies that capture highest percentage of precipitation and also the rate of transpiration is much higher from the vegetation rich areas, where plants uptake water from root zone.

5. The results of analysis show that model efficiency is lower for calibration of daily streamflow. This is due to lack of availability of measured streamflow data at all sub-basins. Therefore, it can be concluded that the semi-distributed model with 24 parameters is data intensive, make it difficult to apply in catchments with scarce data.

6. The shape, size and slope of polygons effectively reflected the difference between two catchments. This variation is mainly due to changes in the rate of conversion of rainfall into runoff from one catchment to another.

7. The rainfall-runoff polygon based methodology proves to be a simple and efficient way of studying the rainfall-runoff conversion mechanism in any catchment, provided there is availability of past and present rainfall runoff data and satellite images.

5.4 LIMITATIONS OF THE STUDY

1. The LU/LC change prediction models do not consider drivers representing agricultural practices and economic growth.

2. Prediction accuracy of LCM and CA-Markov model in predicting the future trend in LU/LC is mainly based on two previous year LU/LC maps.

3. The non availability of cloud free satellite data has limited the analysis of AET only for few years.

4. The hydrological model calibration efficiency is limited due to lack of measured data at different sub basins.

5.5 SCOPE FOR THE FUTURE STUDIES

1. Improving the LU/LC change prediction accuracy by considering more driving factors including agricultural management and economic growth.

2. Developing land use change prediction model which can take up more number of base LU/LC maps instead of taking just two base periods.

3. SMA model can be calibrated and validated by considering small catchment which is surplus with all input data.

4. Hydrologic response characteristics can be studied in detail by considering baseflow contribution separately.

Abushandi, E., and Merkel, B. (2013). "Modelling Rainfall Runoff Relations Using HEC-HMS and IHACRES for a Single Rain Event in an Arid Region of Jordan." *Water Resour. Manag., 27*, 2391–2409.

Akbari, S., Singh, R. (2012). "Hydrological modelling of catchments using MIKE SHE."*IEEE-Int. Conf. On Adv. In Eng., Sci. And Manag.*, 335-340.

Ali, G., Tetzlaff, D., Kruitbos, L., Soulsby, C., Carey, S., McDonnell, J., et al. (2013). "Analysis of hydrological seasonality across northern catchments using monthly precipitation–runoff polygon metrics". *Hydrol. Sci. J.,* 59 (1), 56-72.

Ambsat, K. Sunil., Keshari, K. Ashok and Gosain, K. Ashvani. (2008). "Estimating Regional Evapotranspiration using Remote Sensing: Application to Sone Low Level Canal System, India." 10.1061/ (ASCE) 07339437(2008)134:1(13).

Aspinall, R. (2004). "Modelling land use change with generalized linear models—a multi-model analysis of change between 1860 and 2000 in Gallatin Valley, Montana." *J.of Environ. Manag., 72*, 91–103.

Bastiaanssen, W.G.M (1995). "Regionalization of surface flux densities and moisture indicators in composite terrain. A remote sensing approach under clear skies in Mediterranean climates-Report 109." Agricultural Department, Wageningen, The Netherlands.

Behera, D. M., Borate, N. S., Panda, N. S., Behera, R. P., and Roy, S. P. (2012). "Modelling and analyzing the watershed dynamics using Cellular Automata (CA)–Markov model – A geo-information based approach." *J.of Earth System Sci., 121*(4), 1011–1024.

Beven, K., Warren, R., and Zaoui, J. (1980). "SHE: towards a methodology for physically-based distributed forecasting in hydrology." *Hydrol. forecasting,* 133-137. The Oxford Symposium,IAHS-AISH.

Bhagyanagar, R., Kawal, M. B., Dwarakish, G. S., Surathkal, S., (2012). "Land use/ land cover change and urban expansion during 1983-2008 in the coastal area of Dakshina Kannada district, South India". *J. of Appl. Remote Sens., 6* (1), 63-76.

Biondi, D., Versace, P., Sirangelo, B., (2010). "Uncertainty assessment through a precipitation dependent hydrologic uncertainty processor: An application to a small catchment in southern Italy". *J. of Hydrol., 386, 38–54.*

Blume, T., Zehe, E., & Bronstert, A. (2007). "Rainfall—runoff response, event-based runoff coefficients and hydrograph separation". *Hydrol. Sci. J., 52(5), 843-862.*

Bormann, H., Breuer, L., Graff, T., Huisman, J. A., and Croke, B. (2009). "Assessing the impact of land use change on hydrology by ensemble modelling (LUCHEM) IV: Model sensitivity to data aggregation and spatial (re-)distribution." *Adv. in Water Resour., 32, 171–192.*

Breuer, L., Huisman, J. A., Willems, P., Bormann, H., Bronstert, A., Croke, B. F., et al. (2009). "Assessing the impact of land use change on hydrology by ensemble modeling (LUCHEM) I: Model intercomparison with current land use." *Adv.in Water Resour., 32*, 129–146.

Brunsell, A. Nathaniel and Gillies, R. Robert (2002). "Incorporating Surface Emissivity into a Thermal Atmospheric Correction." *Photogram. Eng. & Remote Sens.,* 68(12).

Butts, B. M., Payne, T. J., Kristensen, M., Madsen, H., (2004). "An evaluation of the impact of model structure on hydrological modelling uncertainty for streamflow simulation." *J. of Hydrol., 298* , 242–266.

Campbell, J. D., Lusch, P. D., Smucker, A. T., and Wangui, E. E. (2005). "Multiple Methods in the Study of Driving Forces of Land Use and Land Cover Change: A Case Study of SE Kajiado District, Kenya." *Hum. Ecol., 33* (6), 763-791.

Changhong, S., Bojie, F., Yihe, L., Nan, L., Yuan, Z., Anna, H., et al. (2011). "Land Use Change and Anthropogenic Driving Forces: A Case Study in Yanhe River Basin." *Chin. Geogr. Sci. , 21* (5), 587–599.

Chen, S. M., Wang, Y. M., and Tsou, I. (2013). "Using artificial neural network approach for modelling rainfall–runoff due to typhoon." *J.of Earth System Sci., 122* (2), 399–405.

Cheng, S.j. (2011). "The best relationship between lumped hydrograph parameters and urbanized factors." *Nat. Hazard., 56*, 853–867.

Chien, H., Yeh, J. F., Knouft, H. J., (2013). "Modeling the potential impacts of climate change on streamflow in agricultural watersheds of the Midwestern United States." *J.of Hydrol., 491*, 73–88.

Choi, W., and Deal, M. B. (2008). "Assessing hydrological impact of potential land use change through hydrological and land use change modeling for the Kishwaukee River basin (USA)." *J.of Environ. Manag., 88*, 1119–1130.

Chow, T. V., Maidment, R. D., and Mays, W. L. (1988). *Appl. Hydrol.*(2010 ed.). Tata McGraw-Hill.

Cornelissen, T., Diekkruger, B., and Giertz, S. (2013). "A comparison of hydrological models for assessing the impact of land use and climate change on discharge in a tropical catchment." *J.of Hydrol., 498* , 221–236.

Costa, H. M., Botta, A., and Cardille, A. J. (2003). "Effects of large-scale changes in land cover on the discharge of the Tocantins River, Southeastern Amazonia." *J. of Hydrol., 283* , 206–217.

Crooks, S., & Kay, A. (2015). "Simulation of river flow in the Thames over 120 years: Evidence of change in rainfall-runoff response?". *J. of Hydrol.: Reg. Stud.,* 4, 172–195.

Daofeng, L., Ying, T., Changrning, L., and Fanghua, H. (2004). "Impact of land-cover and climate changes on runoff of the source regions of the Yellow River." *J. of Geogr. Sci., 14* (3), 330-338.

Delgado, J., Llorens, P., Nord, G., Calder, R. I., and Gallart, F. (2010). "Modelling the hydrological response of a Mediterranean medium-sized headwater basin subject to land cover change: The Cardener River basin (NE Spain)." *J. of Hydrol., 383*, 125–134.

Dijk, v. A., & Bruijnzeel, L. A. (2001). "Modeling runoff interception by vegetation of variaable density using an adopted analytical model. Part 2: Model validation for a tropical upland mixed croping system." *J. of Hydrol., 247*, 239-262.

Elfert, S., and Bormann, H. (2010). "Simulated impact of past and possible future land use changes on the hydrological response of the Northern German lowland 'Hunte' catchment." *J.of Hydrol., 383*, 245–255.

Feyen, L., Vazquez, R., Christiaens, K., Sels, O., and Feyen, J. (2000). "Application of distributed physically based hydrological model to a medium size catchment". *Hydrol. and Earth Sys. Sci., 4* (1), 47-63.

Fleming, M., & Neary, V. (2004). "Continuous Hydrologic Modeling Study with the Hydrologic Modeling System." *J. of Hydrol. Eng., 9* (3), 175-183.

Garcıa, A., Sainz, A., Revilla, A. J., Alvarez, C., Juanes, A. J., & Puente, A. (2008). "Surface water resources assessment in scarcely gauged basins in the north of Spain." *J. of Hydrol., 356*, 312– 326.

Ghosh, S., and Misra, C. (2010). "Assessing Hydrological Impacts of Climate Change: Modeling Techniques and Challenges." *The Open Hydrol. J., 4*, 115-121.

Goldshleger, N., Shoshany, M., Karnibad, L., Arbel, S., & Getker, M. (2009). "Generalising relationships between runoff–rainfall coefficients and impervious areas: an integration". *Urban Water J., 6*(3), 201-208.

Grayson, B. R., Moore, D. I., and McMahon, A. T. (1992). "Physically based hydrologic modeling: Is the concept realistic?" *Water Resour. Res., 26* (10), 2659-2666.

Grimmond, C., & Oke, T. R. (1991). "An Evapotranspiration-interception model for urban areas." *Water Resour. Res., 27* (7).

Haigen, Z., Shengtian, Y., Zhiwei, W., Xu, Z., Ya, L., & Linna, W. (2015). "Evaluating the suitability of TRMM satellite rainfall data for hydrological simulation using a distributed hydrological model in the Weihe River catchment in China." *J. of Geogr. Sci.*, 25(2), 177-195.

Halff, A. M., Halff, H. M., Azmoodeh, M., (1993). "Predicting Runoff from Rainfall Using Neural Network." *Eng. Hydrol.* (pp. 760-765). American Society of Civil Engineers, New York.

Hamel, P., & Guswa, A. J. (2015). "Uncertainty analysis of a spatially explicit annual water-balance model: case study of the Cape Fear basin, North Carolina." *Hydrol.and Earth Sys. Sci., 19*, 839–853.

He, M., and Hogue, S. T. (2012). "Integrating hydrologic modeling and land use projections for evaluation of hydrologic response and regional water supply impacts in semi-arid environments." *Env. Earth Sci., 65*, 1671–1685.

Hogue, S. T., Gupta, H., and Sorooshian, S., (2006). A 'User-Friendly' approach to parameter estimation in hydrologic models. *J. of Hydrol.*, 320, 202–217.

Hong, Wang., Xiaobing, Li., Huiling, Long., Qiao, Yunwei and Li, Ying (2011). "Development and application of a simulation model for changes in land-use patterns under drought scenarios." *Computers and Geosci.*, *37,* 831–843

Huang, S., Zang, W., Xu, M., Li, X., Xie, X., Li, Z., et al. (2015). "Study on runoff simulation of the upstream of Minjiang River under future climate change scenarios." *Nat. Hazards., 75*, 139–154.

Huigen, G M (2004). "First principles of the MameLuke multi-actor modelling framework for land use change, illustrated with a Philippine case study". *J.of Env. Manag., 72*, 5-21.

Huisman, J. A., Breuer, L., Bormann, H., Bronstert, A., Croke, B. F., Frede, H. G., et al. (2009). "Assessing the impact of land use change on hydrology by ensemble modeling (LUCHEM) III: Scenario analysis." *Adv. in Water Resour., 32* , 159–170.

Isik, S., Kalin, L., Schoonover, E. J., Srivastava, P., and Lockaby, G. B. (2013). "Modeling effects of changing land use/cover on daily streamflow: An Artificial Neural Network and curve number based hybrid approach." *J. of Hydrol., 485* , 103–112.

Jain, K. S., and Chaudhry, A. (2003). "Snow and forest cover assessment of Uttaranachal State using IRS 1C WiFS data." *J. of Indian Soc. of remote sens., 31* (2), 91-100.

Jiang, T., Chen, D. Y., Xu, C., Chen, X., Chen, X., and Singh, P. V. (2007). "Comparison of hydrological impacts of climate change simulated by six hydrological models in the Dongjiang Basin, South China." *J. of Hydrol., 336*, 316– 333.

Jimenez-Munoz, Juan., Sobrino, A. Jose., Skokovi, Drazen., Mattar, Cristian., and Cristobal, Jordi (2014). "Land Surface Temperature Retrieval Methods from Landsat-8 Thermal Infrared Sensor Data." *IEEE Geosci. and Remote Sens. Lett.,* 11(10).

Jimenez-Munoz, Juan., Sobrino, A. Jose., Skokovi, Drazen., Soria, G., Julien, Y., Mattar, C., and Cristobal, Jordi (2014). "Calibration and Validation of land surface temperature for Landsat8- TIRS sensor". Proceedings of Land Product Validation and Evolution, ESA/ESRIN Frascati, Italy.

Jing, Z., & Ross, M. (2015). "Hydrologic Modeling Impacts of Post-mining Land Use Changes on Streamflow of Peace River, Florida". *Chin. Geogr. Sci.*, 10.1007/s11769-015-0745-2.

Jing-an, Shao, Chao-fu, Wei, De-ti, Xie (2006). "An insight on drivers of land use change at regional scale." *Chin. Geogr. Sci.,* 16(2), 176-182

Kadioglu, M., & Şen, Z. (2009). "Monthly precipitation-runoff polygons and mean runoff coefficients". *Hydrol. Sci. J.,* 4 (1), 3-11.

Khan, U., Tuteja, K. N., Sharma, A., (2013). "Delineating hydrologic response units in large upland catchments and its evaluation using soil moisture simulations." *Env. Model. and Softw., 46*, 142-154.

Kim, J., Warnock, A., Ivanov, Y. V., Katopodes, D. N., (2012). "Coupled modeling of hydrologic and hydrodynamic processes including overland and channel flow." *Adv. in Water Resour., 37*, 104–126.

Kumar, M., Marks, D., Dozier, J., Reba, M., and Winstral, A. (2013). "Evaluation of distributed hydrologic impacts of temperature-index and energy-based snow models." *Adv. in Water Resour., 56*, 77–89.

Kumar, S. K., Valasala S. N., Subrahmanyam V J., Mallampati M., Shaik K., and Ekkirala P. (2015). "Prediction of future land use land cover changes of Vijayawada city using Remote Sensing and GIS". *Int. J. of Innov. Res. in Adv. Eng.,* **2**(3), 91-97.

Lambe, William, T (1967). "Soil testing for engineers". The Massachusetts Institute of Technology. John Wiley and Sons Inc.

Laouacheria, F., & Mansouri, R. (2015). "Comparison of WBNM and HEC-HMS for Runoff Hydrograph Prediction in a Small Urban Catchment." *Water Resour. Manag.*, 29, 2485–2501.

Latif, S. M. (2014). "Land Surface Temperature Retrival of Landsat-8 Data Using Split Window Algorithm- A Case Study of Ranchi District". *Int. J. of Eng. Dev. and Res.,* 2(4), 2321-9939.

Laxmi, Keerthi (2015), "Evaluation of a satellite-Based evapotranspiration model in a humid tropical region." Doctoral thesis, Dept. of App. Mech., Nitk Surathkal.

Lee, C.L., Huang, S.L., and Chan, S.L. (2008). "Biophysical and system approaches for simulating land-use change." *Landsc. and Urban Plan., 86*, 187–203.

Legesse, D., Vallet-Coulomb, C., and Gasse, F. (2003). "Hydrological response of a catchment to climate and land use changes in Tropical Africa: case study South Central Ethiopia." *J. of Hydrol., 275*, 67–85.

Li, Z., Liu, W.Z., Zhang, X.C., and Zheng, F. (2009). "Impacts of land use change and climate variability on hydrology in an agricultural catchment on the Loess Plateau of China." *J. of Hydrol., 377*, 35–42.

Lin, Y.P., Verburg, H. P., Chang, C.R., Chen, H.Y., and Chen, M.H. (2009). "Developing and comparing optimal and empirical land-use models for the development of an urbanized watershed forest in Taiwan." *Landsc. and Urban Plan., 92*, 242–254.

Lin, Y.P., Wu, P.J., and Hong, N.M (2008). "The effects of changing the resolution of land-use modeling on simulations of land-use patterns and hydrology for a watershed land-use planning assessment inWu-Tu, Taiwan." *Landsc. and Built-up land Plan., 87*, 54-66.

Liou, Y.-A., and Kar, K. S. (2014). "Evapotranspiration Estimation with Remote Sensing and Various Surface Energy Balance Algorithms—A Review." *Energies*, 7, 2821-2849.

Liu, M., Hu, Y., Chang, Y., He, X., and Zhang, W. (2009). "Land Use and Land Cover Change Analysis and Prediction in the Upper Reaches of the Minjiang River, China." *Env. Manag., 43*, 899–907.

Lorup, K. J., Refsgaard, C. J., and Mazvimavi, D. (1998). "Assessing the effect of land use change on catchment runoff by combined use of statistical tests and hydrological modelling: Case studies from Zimbabwe." *J. of Hydrol., 205*, 147-163.

Mackay, S. D., (2001). "Evaluation of hydrlogic equilibrium in a mountainous watershed: incorporating forest canopy spatial adjustment to soil biogeochemical processes." *Adv.in Water Resour., 24*, 1211-1227.

Magar, R. B., and Jothiprakash, V. (2011). "Intermittent reservoir daily-inflow prediction using lumped and distributed data multi-linear regression models." *J. of Earth Sys. Sci., 120* (6), 1067–1084.

Mao, D., and Cherkauer, A. K. (2009). "Impacts of land-use change on hydrologic responses in the Great Lakes region." *J. of Hydrol., 374*, 71–82.

Maskova, Zuzana., Zemek, Frantisek., and Kvet, Jan (2008). "Normalized difference vegetation index (NDVI) in the management of mountain meadows." *Boreal Environ. Res.,* 13, 417-432.

Mauser, W., and Bach, H. (2009). "PROMET – Large scale distributed hydrological modelling to study the impact of climate change on the water flows of mountain watersheds." *J. of Hydrol., 379*, 362-377.

McColl, C., and Aggett, G. (2007). "Land-use forecasting and hydrologic model integration for improved land-use decision support." *J. of Env. Manag., 84*, 494–512.

Merritt, S. W., Alila, Y., Barton, M., Taylor, B., Cohen, S., and Neilsen, D. (2006). "Hydrologic response to scenarios of climate change in sub watersheds of the Okanagan basin, British Columbia." *J. of Hydrol., 326*, 79–108.

Mimikou, M. (1984). "Regional relationships between basin size and runoff characteristics". *Hydrol. Sci. J.,* 29(1), 63-73.

Mishra, S. K., Jain, M. K., Pandey ,R. P., Singh, V. P (2005). "Catchment area-based evaluation of the AMC-dependent SCS-CN-based rainfall–runoff models". *Hydrol. Process.* 19, 2701–2718.

Muller, R. M., and Middleton, J. (1994). "A Markov model of land-use change dynamics in the Niagara Region, Ontario, Canada." *Landsc. Ecol., 9(2),* 151-157.

Nagaraj, M. K., Yaragal, C. S., 2008. "Sensitivity of land cover parameter in runoff estimation using GIS". *ISH J. of Hydra. Eng., 14* (1), 41-51.

Nandakumar, N., and Mein, R. G. (1997). "Uncertainty in rainfall-runoff model simulations and the implications for predicting the hydrologic effects of land-use change." *J.of Hydrol., 192*, 211-232.

Nazir, H. M., Sulaiman, N. A., & Juahir, H. (2015). "Hydrologic response characteristics of a tropical catchment to land use changes: a case study of The Nerus catchment". *Environ. Earth Sci.,* 73, 7533–7545.

Niehoff, D., Fritsch, U., and Bronstert, A. (2002). "Land-use impacts on storm-runoff generation: scenarios of land-usechange and simulation of hydrological response in a meso-scale catchment in SW-Germany." *J. of Hydrol., 267*, 80–93.

Niel, H., Paturel, J.-E., and Servat, E. (2003). "Study of parameter stability of a lumped hydrologic model in a context of climatic variability." *J. of Hydrol., 278*, 213–230.

Niu, J., and Sivakumar, B. (2013). "Study of runoff response to land use change in the East River basin in South China." *Stoch Environ Res Risk Assess* .

Nourani, V., & Saeidifarzad, B. (2016). "Detection of land use/cover change effect on watershed's response in generating runoff using computational intelligence approaches". *Stoch Environ Res Risk Assess,* 1-17. doi:DOI 10.1007/s00477-016-1220-z

Olmedo, C. M., Paegelow, M., and Mas, J. (2013). "Interest in intermediate soft-classified maps in land change model validation: suitability versus transition potential." *Int. J. of Geogr. Infor. Sci., 27(12),* 2343–2361.

Ondieki, C. M. (1997). "Potential of episodic flows in some four representative non-perennial river flow catchments in semi-arid Laikipia district, Kenya." *Env. Monit. and Assess., 45*, 285–299.

Onstad, C.A., Jamieson, D.G., 1970. "Modelling the effects of land use modifications on runoff", *Water Resour. Res.,* 6 (5), 1287-1295.

Ozturk, M., Copty, K. N., and Saysel, K. A. (2013). "Modeling the impact of land use change on the hydrology of a rural watershed." *J. of Hydrol., 497*, 97–109.

Parajka, J., Naeimi, V., Bloschl, G., Wagner, W., Merz, R., and Scipal, K. (2006). "Assimilating scatterometer soil moisture data into conceptual hydrologic models at the regional scale." *Hydrol. and Earth Sys. Sci., 10*, 353–368.

Pektas, O. A., & Cigizoglu, K. H. (2013). "ANN hybrid model versus ARIMA and ARIMAX models of runoff coefficient". *J. of Hydrol.,* 500, 21–36.

Post, A. D., Jones, A. J., (2001). "Hydrologic regimes of forested, mountainous, headwater basins in New Hampshire, North Carolina, Oregon and Puerto Rico." *Adv. in Water Resour., 24*, 1195-1210.

Punmia, B C., Jain, Kumar, Jain., and Jain, Kumar, Arun (2005)."Soil mechanics and foundation". 16th edition, Laxmi publications (p) Ltd, New Delhi.

Qin.Z, Karnieli.A., and Berliner, P (2001). "A mono window algorithm for retrieving land surface temperature from Landsat TM data and its application to the Israel-Egypt border region." Ben Gurion University of the Negev, Israel.

Rajeshwari, A and Mani, N D (2014). "Comparison of cirrus cloud coverage calculated from reanalysis meteorological data with satellite data." Proceedings of the TAC-Conference, Oxford, UK.

Ralha, G. C., Abreu, G. C., Coelho, G. C., Alexandre, Z., Macchiavello, B., and Machado, B. R. (2013). "A multi-agent model system for land-use change simulation." *Env. Model. and Softw., 42*, 30-46.

Ribalaygua, J., Torres, L., Portoles, J., Monjo, R., Gaitan, E., & Pino, M. R. (2013). "Description and validation of a two-step analogue/regression downscaling method." *Theor.l and Appl. Climatol., 114*, 253–269.

Rodríguez-Blanco, M., Taboada-Castro, M., & Taboada-Castro, M. (2012). "Rainfall–runoff response and event-based runoff coefficients in a humid area (northwest Spain)". *Hydrol.Sci. J.,* 57(3), 445-459.

Ruelland, D., Ardoin-Bardin, S., Billen, G., and Servat, E. (2008). "Sensitivity of a lumped and semi-distributed hydrological model to several methods of rainfall interpolation on a large basin in West Africa." *J. of Hydrol., 361*, 96– 117.

Sahua, R., Mishra, S., Eldho, T., (2012). Performance evaluation of modified versions of SCS curve number method for two watersheds of Maharashtra, India. *ISH J. of Hydraul. Eng.* 18 (1), 27–36.

Sang, L., Zhang, C., Yang, J., Zhu, D., and Yun, W. (2011). "Simulation of land use spatial pattern of towns and villages based on CA–Markov model." *Math. and Computer Model., 54*, 938–943.

Sarkar, A., Kumar, R., (2012). "Artificial Neural Networks for Event Based Rainfall-Runoff Modeling". *J. of Water Resour.and Prot., 4*, 891-897.

Schnitzer, M. (1978). "Humic substances: Chemistry and reactions". In: Soil organic matter, M. Schnitzer and S.U. Khan, Ed. Elsevier Scientific Publishing Co., New York. l- 64.

Schreider, Y. S., Jakeman, A. J., Letcher, R. A., Nathan, R. J., Neal, B. P., Beavis, S. G., (2002). "Detecting changes in streamflow response to changes in non-climate catchment condition: farm dam development in the Murray-Darling, Australia." *J. of Hydrol., 262*, 84-98.

Schulz, J. J., Cayuela, L., Echeverria, C., Salas, J., and Benayas, M. J. (2010). "Monitoring land cover change of the dryland forest landscape of Central Chile (1975–2008)." *Appl. Geogr., 30*, 436–447.

Shen, C., Phanikumar, S. M., (2010). "A process-based, distributed hydrologic model based on a large-scale method for surface–subsurface coupling." *Adv. in Water Resour., 33*, 1524–1541.

Shirke, Y., Kawitkar, R., Balan, S., (2012). "Artificial Neural Network based Runoff Prediction Model for a Reservoir". *Int. J. of Eng. Res. and Technol., 1* (3).

Singh, V., Bankar, N., Salunkhe, S. S., Bera, K. A., Sharma, J. R., (2013). "Hydrological stream flow modelling on Tungabhadra catchment: parameterization and uncertainty analysis using SWAT CUP." *Curr. Sci., 104* (9), 1187-1199.

Siriwardena, L., Finlayson, B. L., and McMahon, T. A. (2006). "The impact of land use change on catchment hydrology in large catchments: The Comet River, Central Queensland, Australia." *J. of Hydrol., 326* , 199–214.

Skokovic, D and Sobrino, J.A (2014). "Estimation of land surface temperature of dindigul district using landsat8 data." *IJRET*, 3(5).

Sobrino A.J., Gomez M., Jimenez-Munoz C.J., Olioso A. (2007). "Application of a simple algorithm to estimate daily evapotranspiration from NOAA–AVHRR images for the Iberian Peninsula." *Remote Sens. of Environ.,* 110, 139–148.

Sobrino.J.A, Gomez M., Jimenez-Munoz C.J., Olioso A and Chehbouni, G. (2005). "A simple algorithm to estimate evapotranspiration from DAIS data: Application to the DAISEX campaigns." *J. of Hydrol.,* 315,117–125.

Sridhar Venkataramana (2007). "Evapotranspiration estimation and scaling effects over the Nebraska Sandhills". *Great Plains Research*, 17, 35-45.

Sriwongsitanon, N., & Taesombat, W. (2011). "Effects of land cover on runoff coefficient". *J. of Hydrol.,* 410, 226–238.

Straub, D. T., Melching, S. C., & Kocher, E. K. (2000). "Equations for Estimating Clark Unit-Hydrograph Parameters for Small Rural Watersheds in Illinois."

Subramanya, K. (2008). *Engineering Hydrology* (2010 ed.). Tata McGraw-Hill.

Sudheer, K. P., Gosain, A. K., Ramasastri, K. S., (2002). "A Data Driven Algorithm for Constructing Artificial Neural Network Rainfall-Runoff Models." *Hydrol. Process., 16* (6), 1325-1330.

Tang, L., Yang, D., Hu, H., and Gao, B. (2011). "Detecting the effect of land-use change on streamflow, sediment and nutrient losses by distributed hydrological simulation." *J. of Hydrol., 409*, 172–182.

Thanapakpawin, P., Richey, J., Thomas, D., Rodda, S., Campbell, B., and Logsdon, M. (2006). "Effects of landuse change on the hydrologic regime of the Mae Chaem river basin, NW Thailand." *J. of Hydrol., 334*, 215– 230.

Tian, Y., Xu, Y.P., Zhang, X.J., (2013). "Assessment of Climate Change Impacts on River High Flows through Comparative Use of GR4J, HBV and Xinanjiang Models." *Water Resour. Manag., 27*, 2871–2888.

Tong, T. Y., Sun, Y., Ranatunga, T., He, J., and Yang, J. Y. (2012). "Predicting plausible impacts of sets of climate and land use change scenarios on water resources." *Appl. Geogr.,* 32, 477-489.

Ty, V. T., Sunada, K., Ichikawa, Y., Oishi, S., (2012). "Scenario-based Impact Assessment of Land Use/Cover and Climate Changes on Water Resources and Demand: A Case Study in the Srepok River Basin, Vietnam—Cambodia." *Water Resour. Manag., 26*, 1387–1407.

User Manual: Hydrologic Modeling System HEC-HMS. US Army Corps of Engineers. Hydrologic Engineering Center.

Vaezi, A. (595–604). "Modeling Runoff from Semi-Arid Agricultural Lands in Northwest Iran". *Pedosphere*, 24(5), 2014.

Valent, P., Szolgay, J., and Riverso, C. (2012). "Assessment of the uncertainties of a conceptual hydrologic model by using artificially generated flows." *Slovak J. of Civil Eng., 20* (4), 35-43.

Veldkamp, A., P.H. Verburg., K. Kok., G.H.J. de, Koning., J. Priess and A.R. Bergsma (2001). "The need for scale sensitive approaches in spatially explicit land use change modeling." *Env. Model.and Assess., 6*, 111–121.

Verburg H. Peter., Schot P. Paul., Dijst J. Martin and Veldkamp, A (2004). "Land use change modelling: current practice and research priorities." *GeoJ., 61*, 309–324.

Verburg, H. P., Overmars, P. K., Huigen, G. M., Groot, T. W., and Veldkamp, A. (2006). "Analysis of the effects of land use change on protected areas in the Philippines." *Appl. Geogr., 26*, 153–173.

Verburg, H. P., Schot, P. P., Dijst, J. M., and Veldkamp, A. (2004). "Land use change modelling: current practice and research priorities." *GeoJ., 61*, 309–324.

Verburg, P H., Veldkamp, A., Fresco, L O (1999). "Simulation of changes in the spatial pattern of land use in China". *Appl. Geogr.,*19, 211-233.

Verma, K. A., Jha, K. M., and Mahana, K. R. (2010). "Evaluation of HEC-HMS and WEPP for simulating watershed runoff using remote sensing and geographical information system." *Paddy Water Environ , 8*, 131–144.

Viney, R. N., Bormann, H., Breuer, L., Bronstert, A., Croke, B. F., Frede, H. G., et al. (2009). "Assessing the impact of land use change on hydrology by ensemble modelling (LUCHEM) II: Ensemble combinations and predictions." *Adv. in Water Resour., 32*, 147–158.

Visessri, S., & McIntyre, N. (2015). "Regionalization of hydrological responses under land-use change and variable data quality". *Hydrol. Sci. J.,* 1-19. doi:10.1080/02626667.2015.1006226

Walkley, A. and Black, I. A. (1934). "An examination of the Degtjareff method for determining soil organic matter, and a proposed modification of the chromic acid titration method". *Soil Sci.,* 37, 29-38.

Wang, G., Zhang, J., Pagano, T., Xu, Y., Bao, Z., Liu, Y., et al. (2015). "Simulating the hydrological responses to climate change of the Xiang River basin, China". *Theoret. and Appl. Climatol.*, DOI 10.1007/s00704-015-1467-1.

Wang, S., Zhang, Z., McVicar, R. T., Zhang, J., Zhu, J., and Guo, J. (2012). "An event-based approach to understanding the hydrological impacts of different land uses in semi-arid catchments." *J. of Hydrol., 416–417 ,* 50–59.

Wang, S., Zheng, X., and Zang, X. (2012). "Accuracy assessments of land use change simulation based on Markov-cellular automata model." *Proc. Env. Sci., 13*, 1238 – 1245.

Warburton, L. M., Schulze, E. R., Jewitt, P. G., (2012). "Hydrological impacts of land use change in three diverse South African catchments." *J. of Hydrol., 414–415*, 118–135.

Westmacott, R. J., and Burn, H. D., (1997). "Climate change effects on the hydrologic regime within the Churchill-Nelson River Basin." *J. of Hydrol., 202* , 263–279.

Wibig, J., Maraun, D., Benestad, R., Kjellstrom, E., Lorenz, P., & Christensen, B. O. (2015). "Chapter 10: Projected Change—Models and Methodology". *DOI 10.1007/978-3-319-16006-1_10*, 189-2015.

Wijesekara, G. N., Gupta, A., Valeo, C., Hasbani, J. G., Qiao, Y., Delaney, P., et al. (2012). "Assessing the impact of future land-use changes on hydrological processesin the Elbow River watershed in southern Alberta, Canada." *J. of Hydrol., 412–413*, 220–232.

Wooldridge, S., Kalma, J., Kuczera, G., (2001). "Paremeterization of a simple semi-distributed model for assessing the impact of hydrologic response." *J. of Hydrol., 254*, 16-32.

Wu, K., Johnston, A. C., (2007). "Hydrologic response to climatic variability in a Great Lakes Watershed: A case study with the SWAT model." *J. of Hydrol., 337*, 187– 199.

Xu, C. Y., and Singh, V. P. (1998). "A Review on Monthly Water Balance Models for Water Resources Investigations." *Water Resour. Manag., 12*, 31–50.

Ye, X., Zhang, Q., Liu, J., Li, X., Xu, C.Y., (2013). Distinguishing the relative impacts of climate change and human activities on variation of streamflow in the Poyang Lake catchment, China. *J. of Hydrol. 494*, 83–95.

Yu, W., Zang, S., Wu, C., Liu, W., and Na, X. (2011). "Analyzing and modeling land use land cover change (LUCC) in the Daqing City, China." *Appl. Geogr., 31*, 600-608.

 YueChen, L., and ChunYang, H. (2008). "Scenario simulation and forecast of land use/cover in northern China." *Chin. Sci. Bullet. , 53* (9), 1401-1412.

Zak, R. M., Cabido, M., Caceres, D., and Diaz, S. (2008). "What Drives Accelerated Land Cover Change in Central Argentina? Synergistic Consequences of Climatic, Socioeconomic, and Technological Factors." *Env. Manag., 42*, 181–189.

Zheng, X.-Q., Zhao, L., Xiang, W.-N., Li, N., Lv, L.-N., and Yang, X. (2012). "A coupled model for simulating spatio-temporal dynamics of land-use change: A case study in Changqing, Jinan, China." *Landsc. and Urban Plan., 106*, 51–61.

Zhou, F., Xu, Y., Chen, Y., Xu, C., Gao, Y., and Du, J. (2013). "Hydrological response to Built-up landization at different spatio-temporal scales simulated by coupling of CLUE-S and the SWAT model in the Yangtze River Delta region." *J. of Hydrol., 485*, 113–125.